Abstract

Several studies claim that wind power will play a major role in the energy supply of the European Union, forecasting 70 GW of new installed capacity in the next five years. Given the accelerated growth that offshore wind power is experiencing, many challenges are to be addressed in the next few years and substantial improvements are to be expected. Offshore wind farms (OWF) are expected to increase in rated power and in distance from shore, thus increasing the relevance of the transmission system. Therefore, a detailed technical-economic analysis is necessary to estimate which is the optimal transmission system to transmit the power generated at the OWF.

This thesis presents a technical-economic analysis of power transmission systems for OWF. The aim of this work is to determine the most suitable power transmission technology for a given set of OWF characteristics. Costs and losses of different proposed technologies are investigated: high-voltage alternating current (HVAC), high-voltage direct current (HVDC) based on voltage-source converters (VSC), and low-frequency alternating current (LFAC). For the technical part of the analysis, the strengths and weaknesses of each technology are exposed, as well as the role of the main components investigated. Regarding the economic side of the thesis, the costs of the major components of each transmission system are associated to cost functions, and their losses modelled. Availability of the components is also considered, as well as the variability of the self-made cost functions. The self-made cost functions, being contributions of this work, are provided for public use. The costs of the whole transmission system including losses are obtained as a function of a range of variables (transmission length, rated power, voltage level, etc.). Additionally, the employed cost functions and loss calculations are summarized in a spreadsheet, which is openly available upon request.

Besides giving the cost functions, the technical-economic analysis is applied to a set of case studies to draw a comparison between a range of proposed transmission systems. The obtained results indicate that the break-even point between HVAC and HVDC is to be found in the 50-100 km range, approaching 50 km in the case of large OWF (e.g. 1000 MW). Additionally, the studied cases also reveal that LFAC could result the most suitable option in the 50-70 km range.

Acknowledgements

Few bachelor thesis lead to the writing of an academic paper. It is said that those who do, either work on a leading-edge technology or benefit from a very good supervisor. For this case, it is unquestionable that without the help and dedication of Rodrigo Teixeira Pinto, this would have never been possible. His help and has driven myself to discover such an interesting academic field such as power transmission, and I am infinitely thankful for that. I would have never worked so hard and achieved this work without him. Many thanks, Rodrigo; and congratulations on the birth of your child, Vito.

I would also like to particularly thank Oriol Gomis for his attitude, for giving me the opportunity to work with Rodrigo, and for giving me the chance to be involved in such a great team at the CITCEA. Thanks to Muhammad Raza for his powerful advices, and for his infinite patience resolving my doubts.

I would also like to mention Professor Josep A. Sànchez for his help and advice on the statistics part of the modelling equations, strengthening this present work.

Thanks to my family for their support, and especially to Sofía, as you have dealt with my frustrations, angers, and joy when building this work. Your support and love is beyond what I could ask for.

Summary

List of Acronyms

CCV	Cycloconverter
GIS	Gas-insulated switchgear
HVAC	High-voltage alternating current
HVDC	High-voltage direct current
LCC	Line-commutated converter
LFAC	Low-frequency alternating current
MVAC	Medium-voltage alternating current
NPV	Net present value
OWF	Offshore wind farm
VSC	Voltage-source converter

Preface

The thesis contributions are:

- analysis of the economic feasibility of offshore wind farms (OWFs) connected with low-frequency ac (LFAC) transmission systems as an alternative power transmission technology;
- providing the scientific community with new cost functions for voltage-source converters, HVDC cables and GIS switchgears;
- adapted cost functions for HVDC-VSC offshore platforms and LFAC offshore platforms;
- providing a tool that calculates the capital costs and losses of a subsea power transmission system, as a function of the offshore wind farm characteristics, with variable configuration and different technologies, including the system availability. The newly developed cost functions have been included in this tool, in addition to cost functions available in the literacy, resulting in a powerful cost-estimator;
- exposing a detailed methodology on general loss calculation of the considered components.

1. Introduction

1.1. Offshore wind energy

Wind energy is nowadays a growing trend. As it can be seen in Figure 1, the wind industry has experienced a sustained growth over the last decade. Wind energy provides a reliable, clean, safe and competitive alternative in comparison with other energy sources, such as fossil fuels. Most countries have plans for increasing the production of electricity related to renewable energy, by means of wind power: only in Europe, forecasts predict 70 GW of new wind power plants for the next five years [1] [2].

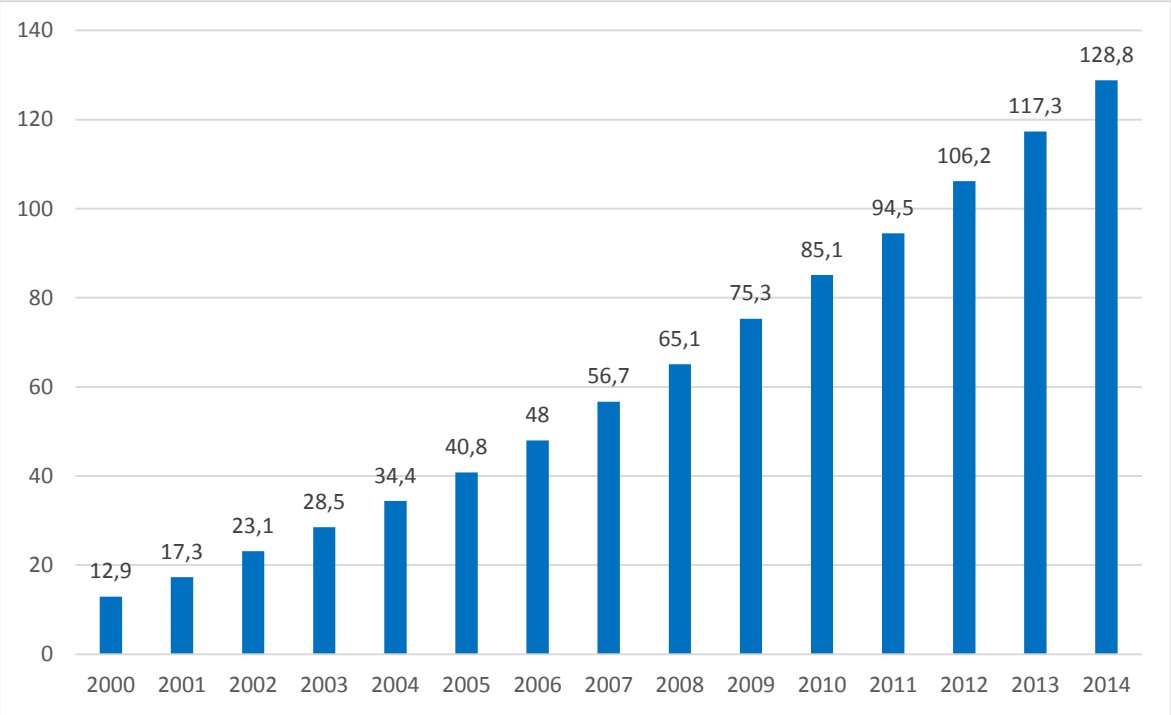

Figure 1 Cumulative capacity installed in EU (GW) (data source: [3]).

In 2012, the EU reached the 100 GW milestone of installed capacity, confirming the fast growth that wind energy is experiencing in the last decade. In fact, it is estimated that wind energy will supply alone 25.7% of EU's electricity demand by 2030, according to the European Wind Energy Association (EWEA) [4].

However, wind farms occupy a large amount of space compared to conventional power plants, produce noticeable undesired noise and have a considerable visual impact. Therefore, placing wind farms offshore is a convenient alternative, even offering significant advantages over land based wind systems, since with higher annual mean wind speeds, a higher energy yield is obtained. Countries such as Germany, Denmark, Sweden, the Netherlands, and China are currently operating offshore wind farms (OWFs) and many others have wind farms in development [1].

The first offshore wind farm was inaugurated in 1991, 2.5 km off of the Danish coast, featuring eleven 450 kW turbines for a total capacity of 4.95 MW [5]. Until 2001, the development of offshore wind was unstable and irregular, dependent of small near-shore projects in Danish and Dutch waters, with capacities of less than 1 MW. In 2001, with 20 turbines and a total capacity of 40 MW, the first "utility-scale" wind farm was built in Danish waters, the *Middlegrunden* project [6]. Figure 3.1-2 shows that offshore wind is experiencing substantial growth; after the first years of initial developments, and that nowadays large-scale offshore wind farms, e.g. 630 MW (London Array wind farm, 2013), are currently operating.

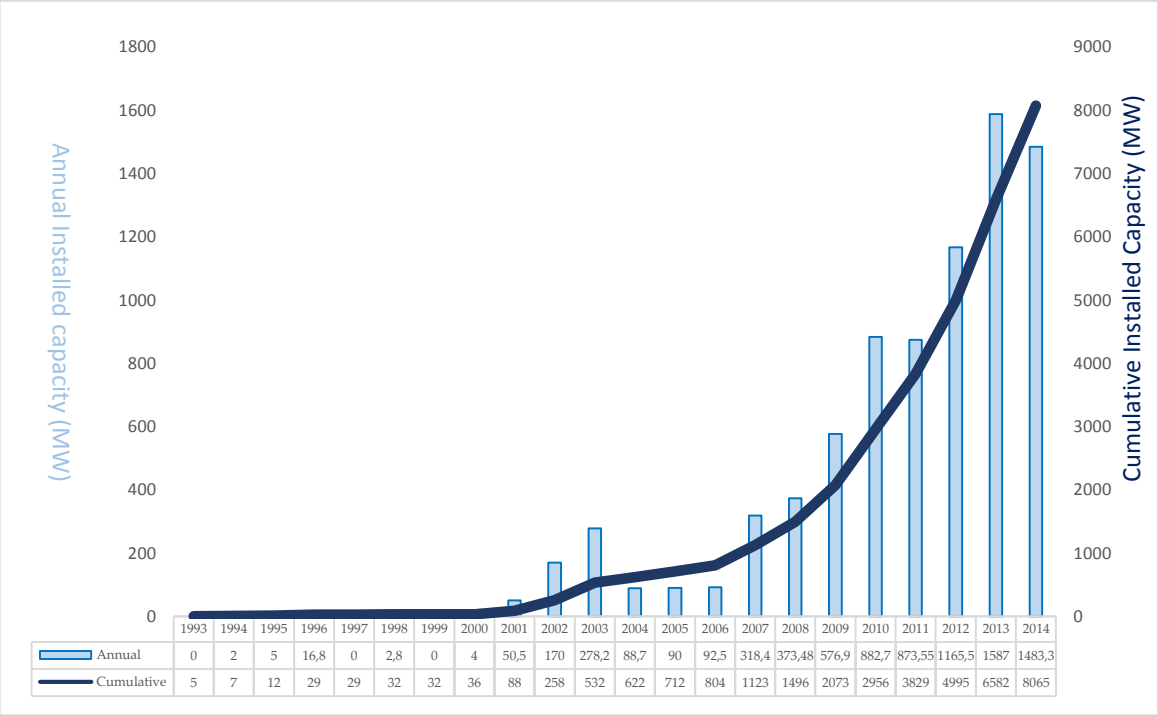

	1993	1994	1995	1996	1997	1998	1999	2000	2001	2002	2003	2004	2005	2006	2007	2008	2009	2010	2011	2012	2013	2014
Annual	0	2	5	16,8	0	2,8	0	4	50,5	170	278,2	88,7	90	92,5	318,4	373,48	576,9	882,7	873,55	1165,5	1587	1483,3
Cumulative	5	7	12	29	29	32	32	36	88	258	532	622	712	804	1123	1496	2073	2956	3829	4995	6582	8065

Figure 2 Cumulative and annual offshore wind installations (MW) (data source: [2]).

Offshore wind developments are also being considered outside of the EU. For instance, the Chinese government has set ambitious targets of 5 GW of installed offshore wind capacity by 2015 and 30 GW by 2020, which could make China the country with the highest installed

capacity offshore.

Given the strong growth that offshore wind power is experiencing, many challenges are to be addressed in the next few years and substantial improvements are to be expected, some of which related with cost reduction measures and resource optimization [7] . Offshore wind levelized cost of energy (LCoE[1]) is nowadays around 140 €/MWh, but is expected to diminish to 90 €/MWh around 2030 [4], making it a tough competitor to fossil fuels [8].

1.2. Problem description

Offshore wind farms consist of arrays of turbines linked together in a given layout. The energy generated by the turbines is directed through distribution cables to a collection point, and then transmitted to the grid. This last step represents the challenge that will be analyzed in this thesis (coloured in red in the following figure).

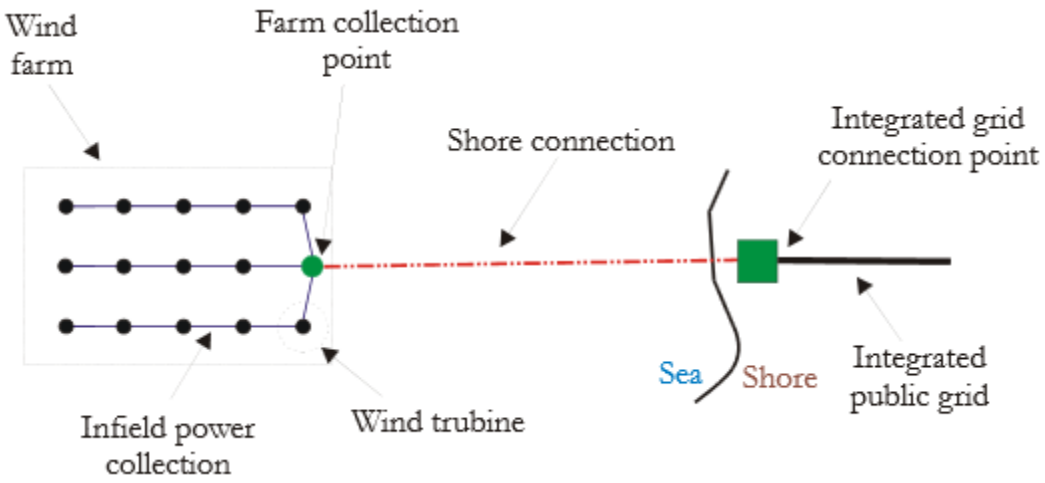

Figure 3 Schema of an offshore wind farm [9].

In the beginning of the offshore wind industry development, as the distances to shore were considerably small and the amount of energy to be transmitted was relatively low, the transmission of this energy was not as challenging, and usually ac transmission systems at

[1] LCoE – Levelized Cost of Electricity incorporates all the costs incurred during the life of a power station, including for example CAPEX, O&M (operations and maintenance), fuel and decommissioning costs, and divides the discounted sum of those costs by the discounted lifetime output from the power station, resulting in a lifetime average (levelized) cost per unit of electricity.

medium voltage were involved.

However, as it can be seen in Figure 4, the rated power of offshore wind farms has largely grown in the last few years, and it is expected to increase more in the next decades [2] [4]. Furthermore, offshore wind farms are built nowadays at an appreciable distance from coastline – e.g. 121 km in the case of Bard 1 OWF – and this trend is expected to continue over the next decades [10]. Those two factors consequently increase the importance of the power transmission, thus making the transmission technology a crucial decision factor.

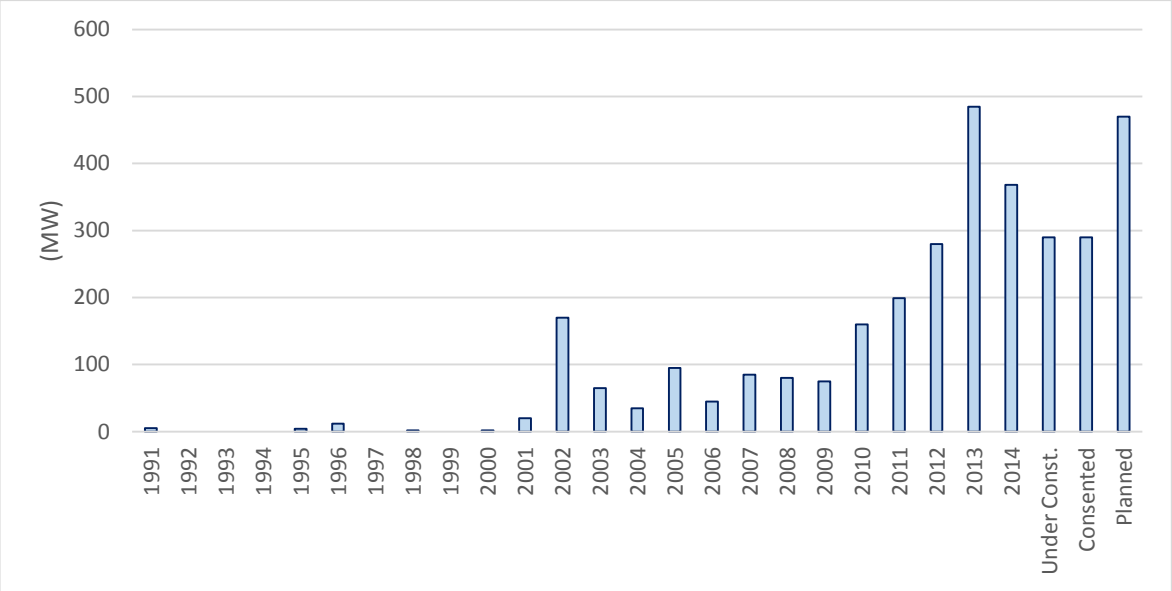

Figure 4 Average installed capacity of offshore wind farms (Data source: [10])

In fact, an increase on capacity corresponds with an increase in transmitted energy, which necessarily implies cables with higher voltage and power ratings. The number of cables, voltage level, and the technology used, are all factors that influence the cost and losses of the connection, and therefore have a significant influence on the wind farm profit.

In addition, as the distance to shore increases, those factors have greater importance as costs and losses can be much higher with long shore connections. Table 1 shows a cost breakdown

Table 1 Cost breakdown of an offshore wind farm. Source: [11]

Capital investment cost	*2,4 - 3,6 M€/MW*
Wind turbine cost share	30 - 50%
Power transmission cost share	15 - 30%
Construction cost share	15 - 25%
Other capital cost share	8 - 30%

of an OWF, estimating power transmission costs between 15% and 30% of the total cost, the latter applying for more isolated OWF.

It has been stated so far that OWF are expected to increase in rated power and in distance from shore, thus increasing the relevance of the transmission system. Therefore, a detailed technical-economic analysis is necessary to estimate which is the optimal transmission system to transmit the power generated at the OWF. Consequently, the research question driving the present work is presented as:

Which would be the most suitable transmission system for a particular offshore wind farm, in terms of costs, loss reduction, and technical feasibility?

1.3. Problematic overview

The query in the research question is the suitability of high-voltage alternating current (HVAC) transmission systems. As the overwhelming majority of power transmission systems are HVAC, what are the reasons behind considering other technologies? In fact, the main issue with HVAC, setting aside other matters, is that the transmission capability of HVAC subsea cables is limited. The presence of reactive power compromises the transmission of active power, particularly in long transmissions and higher voltages. This issue is further developed in Section 2.1.2 .

On the other hand, high-voltage direct-current (HVDC) overcomes most of the HVAC transmission system flaws (see Section 2.3.1), but comes at a higher base cost (ac-dc converters mainly). Furthermore, distance-dependent costs are lower for HVDC than for their HVAC counterpart, which leads to a break-even point where HVDC transmission system costs become lower. Figure 5 illustrates this fact.

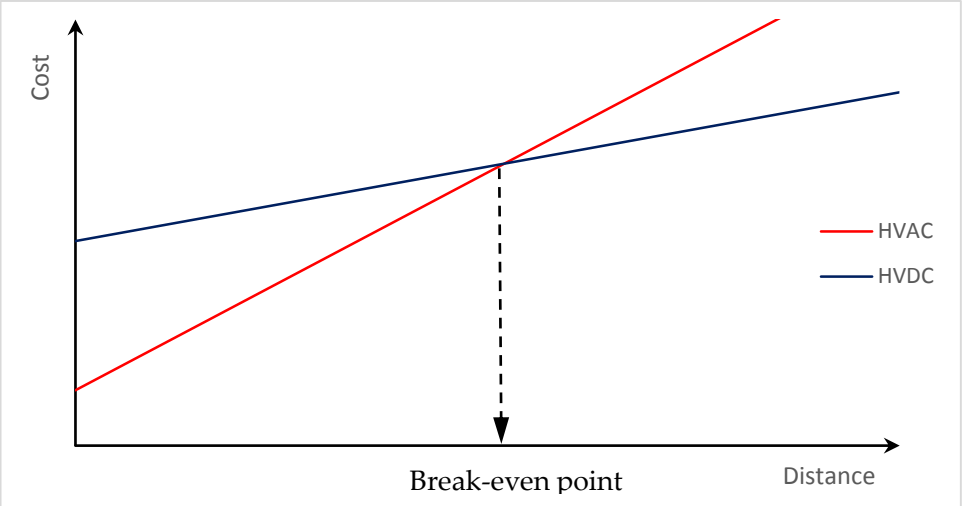

Figure 5 Qualitative chart of HVAC and HVDC transmission systems costs

As the distance rises, costs and losses of HVAC subsea transmission systems overcome the costs of the HVDC alternative. The distance at which the break-even point occurs depends on many factors (e.g. rated power of the OWF or the voltage level of both transmission systems), but generally falls in the 50-100 km range, depending on considered configurations [11] [12], with recent reports favouring 50 km [13] [14]. Determining the break-even distance as a function of the transmission characteristics is one of the main goals of this work, and it is considered that it will be helpful to the scientific community working on power transmission or on OWF concepts.

Table 2 shows data of recently commissioned OWF. None of both transmission technologies is clearly dominant in recently commissioned OWF, although remotely located OWF transmit their power by means of HVDC systems (e.g. Bard 1, Borkum West 2, Nordsee Ost and Meerwind Süd), whereas the ones nearer to the grid employ HVAC systems (Anholt, Greater Gabbard and London Array 1).

Table 2 Recently-commissioned OWF

Offshore wind farm	*Transmission length [km]*	*Rated power [MW]*	*Transmission type*	*Commissioning year*
Anholt (Denmark)	25	400	HVAC	2013
Bard 1 (Germany)	121	400	HVDC	2013
Borkum West 2 (Ger.)	75	400	HVDC	2013
Greater Gabbard (UK)	46	506	HVAC	2012

London Array 1 (UK)	55	630	HVAC	2013
Nordsee Ost (Ger.)	85	295	HVDC	2013
Meerwind Süd (Ger.)	85	288	HVDC[2]	2013

Additionally, another technology is suggested amongst the reviewed literature: low-frequency alternating current (LFAC) [15]. It can be understood as a compromise between HVAC and HVDC [16]. The conversion from low frequency to 50 Hz is supposed to be less expensive than from ac to dc, as well as distance-dependent costs should be lower than for HVAC, suggesting that LFAC would be competitive in the 30-150 km range [17] [18]. That would translate in a cost pattern similar to the one shown in Figure 6. Nevertheless, the technical feasibility of LFAC for OWF power transmission is still being discussed as specialists do not agree on various aspects, such as the conversion topology, and hitherto[3], no OWF power transmission has employed the LFAC technology.

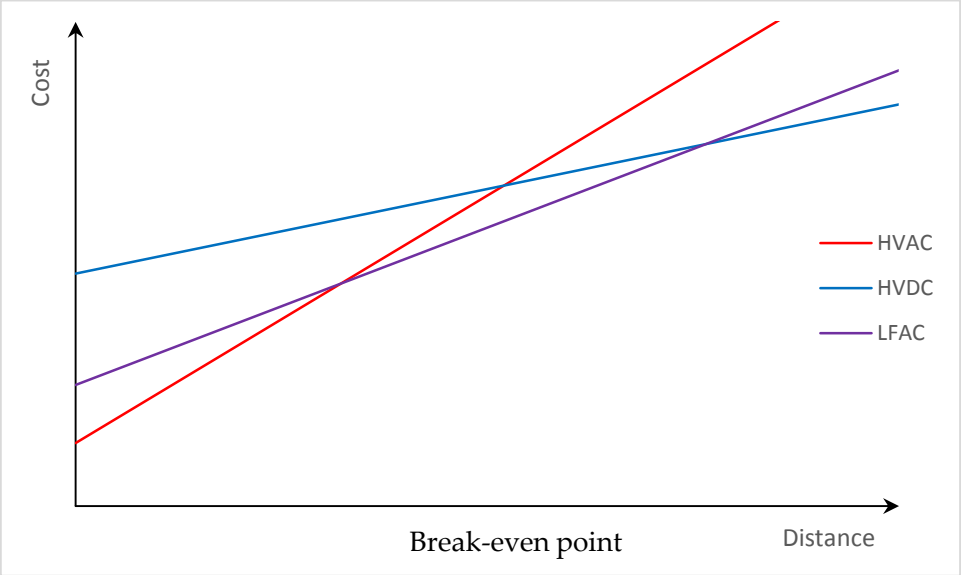

Figure 6 Expected cost function of LFAC

[2] Nordsee Ost and Meerwind Süd share the same HVDC 576 MW offshore hub

[3] June 2015.

1.4. Objectives

This thesis is conceived as a technical-economic analysis of the different technologies for power transmission in offshore wind farms. The purpose of this work is then to determine the optimum transmission technology for a given offshore wind project. The main objectives underlying this matter are the following:

- present technical considerations, as well as advantages and disadvantages of the considered technologies;
- achieve an accurate economic analysis for HVAC and HVDC transmission systems, treating the OWF characteristics as well as the transmission characteristics as variables;
- analyse the economic feasibility of LFAC, by estimating its costs and comparing them to HVAC and HVDC.

The thesis main chapters are consequently the following:

- Chapter 2 presents the technical background of HVAC, MVAC, HVDC and LFAC transmission systems, though a literature review. The general performance of each technology is analysed, highlighting their strengths and weaknesses. Moreover, the role of the main components in each technology is described. MVAC is included as it was used for some OWF, but will not be given the same level of attention (see section 2.2)
- Chapter 3 draws the technical-economic analysis, by building cost functions of every component as well as modelling the system losses, whilst considering technical decisions over the system configuration. A deeper look at HVAC and HVDC is made in Section 0, including the cost functions variability, which should enhance the validity of the results;
- Chapter 4 applies the technical-economic model to a real case, discussing the obtained results against real data;
- The utilized cost functions are included in a spreadsheet, which calculates the cost of the considered transmission technologies for any data introduced by the user. A cost sensitivity analysis is included, as well as the possibility to modify technical decisions, or inputs. This spreadsheet is intended to make accessible the results of this present work.

Regarding the methodology, a thorough literature review has been made to back up its technical background, as well as to support the modelling decisions made in the thesis. For the economic analysis, the procedure has been to build self-made cost functions when the collected data allowed. In other cases, not enough data has been obtained to determine the costs patterns, and cost functions used by other researchers have been employed. If none of the previous was possible, justified assumptions have been made.

1.5. Scope

This thesis focuses on the transmission system of offshore wind farms, from the offshore substation to the onshore substation: power cables, transformers and power converters are the main studied components. Furthermore, losses and cost patterns of those devices are very relevant to this work. More precisely, this thesis analyses technical considerations of different technologies regarding power transmission. Once the technical considerations are analysed, the economic analysis will take place. For emerging technologies, such as LFAC, some elements whose technical feasibility is not proven will still be considered.

Everything outside the transmission system is outside the scope of this work. That implies that the wind farm turbines, infield collection cables (i.e. anything related to the inner workings of the wind farm) is out of the scope of this project. Additionally, it will be assumed that no grid reinforcements or grid modifications due to the injection of bulk power will are necessary at the point of common coupling onshore.

A study on the economic viability of an offshore wind farm, analysing the profitability (net present value, internal return rate, etc.) of the investment will not be considered, because to do that the costs of the wind turbines, collection system, wind availability, would have to be accurately studied, and that would not necessarily affect the obtained results for the transmission system technology.

Regarding the economic analysis, this project focuses on building the cost functions and establishing costs patterns of the power transmission system, thus determining the costs of the components and evaluating their losses. This type of economic analyse will be more useful to other researchers than analysing the economic viability of an OWF, as the cost functions

obtained can be adapted to other studies, e.g. to estimate the cost of other subsea power transmission systems.

2. Technical Background

In this Chapter, technical information of the considered power transmission technologies is presented. The functioning of each technology is described, and the role of the main necessary components is analysed. The described components are relevant for the technical-economic analysis, performed in Chapter 3, and are included in the cost models.

2.1. HVAC

Nowadays, HVAC is the most common method used for power transmission [19]. Until recent years, it was the only technology employed regarding offshore wind farms, along with MVAC [20].

Since the development of transformers, which allow for high power and insulation levels, have overall lower loses, and relatively simple operation and maintenance, HVAC has been the dominant technology for electricity transmission all over the world. Regarding offshore wind farms, it was indeed the main technology in the early years of development, when wind parks had a small rated capacity and were built close to shore. Nevertheless, nowadays, the offshore wind farm characteristics determine whether HVAC is the optimal option.

In the following sections, HVAC offshore transmission systems will be described, their basic functioning and disadvantages will be presented, and the role of the main components will be analysed.

2.1.1. General Description

The basic functioning of an HVAC transmission is the following: the power produced by the wind farm at medium-voltage alternating-current[4] (MVAC) is sent to an offshore substation, which contains a power transformer, which steps up the voltage to values typically between 110kV and 275kV. The power is transmitted at this voltage through subsea cables, generally buried until it finally reaches the onshore substation, where the connection to the grid is made. Other components, such as switchgears and reactive power compensation systems are necessary to guarantee the power transmission.

[4] Typically 30-36 kV.

Figure 7 illustrates a basic scheme of an HVAC offshore transmission system (note that although ac systems generally have three phases, only one phase is represented).

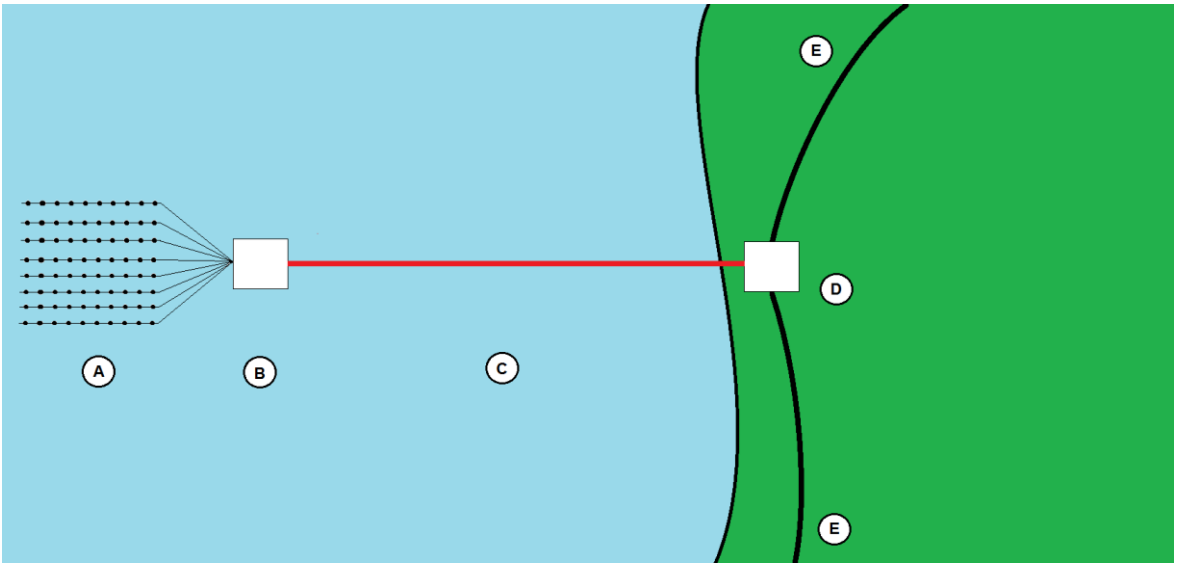

*Figure 7 General Scheme of an HVAC transmission, per phase. **A**: Offshore wind farm, infield power is transmitted at medium voltage to the offshore substation (**B**). **B**: Offshore substation, containing various electrical devices, notably the step-up power transformer and switchgear, as well as reactive power compensation systems. **C**: HVAC three-phase subsea line, which carries power from the offshore substation (**B**) to the onshore substation (**D**), at high voltage. **D**: Onshore substation, the connection with the grid is produced. Reactive compensation systems and switchgears may also be present, as well as a power transformer if the grid voltage level differs from the HVAC voltage level (**C**).*

2.1.2. HVAC transmission losses

This section aims to give an overview about the losses (and reactive power generation) of HVAC transmission systems, to understand its limitations. Detailed loss evaluation for HVAC is developed in Section 3.4.4.

Most losses, up to 60% (see Chapter 4), regarding the transmission system of an OWF are in fact located at the submarine cables. There are two types of losses, depending on the nature of the involved power: reactive losses[5] (capacitive and inductive) and active losses (ohmic and dielectric losses).

[5] Although called reactive "losses", it does not configure a loss of energy, but a form of energy which is generated in ac systems and that cannot be utilized.

In fact, the reason behind stepping up the transmission voltage is to substantially reduce ohmic losses, which are proportional to the square of the current amplitude (see (1)). At a given power, doubling the voltage halves the current, hence reducing ohmic losses by a quarter. With this in mind, in theory, the more the voltage is raised, the more the ohmic losses are decreased.

$$P_{losses} = 3 \cdot {I_{cable}}^2 \cdot r \cdot d \qquad Q_L = 3 \cdot {I_{cable}}^2 \cdot 2\pi \cdot f \cdot L \cdot d \qquad (1)$$

where;

P_{losses}: Ohmic losses in the cables [W];

Q_L: Reactive power produced by inductive effects [VAr];

I_{cable}: Cable current intensity [A];

f : Electric frequency [Hz];

r: Line resistance [Ohm/km];

L: Line inductance [H/km];

d: Line length [km].

The formulae for inductive and ohmic losses are shown above. Ohmic losses in ac are due to the conductor resistivity, the skin effect and the proximity effect (refer to Section 3.4.4.1 for further details on the ac resistance, and on proximity and skin effect); whereas inductive losses are due to the displacement between voltage and current, which can happen in ac systems. On the other hand, subsea cables have a lower inductance than overhead lines due to the lower spacing between conductor and the earth. Both inductive and ohmic losses are current-square dependent. Bearing that in mind, to lower the losses, the highest possible voltage should be established.

However, regarding offshore transmission, other types of losses are also significant and may considerably reduce the transmitted power, thus plundering the efficiency of the whole transmission. Ohmic and inductive losses are both dependent of the square of the current, and are tackled by rising the voltage level. On the other hand, cables generate capacitive power

(capacitive "losses") proportionally to the voltage squared, as shown in (2). It can be noticed that these capacitive "losses" are not load-dependent, as they are a function of the voltage level, and not dependent on the transmitted current.

$$Q_c = 3 \cdot \left(\frac{U_{RMS}}{\sqrt{3}}\right)^2 \cdot 2\pi \cdot f \cdot C \cdot d \quad (2)$$

where;

Q_c: Reactive power produced by capacitor effects [VAr];

U_{RMS}: Phase to phase voltage level [V];

f : Electric frequency [Hz];

C: Line capacitance [F/km];

d: Line distance [km].

Usually, the capacitive "losses" are of lesser importance in overhead HVAC transmission lines, except for very long transmission distances, as the capacitance of those lines is smaller than in HVAC underground or submarine cables. However, in subsea transmission lines, due to proximity between conductors and the sheath, the capacitance is much higher. In fact, while for overhead lines the capacitance lies in the 9-14 nF range, subsea cable capacitance falls in the 200-300 nF range, i.e. 20 times higher [21]. On the contrary, inductive reactive power is lower in subsea cables than in overhead lines, typically the inductance of subsea cables is the half of the overhead lines inductance [21].

Thus, the more the voltage is risen to reduce ohmic and inductive losses (mainly ohmic losses), the more the capacitive "losses" increase. In reality, as those "losses" are voltage-square dependent, they become an overwhelming problem, particularly in long subsea cables. In fact, as the reactive power produced by the cable capacitance rises, the real power which could be transmitted decreases. In fact, the cable apparent power can be calculated as:

$$S = \sqrt{(P_{transmitted} + P_{losses})^2 + {Q_{tot}}^2}\ , \qquad where\ Q_{tot} = Q_L - Q_c, \quad (3)$$

where;

$P_{transmitted}$: Power transmitted and delivered to the grid [W];

Q_{tot}: Total reactive power produced by inductive and capacitive effects [VAr];

S: Apparent power [VA].

For a given voltage level and a given current intensity, the apparent power S remains more or less constant throughout the cables. Consequently, an increase in reactive power implies a decrease in active power, thus plundering the efficiency of the whole transmission. This concept is illustrated in Figure 8. It shows the transmittable active power of an 800 mm² three-core cable with respect to distance, for different voltage levels. The higher the voltage level, the higher the generated reactive power per kilometre of cable. Hence, for high voltage levels, the reduction of the active power transmission capability is steeper.

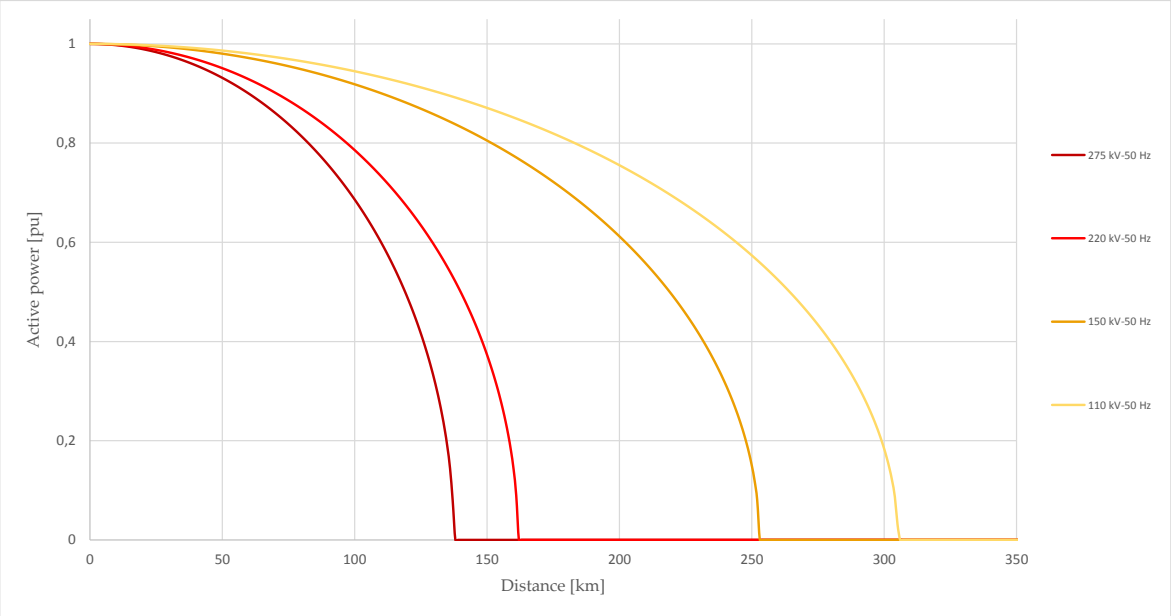

Figure 8 Active power transmission capability of subsea 800mm² three-core cables at different voltage levels, with compensation at both ends of the cable

Note that this fact indicates that the ac cables must be rated higher than the active power they are supposed to transmit. For example, the 275 kV cable is only able to carry 50% of its rated power as active power for a transmission length of approximately 120 km, the rest being reactive power. Consequently, for a 275 kV 120 km transmission system, the cables should be rated the double of the power they must transmit, resulting in higher costs. This is a very deterrent fact for HVAC subsea transmission.

The same concept can be understood by analysing the current behaviour throughout the cables. Figure 9 illustrates the model of a short transmission line [22].

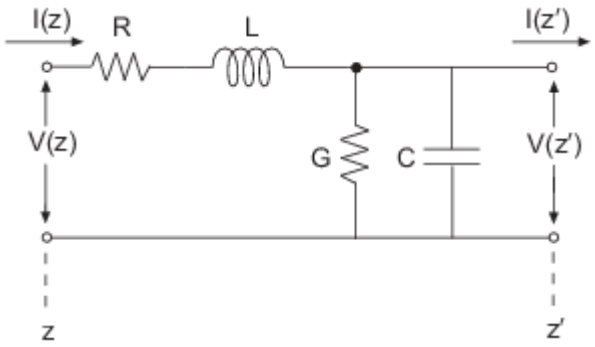

Figure 9 : Transmission Line model for short distances [22].

As shown in Figure 9, the current in the transmission system can be split on its active component, responsible for the transmission of active power, and its reactive component, which is related to the inductive and capacitive elements of the transmission systems.

Finally, it can be observed that there is a parallel conductance G that has not been mentioned yet. This conductance models the dielectric losses, which are active losses that are voltage-square dependent (see Section 3.4.4.3), being proportional to the capacitive reactive power as shown in (4):

$$P_{dielectric} = Q_c \cdot \tan\delta \tag{4}$$

where tan(δ) is a material-dependent factor, typically around 0,004 [23].

In conclusion, it could be said that ac systems present some challenges that can compromise its power transmission capability. Furthermore, the voltage level decision must take into account two facts: a higher voltage level will require more reactive power compensation and may compromise the power transmission performance; nevertheless lowering voltage level implies increasing ohmic losses, hence reducing transmission performance.

Next, through Sections 2.1.3 to 2.1.6, the main components of an HVAC offshore transmission system will be analysed.

2.1.3. Subsea cables

Subsea cables must carry the power between the offshore substation and the onshore substation. They are a critical component of the transmission, that determines most of the losses and reactive power, as the entire power generated reaches the grid through them.

The first choice to be made regards the number of cores. Either one three-core cable or three single-core cables can be employed for three-phase systems, where the latter option is preferred for bulk power transmission. Considering that three single-core cables need less cross-section than three-core cables, a lesser amount of copper is needed, reducing the costs [24].

However, to lay three cables symmetrically is costlier than laying one single cable. Additionally, to keep the system symmetrical, transposition of the cables is needed at certain intervals. With transposition is meant that the single-phase cables have to change in relative position to keep the system balanced. According to [24], this operation has to be done approximatively every 50 km. The screens of the cables have to be cross-bonded as well to eliminate sheath-circulating currents. The cost of transposition is high, especially at sea where it is a real technical challenge and increases the cables installation cost. Therefore, the preferred option for offshore ac transmission is to employ three-core cables.

The other critical choice to be made is the insulation material. In fact, cables are classified by their insulation material, which strongly influence the cable electrical performance and behaviour [22]. For offshore transmission systems, cross-linked polyethylene (XLPE) insulated cables are recommended by manufacturers [25]. Cross-linked polyethylene has been used for submarine cables since 1973 and for underground land cables even before [25]. XLPE is made by cross-linking chains of low-density polyethylene to form three dimensional networks. The XLPE material has excellent insulating properties and a high level of performance. Moreover, its dielectric loss factor is notably low compared to other insulation materials (five times less than other materials, such as paper oil or polyethylene rubber [26]).

Regarding the conductor, either copper or aluminium are possible. Copper is usually preferred, as it has a high conductivity (lower ohmic losses) and can carry a larger amount of power for a given section. In fact, to achieve the same conductivity, aluminium cables need a cross section 50% higher [27]. Alternatively, aluminium cables cost less but are more difficult to install [27]. Therefore, aluminium becomes a more interesting option when copper prices rise.

Figure 10 72kV three-core power cable [28]

2.1.4. Power Transformer

A transformer is a basic device in power distribution and power transmission. The role of a power transformer is to vary levels of voltage between two circuits by means of electromagnetic induction. Basic characteristics of a transformer are its nominal power, which indicates the maximum power it can operate in steady state; and its turn ratio, which indicates the voltage transformation ratio. There is the need of transformers whenever voltage levels have to be varied. In addition, more than one transformer is needed at the same point when carrying large amounts of power, as generally individual transformers cannot withstand loads

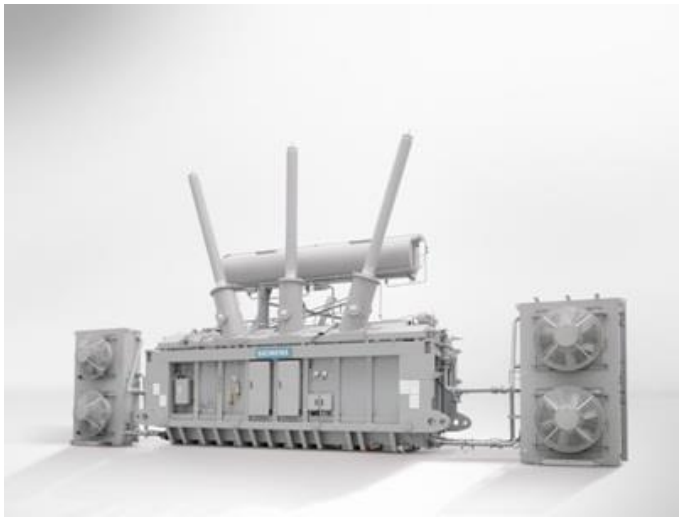

Figure 11 Large Power Transformer (Source: Siemens)

bigger than 1000 MVA [29],as well as various transformers operating at the same point increase reliability.

In OWF, the collection systems are usually in medium voltage (33kV) and, for HVAC transmission purposes, the voltage must be increased to higher voltage values, usually between 110kV and 275 kV [28]. Along with other equipment, the group of offshore transformers is mounted on an offshore substation near the wind farm. At the end of the transmission, the other group of transformers varies the voltage level to meet the grid voltage. This latter group of transformers is not necessary in case the transmission voltage matches the grid connection voltage.

Large power transformers have overall very high efficiency, being reported as high as 99,85% [30]. Its losses come from copper windings (load-dependent ohmic losses), and from the iron core (non-load dependent). Transformer loss calculations are furtherly developed in Section 3.4.4.7.

2.1.5. GIS Switchgear

A switchgear is a main protective element of a transmission system. Adapted to high voltages and high current; it helps connecting and disconnecting in case of a fault or short-circuit, and one of its main components is a circuit breaker [25]. Whenever there is a fault, the circuit breaker helps in disconnecting the circuit and quenching the fault current. On the other hand, the switchgear also contains measuring instrumental systems to monitor the transmitted power.

As for offshore applications, gas insulated switchgears are mostly employed [25]. Moreover, gas-insulated switchgear are more compact and have smaller dimensions than conventional switchgears, thus making them more suitable to be mounted on an offshore substation, where space is critical. This component will be included in the cost models.

2.1.6. Reactive power control

As discussed in Section 2.1.2, electrical systems, notably buried cables, produce reactive power. Reactive power must be compensated to prevent a decrease in active power. Furthermore, TSO have strict requirements on power factor values, which must be respected to inject power into the grid [31]. There are different strategies and different devices used for reactive compensation. Note that as the reactive power produced in subsea cables is mostly

capacitive, reactive compensators must produce inductive power.

As for strategies, the most common is to split power compensation between onshore and offshore substations [13]. Nevertheless, compensating reactive power offshore implies a bigger substation, thus increasing the offshore foundation costs. Other strategies are possible, such as installing all the compensators onshore to reduce costs. Figure 12 illustrates this concept. As shows in the figure, even at low distances such as 50 km other strategies than 50/50 splitting imply a noticeable reduction of the transmitted power.

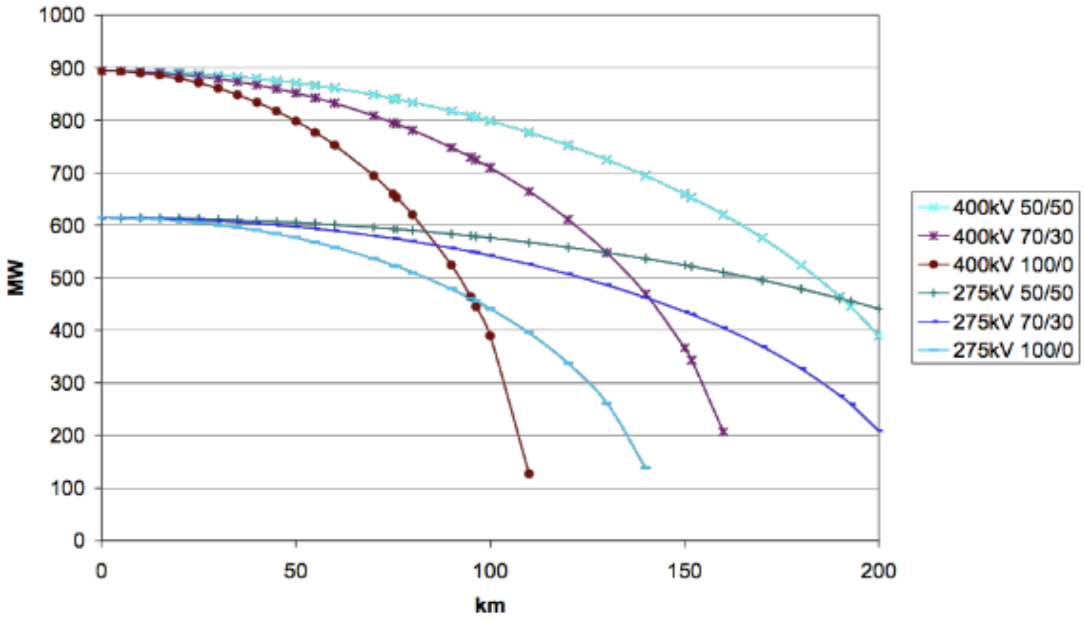

Figure 12 Transmitted power as a function of distance, for different voltage levels and different reactive compensating strategies. Source: [13]

Regarding reactive power compensation devices, there are two generally options: fixed-value compensators, and variable compensators. On one side, fixed-value compensators, such as shunt reactors, are cheaper and occupy less space, but they cannot adjust their VAr ratings to match power fluctuations. On the other side, variable compensators such as STATCOMs (Static Synchronous Compensator) are more expensive, but trough power electronics they can aim to compensate the exact value desired at each moment.

Due to the nature of wind, current generated by the OWF is variable; hence, the reactive power produced also fluctuates. Nevertheless, the current only affects the inductive reactive power, which was found to be generally two orders of magnitudes smaller than the capacitive reactive power. Therefore, variations in the reactive power generated by the transmission system are

of less than 1% . Consequently, variable compensators are only needed when there are very strict requirements at the grid coupling point, i.e. when it is required complete reactive power compensation[6].

For this work, shunt reactors will be considered at the offshore wind farm, and a STATCOM will be considered onshore whenever they are necessary to meet the grid code requirements.

[6] If a power factor of 1 is required (i.e. no reactive power at the grid point of common coupling), it must be ensured that full compensation is made. For this purpose, STATCOMS are more suitable as they can adjust its value to exactly compensate all the reactive power.

2.2. MVAC

In functioning aspects, medium voltage alternative current (MVAC) is very similar to HVAC, but operates at a lower voltage. In fact, in MVAC, the voltage is not stepped up at the sending point, hence the produced power is transmitted at the same voltage level as the infield wind farm voltage level.

Consequently, transmission transformers are not needed and initial costs are reduced. Moreover, the offshore substation can be spared, as there is no need of adapting the voltage level. On the other hand, operating with a lower voltage implies a greater current. As very large ampacities tend to be avoided, numerous three-phase systems are needed to transmit notable amounts of power. In fact, ohmic losses can be potentially much higher than in HVAC, as ohmic losses are dependent on the current squared.

Therefore, MVAC is suitable if those losses can be constrained, i.e. with small wind farms or very short distances to shore. It is suggested that MVAC would be suitable for OWF rated less than 200MW, and less than 20 km far from the grid coupling point [22]. However, even that is questionable: e.g., the Nysted 1 wind farm, rating 165,6 MW and with a transmission length of 10,75 km , employs HVAC at 132 kV for the transmission system, most likely to reduce the transmission losses.

2.3. HVDC VSC

2.3.1. Why DC?

Since transformers made ac systems won the war of currents in early 20th century, ac has been the preferred method for power transmission. Direct current has been mostly relegated for years to other fields, such as electronics and some chemical industrial processes.

However, starting from the 1970's, dc started to be considered an interested method for bulk power transmission. It has been shown in Section 2.1.2 that ac systems present some disadvantages, related to reactive capacitive power and its consequences on power transmission capability, particularly when transmitting larges amount of power through subsea cables.

DC systems, on the other hand, do not present any sort of reactive power. In fact, capacitive and inductive effects are a consequence of the sinusoidal variations of voltage and current, as reactive power is a function of the frequency, as can be seen in (1) and (2). If voltage and current do not oscillate (i.e. the frequency is null), line inductance and line capacitance effects are null in steady state. Therefore, dc systems are only limited by ohmic losses, as inductive and capacitive effects are not present. Consequently, there is no need to compensate the reactive power produced by the cables, lowering the transmission system cost. On the other hand, the absence of reactive power increases system stability, virtually permitting power to be transmitted with a dc connection for very long distances [12].

Moreover, as skin and proximity effect are inherent to ac systems, they do not affect dc systems. Therefore, for two equivalent systems, the ac line resistance is higher than the dc one; hence, active (ohmic) losses in dc lines are lower. In fact, it is equivalent to say that the equivalent cross section between ac and dc is lower in the latter, which decreases cable costs.

Besides that, direct current allows for different ac grids to be linked asynchronously. Therefore, it can help system stability and prevent cascading failures, by stopping faults or overloads from propagating. Changes in load that would cause portions of an ac network to become unsynchronized and to separate, would not similarly affect a dc link, and the power

flow through the dc link can be used to stabilize the ac network [12].

2.3.2. General functioning

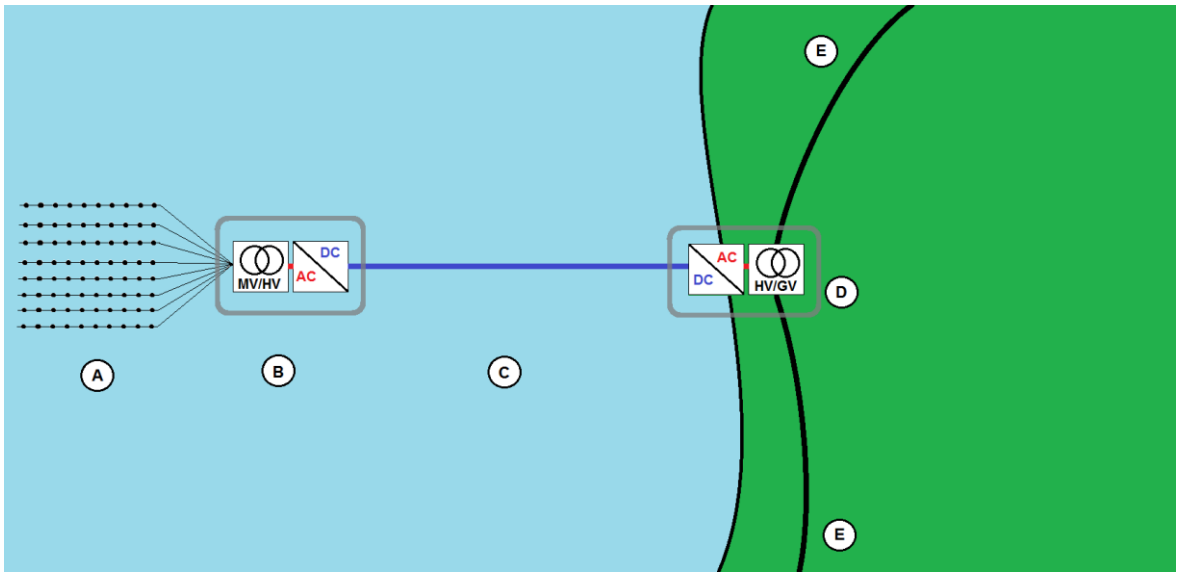

*Figure 13 : General scheme of an HDVC transmission line **A**: Offshore wind farm, infield power is transmitted at medium voltage to the offshore substation (B). **B**: Offshore substation, containing various electrical devices, notably the step-up power transformer and the converter. **C**: HVDC line, which carries power from the offshore substation (B) to the onshore substation (C), at high voltage. **D**: Onshore substation, where the connection with the grid is made and the energy is converted back to ac, contains mainly the other converter station, and may contain a group of transformers, to meet the grid voltage level. Other electrical equipment are also present. **E**: Overhead line from the ac grid.*

The power collected at the inner distribution cables at medium voltage ac is driven to the offshore substation, where the voltage level is stepped up to a value suitable for the converter station. Then, the converter station, allocated in the offshore substation, converts voltages and currents from ac to dc. The power is transferred by dc cables to the onshore substation, where the power is converted inversely from dc to ac. The voltage level is then adapted to the grid voltage by another transformer, and the connection with the grid is produced. Note than for large power transmission, various converters and transformers may be necessary at the same spot.

2.3.3. Converter station technologies

Converting the power from ac to dc efficiently has been historically an overwhelming challenge. Although ac/dc converters have been used in electronics and other low voltage applications, converting bulk power (higher than hundreds of MW) from ac to dc was not feasible until recent decades. There are currently two dominant technologies in use in these high-power converters: line-commutated converters (LCC) and voltage-source converters

(VSC).

2.3.3.1. Line-commutated converter

Most of HDVC converters in operation are LCC [32]. Modern LCC are based on controllable switching devices, employing thyristor valves to perform the commutation. In a LCC, the dc current does not change its direction; it flows through a large inductance and can be considered almost constant. On the ac side, the converter behaves approximately as a current source, injecting both grid-frequency and harmonic currents into the ac network. For this reason, LCC for HVDC is also known as a current-source converter. Because the direction of current cannot be varied, reversal of the direction of power flow (when required) is achieved by reversing the polarity of dc voltage at both stations [32].

LCCs rely on a strong ac system to function. In fact, an ac voltage is necessary to allow the commutation from one switching device to another. Consequently, LCCs depend upon a synchronous ac grid to ensure the electricity conversion. Moreover, a line-commutated converter in steady-state operation at 1 p.u. (rated) active power will consume 0.6 p.u. of reactive power [33], which has to be compensated with capacitor banks, thus implying a larger substation size. Nevertheless, LCCs have lower losses than their counterpart – VSC converters – does; LCC losses are indeed reported as 0.7% of the converted power [34].

Despite the lower losses, an HVDC LCC substation needs much more space. Compared to a VSC-HVDC station, a complete LCC ones needs double the space [35]. This is mainly due to the need of capacitor banks as mentioned, and filter banks to cope with the harmonics. LCC converters generate harmonics, which are to be filtered [36]; hence implying that there is need to accommodate filters in the substations. According to [33], an LCC substation in the hundred-MW range would need between 1600 and 5000 m2 only for the filter banks.

Even though LCC converters are an interesting option for bulk power transmission, they are not suitable for offshore applications[7]. Taking in consideration that the cost of an offshore platform is highly dependent on its size (the more the needed space, the bigger the offshore structure), installing an LCC converter would translate in a strong increase in the offshore

[7] However, it has been stated that some of the LCC issues for offshore wind (such as the space needed for filter banks) could be resolved with alternative control strategies [65].

substation cost. Additionally, LCC need a strong ac grid to properly commutate the current between the thyristor valves and it is not capable to provide black start capability to the offshore wind farms [9]. Therefore, there is not a single offshore wind farm operating with an LCC converter. Consequently, LCC converters will not be considered as an option in the present work.

2.3.3.2. Voltage-source converter

Alternatively, VSCs overcome most of the LCC challenges regarding offshore transmission, and offer other significant advantages. It is an incipient technology; the first VSC converted being installed onshore in 1997. The use of those converters in offshore transmission is relatively new, as the first VSC converter was installed offshore in 2005. Back then they used two-level topologies, whereas nowadays, VSC employ modular multi-level converter (MMC) concepts.

VSC are based on IGBT transistors, which are fully controllable – they can be turned both on and off – on contrary to the thyristors used in LCC converters. Furthermore, in VSCs the active and the reactive power can be controlled independently, so there is no need for reactive power compensation [37]. Additionally, in VSC converters reversal of the power flow is done by reversal of the current – again on the contrary to LCC converters, where the voltage polarity is inverted – thus making them more suitable for dc grid applications [38]. Moreover, as their ac voltage has a low harmonic content, the need for filters is greatly reduced or even eliminated [39].

Another factor which makes VSC converters more interesting for offshore applications is their black start capability. In case of a blackout, VSC converters can lead the grid restoration (provided its capacitors are charged and can function as a voltage source) as they are not dependent on an ac grid to function, nor require an external power supply. According to [40], VSC converters make restoration of the system more reliable and less complicated, by providing a stable frequency and voltage during the recovery process.

On the other hand, one of the main drawback of VSC converters is their losses. Initially, losses on the first VSC converter were reported as 3% of the converted power for the first designs [41]. Nowadays, modern modular multi-level converters achieve less than 1% losses per converter [42].

In conclusion, MMC VSC converters have been proved to be more suitable for offshore wind power-conversion than LCC converters. Notably their reactive power control and lower need for space makes them the preferred option for offshore HVDC power transmission technology. Table 3 compares the main features of both LCC and VSC technologies.

Regarding the converter configuration, different topologies are possible (e.g. bipolar topology, or homopolar topology) with various configurations of converters and cabling systems [12]. Regarding the converters, to diminish the transmission system costs, this thesis will consider a configuration with only one single converter per converter station, i.e. one converter offshore and one converter onshore.

Table 3 Comparison between LCC and VSC converter technologies

	LCC-HVDC	*VSC-HVDC*
Maximum rated values per converter	2000MW ± 800 kV (onshore)	1800MW ± 500 kV [43]
Transistors	Partially controllable, thyristors	Fully controllable, IGBT
Losses	0.7%	1%
Volume	V_0	$0.5 \cdot V_0$
Black start capability	No	Yes
Power reversal	Invert voltage polarity	Invert current flow
Control of reactive power	Uncontrolled. Approximatively rated as 60% of the active transferred power	Control of the reactive power produced

2.3.4. HVDC VSC cables

Compared to ac subsea cable, dc cables can carry a notably higher active power. As there is no capacitive or inductive effects (see Sections 2.1.2 and 2.3.1), there is no reactive power produced in steady state. Moreover, as stated in Section 2.3.1, since proximity and skin effect are inexistent in dc conductors, the dc line resistance is lower for a given cross section, compared to ac cables, thus giving lower cable losses.

Furthermore, as dc systems are not affected by reactive power (refer to Section 2.3.1), or the dielectric as losses calculated in (4), the choosing of the voltage level is not theoretically constrained; being only limited by the cable technology at and 500kV [43]. Therefore, with lesser losses and higher voltage levels, each dc cable is able to transmit higher power than ac

cables [13] [9].

When a monopolar topology is desired (i.e. single converter on each side), either one single cable or two cables can be used [12]. The use of a single cable implies that the return path is made by means of a ground return. Alternatively, two cables at opposite polarity can be employed [9]. This latter case, which consists in single converters with two cables at opposite polarity, is called a symmetric monopole. When employing two cables, both are laid in the same trench and, consequently, the two magnetic fields at opposite polarity will nearly cancel each other. In contrast, single-cable dc systems are not allowed in some countries due to the high electromagnetic field that is generated [9]. Therefore, symmetric systems are preferred and will be considered for the technical-economic analysis performed in this thesis.

As for any power cable, copper is preferred in general as the conductor material for its excellent conductivity compared to other materials, as exposed in Section 2.1.3. Nevertheless, aluminium cables may be employed, particularly in onshore applications [9]. Regarding the cable insulation, extruded XLPE is the preferred option [44].

2.3.5. Further implications of HVDC: MTDC networks

Multi-Terminal dc networks (MTDC) has been the subject of intense research lately [45] [46] [47]. The inherent capabilities of HVDC for bulk power transmission imply that in the long term, with a constant growing of energy demand, large dc grids will be necessary [48]. VSC-HVDC systems are much more suitable for multi-terminal dc networks than LCC-HVDC [45]. Therefore, employing HVDC-VSC power transmission systems for offshore wind farms, besides any economic advantage or loss reduction, would prepare offshore wind for future dc grid integration.

2.4. LFAC

Low-frequency alternating current (LFAC) is supposed to offer the possibility to combine the best of HVDC and HVAC, while eliminating most of their technical disadvantages [49]. Hitherto, LFAC transmission systems have not been applied to OWF, but they are the subject of intense research [15] [17] [18] and [49] to [50]. This Section highlights the main benefits and drawbacks of LFAC.

2.4.1. LFAC principle

The main drawback of HVAC cables, their reduction of the power transmission capability as the cable length grows, is partially mitigated with LFAC. While HVDC eliminates any reactive current, LFAC maintains them, but at a lesser degree than HVAC. By employing a lower electric frequency, the reactive power is proportionally reduced. This fact drives two consequences: firstly, less costs associated with the reactive power compensation. Secondly, any reduction of the transmittable active power happens at higher distances.

Figure 14 shows the power transmission capability of three LFAC and HVAC cables, with LFAC employing 50/3 Hz as the electric frequency. While the 150 kV cable has its power transmission capability reduced to a 60% at approximatively 200 km, this occurs at 600 km for the low frequency cables. Consequently, the cables must not be overrated as much as the HVAC cables to guarantee a certain power transmission capability.

It should also be noted that with lower capacitive reactive power, higher voltages could be applied to LFAC cables without being concerned with the reduction of the transmittable active power.

Additionally, as the ac resistance increase due to the proximity and skin effects is proportional to the frequency, the effective resistance of LFAC cables is lower than their HVAC equivalent, thus presenting also lower ohmic losses. Furthermore, as the reactive power is lower in LFAC cables, its dielectric losses would also be lower.

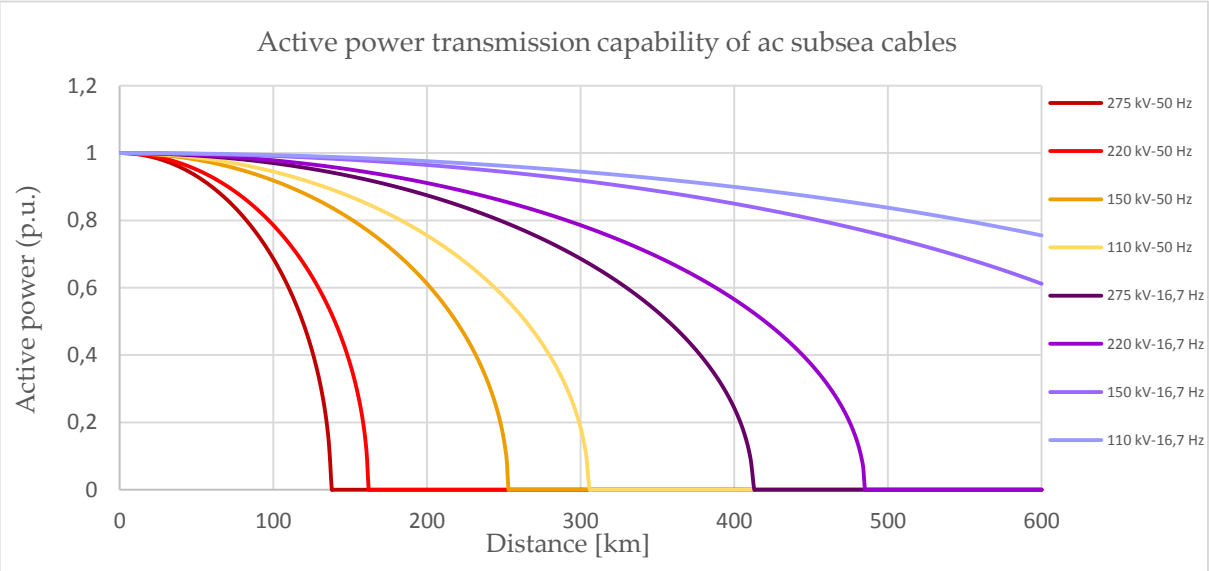

Figure 14 Power transmission capability of HVAC and LFAC cables [51]

To lower the harmonic content, it has been stated that the frequency should be set lower than a third of the standard frequency [17]. In fact, all the consulted articles consider 50/3 Hz (20 Hz on 60 Hz systems) as the standard LFAC frequency [50] [52] [17] [18]. Therefore, this present work is also considering 50/3 (and 20 Hz) for LFAC.

For obtaining a transmission system with a lower frequency, two different general configurations are available. The first configuration considers that the power is generated at standard frequency (50 or 60 Hz), and then converted to low frequency at the offshore substation, and back to the standard frequency at the onshore substation.

On the other hand, the second configuration proposes that the power is already generated by the turbines at low frequency. The latter implies that both the infield power collection and the power transmission is made at 50/3 Hz, thus eliminating the need of a frequency conversion in the offshore substation [50]. However, producing the power at low frequency would mean a redesign of the turbine transformers, although that has been considered feasible [50].

For this work, the latter option will be considered. It is thought that the first configuration (ac-ac conversion at the onshore and offshore substation) will most probably result more expensive than performing a single conversion operation. Furthermore, two conversion operations imply two converter devices, but it also implies that the offshore substation must accommodate those converters, which translates into higher costs. Regarding the transmission

costs, generating the power at low frequency should be more cost-effective[8].

Figure 15 illustrates the considered LFAC configuration, with both the transmission and the power generation at low frequency.

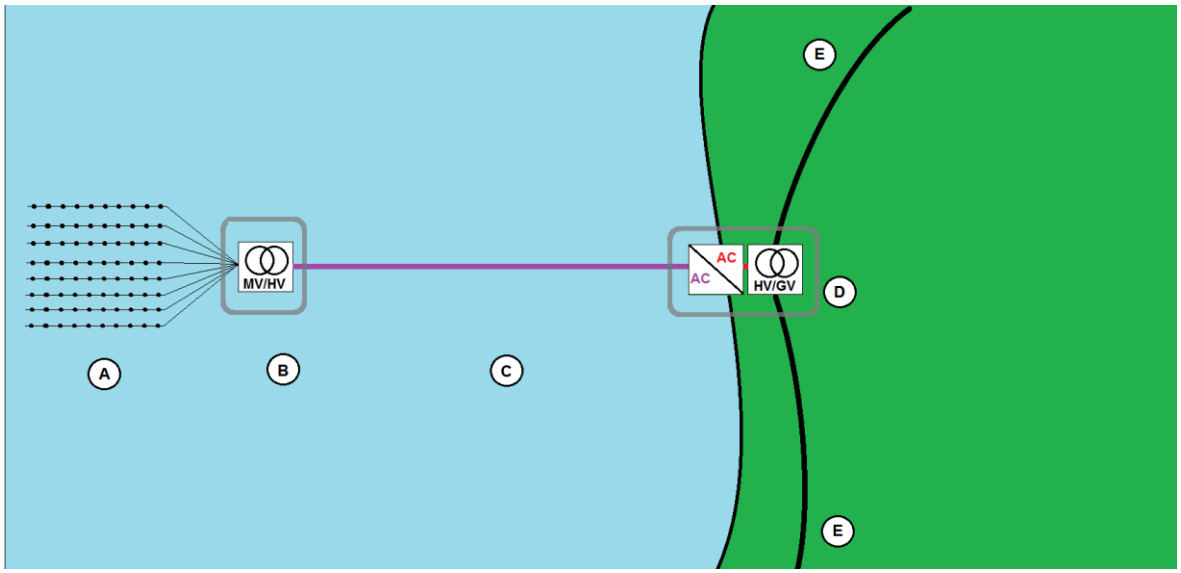

*Figure 15 General scheme of the considered LFAC transmission line **A**: OWF, infield power is transmitted at medium voltage and low frequency to the offshore substation (B). **B**: Offshore substation, containing various electrical devices, notably the step-up low-frequency power transformer. **C**: LFAC line, which carries power from the offshore substation (B) to the onshore substation (C), at high voltage and low frequency. **D**: Onshore substation, where the connection with the grid is made and the energy is converted to standard grid frequency. Contains mainly the ac/ac converter station, and may contain a group of transformers, to meet the grid voltage level. Other electrical equipment is also present. **E**: Overhead line from the AC grid.*

As for any transmission system, the voltage is stepped up for transmission purposes. This is done at the offshore substation by means of low-frequency-adapted transformers. The power is then transmitted at high voltage up to the onshore substation, where the voltage is stepped down and the frequency is changed to the standard grid frequency. This latter conversion operation can be done in numerous ways, and the different options will be analysed in Section 3.6.4.

The following sections analyse how the conversion operation can be made, and which are the differences between a low-frequency transformer and a standard step-up transformer. Additionally, the literacy indicates that ac XLPE cables can also be employed for LFAC [49].

[8] Nevertheless, the cost of redesigning the turbine transformers may surpass the benefits of a single converting operation. However, this is out of the scope of this present work, which focuses on the power transmission.

Regarding LFAC reactive compensation devices, no dedicated studies have been found, although it is suggested that no reactive compensation may be necessary below 25 Hz [53]. On the other hand, [54] states that the physical size of the reactive power compensation systems are independent of the frequency, which means the same cost for each MVAr of reactive compensation.

2.4.2. Low frequency Transformers

The role of those transformers is the of their HVAC counterpart: they must step up the voltage level from the collection system medium voltage to the transmission high voltage at the offshore substation, and change it to the grid voltage level at the onshore substation. However, as they operate at a lower frequency, they present some differences compared to standard step-up transformers.

Their main difference is size related. For the same rated power, a lower frequency requires a larger transformer size and weight [50], which necessarily means a bigger offshore structure and consequently higher costs for both the transformers and the offshore structure [54] [55]. Table 4 shows a comparison between a 200 MVA three-phase transformer at standard and low frequency [18]. Size and weight of the 16,67 Hz transformer is around the triple of the 50 Hz transformer, and costs behave similarly, although they will be studied in more detailed in Section 3.6.2.

Table 4 Data for 200 MVA three-phase 16,67 and 50 Hz transformers

frequency	*Weight*	*Volume*	*Approximate cost*
50 Hz	125 t	52,52 m^3	5 M€
16,67 Hz	374,26 t	157,24 m^3	15 M€

On the other hand, the transformer core losses, which are frequency-dependent, are decreased compared to standard frequency transformers. The core losses can be reduced to a half of their value at 50 Hz, and consequently the total transformer losses (windings and core losses) are also decreased, e.g. by 10% [18].

2.4.3. LFAC power converter

There are different proposed devices to convert the 16,67 Hz transmitted power into standard frequency. Predominantly cycloconverters and back-to-back VSC (B2B-VSC) are suggested to perform the conversion. Note that this matter remains the most discussed issue about LFAC as researchers do not agree which method is the most suitable for converting the frequency [18] [50] [52]. This section analyses both options, drawing a comparison of their advantages and disadvantages.

Cycloconverters (CCV) are thyristor-based ac-ac converters, which rely on the ac grid to effect the commutation. However, they generate a high harmonic content, thus large filtering is required and the power quality is compromised (see Figure 16).

Moreover, cycloconverters stations require a large footprint to accommodate the filters, although that is not a great downside as space is not as critical in the onshore substation as in the offshore substation. Additionally, CCVs do not have an independent control of the reactive power, needing reactive compensation devices as they always generate inductive reactive power [50]. It should be also considered that CCVs are, just as the HVDC LCC converters, vulnerable to grid faults, as they require an ac grid to perform the commutation [17]. Nevertheless, the advantages of employing a CCV are its reduced cost and losses [18], compared to a B2B-VSC, as well as increased reliability since CCV is a mature technology.

On the other hand, a B2B-VSC scheme imply an independent control of active and reactive power, black start capability, as well as no filtering, but comes with higher losses and costs

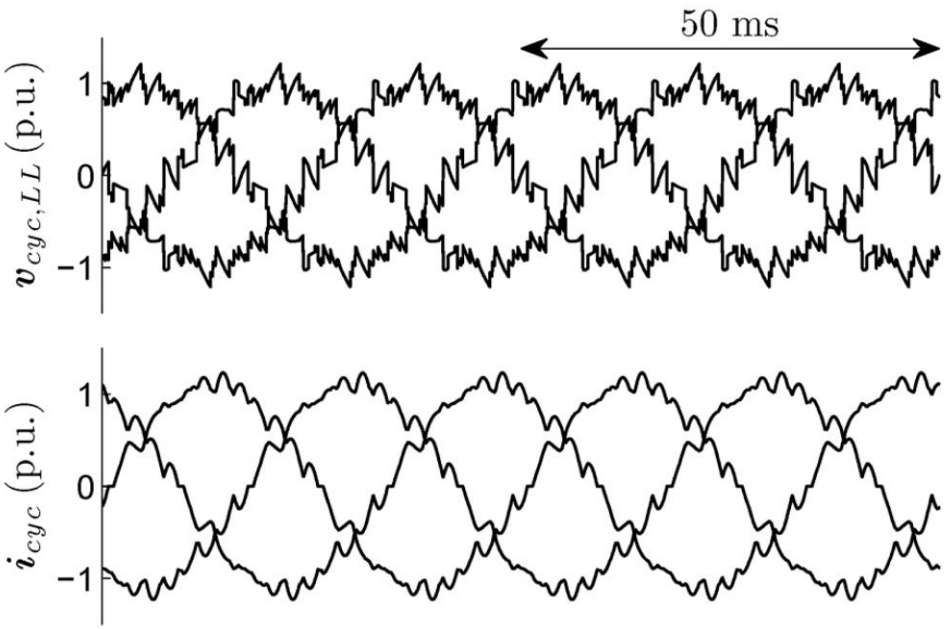

Figure 16 Voltage and current waveforms at the grid side of a CCV [46].

(Section 2.3.3.2 has covered the VSC in detail). Table 5 summarizes the main differences between CCVs and BtB-VSC as power converters.

Table 5 Comparison between CCV and BtB-VSC as power converters for LFAC

	CCV	***B2B-VSC***
Transistors	Partially controllable, thyristors	Fully controllable, IGBT
Substation footprint	Large space needed for filters	Low space needed
Black start capability	No, poor fault ride-through capability	Yes
Cost	lower	higher
Losses	lower	higher
Control of reactive power	Uncontrolled. Approximatively rated as 60% of the active transferred power	Control of the reactive power produced

It is unclear in the related literature which of the two options should be considered. Contrarily

to LCC-HVDC transmission systems, the CCV would be installed only onshore, hence, in principle the impact of the larger space is not as critical. Although the CCV has lower costs and losses, it does not have black start capability and provided a lower power quality. Due to the latter reason, some researchers do not even consider CCV as a feasible option [49], although others state that their lower cost would make LFAC competitive. As there is no clear preferred option in literature, both options will be considered for this work. Nevertheless, if voltage-source converters continue to benefit from reduced losses and costs reductions, over the next years they will probably be the preferred option.

3. Cost modelling

The main purpose of this work is to provide a tool, based on a technical-economic analysis, which determines the electrical transmission costs from the OWF collection point to the grid coupling point, and calculates the break-even distance between HVDC and HVAC transmission technologies. This chapter gives firstly a general description on how the model functions. Secondly, for HVAC[9], HVDC and LFAC, it explains how the cost models have been achieved, and the technical considerations employed. Note that losses and costs are treated separately for each component (i.e. the cable losses are treated in a different Chapter than the cable costs), as their calculation takes a different approach. All the cost functions are summarized in a spreadsheet, to make the cost and loss calculations of the entire power transmission system.

3.1. Tool description

The tool works the following way: first, the user introduces the main data regarding the offshore wind farm (see Section 3.2). Second, to calculate the cost for each transmission technology, the user introduces additional inputs for each. The tool then determines the costs (including losses) for each technology, returning them as a function of the transmission distance. Note that the main aim of these models is to calculate the break-even point between different technologies, and to estimate the capital costs of the power transmission from the OWF collecting point to the grid. Other associated costs, such as grid reinforcements or insurance costs, are out of the scope of this work.

An approach to minimize the number of inputs has been utilized, whenever it has been possible. In fact, the user is not expected to know deeply about specific variables, and the intention is to perform the calculations with the minimum number of variables introduced by the user. Moreover, due to the reduced number of data available to establish the cost functions, linear functions are mostly employed. Detailed statistical data of every cost function can be found in the Appendix 3.

To start, the user has to introduce the main inputs, common to all technologies (see Section

[9] MVAC costs are treated in a sub-section of HVAC (see Sub-section 3.4.5).

3.2), which describe the OWF. Then, for each considered technology (HVAC, MVAC, HVDC and LFAC), the user must decide on some additional inputs (e.g. the voltage level) to perform the calculations that determine the break-even point. For HVAC, LFAC, and HVDC, the user is provided with values which indicate the suitability of the introduced parameters regarding the transmission capability (see Section 3.9)

For every technology, costs are divided in two categories: the costs that are independent of the line length, the base costs; and the costs that are proportional to the line length, the distance-dependent costs. Additionally, the models are implemented in a spreadsheet, thus making modifications in the inputs an accessible task.

3.2. OWF variables

Regarding the cost calculations, the main inputs are related with the OWF parameters. To achieve the model, the variables shown in Table 6 are taken as principal and commune to all models.

Table 6 Model basic variables

Base variables	*Description*	*Units*
P_{OWF}	Nominal active power produced by all the turbines, at full load i.e. the offshore wind park rated power	MW
c_{OWF}	Capacity factor	(p.u.)
C_{energy}	Energy selling price (feed-in tariff)	€/MWh
t_{OWF}	OWF expected lifespan	years
i	Discount rate	%

Although any value can be chosen for those variables, some recommendations are made. This technical-economic analysis is aimed for large OWFs, thus P_{OWF} should be in the hundreds of MW range. The capacity factor, which is indeed the utilization rate, is reported in the 40-50% range (0.4 to 0.5 p.u.), according to [56]. Therefore, it is set by default at 0,4. The energy selling price considered is by default as 50 €/MWh, but higher prices can be encountered if subsides

are taken into account[10] (e.g. the feed-in price for an OWF in Germany is at 190€/MWh [57]). Finally, regarding the expected lifespan, industry predictions are in the 20-25 years range and, consequently, t_{OWF} is taken as 20 years by default.

3.3. Loss cost calculation methodology

The losses cost is calculated as the cost of non-sold energy. Firstly, for each electrical device, the power losses are estimated. Each technology contains its own section detailing the power loss calculation. Secondly, the yearly cost of these losses is calculated with the energy selling price as given in (5). Thirdly, the net present value of those losses throughout the OWF operational time is calculated for a given discount rate, show in (6).

$$Cost_{yearly_j} = P_{losses_j} \cdot 8765{,}81 \cdot C_{energy} \tag{5}$$

where,

P_{losses_j}: generated losses of the device "j" [MW].

The average number of hours in a year is taken as 8765,81.

$$NPV_{losses_j} = Cost_{yearly_j} \cdot \frac{1 - \left(\frac{1}{1+i}\right)^{t_{OWF}+1}}{1 - \left(\frac{1}{1+i}\right)} \tag{6}$$

With NPV_{losses_j} in € and t_{OWF} in years.

The loss factor cost is therefore, for convenience, defined in €/W by (7). This factor will be used for loss cost calculation throughout the entire thesis.

$$F_{loss} = 8765{,}81 \cdot C_{energy} \cdot 10^{-6} \cdot \frac{1 - \left(\frac{1}{1+i}\right)^{t_{OWF}+1}}{1 - \left(\frac{1}{1+i}\right)} \tag{7}$$

[10] Energy selling price for OWF often benefits from subsidies, i.e. the energy selling price is guaranteed at a certain level. For example, a recent round (2015) in the UK guarantees selling price in the range of 80-120 £/MWh for newly commissioned OWF (approx. 111-166 €/MWh) [64].

3.4. HVAC cost

3.4.1. HVAC common variables

To effect the calculations, the user must decide the following variables:

Table 7 HVAC main inputs

Variables	*Description*	*Units*
$U_{RMS,HVAC}$	Phase to phase voltage level of the transmission cables	V
S_{HVAC}	Cable cross section	mm²
f	Electric line frequency	Hz
$n_{cables,HVAC}$	Number of three-core cables	-

The electric line frequency is chosen by default as 50 Hz, but it is modifiable as it could be interesting to introduce other values, such as 60 Hz, which is the frequency in North America and in parts of South America and Asia. The voltage level should be chosen between 110 kV and 275 kV, as the cost equations have been modelled in this range only.

In fact, no data has been found for OWF regarding subsea HVAC transmission systems operating at higher voltage levels, most probably due to increased reduction of active power transmission capability (see Section 2.1.2). The standardized voltage levels for subsea transmission are 110 kV, 132 kV, 150 kV, 220 kV and 275 kV. For the cable cross section, the user must choose from a list of standardized values.

Once the conductor cross-section has been chosen, the three-core cable ampacity (i.e. the maximum intensity that each cable core can withstand) is deduced from values given by suppliers [28], reported in Table 8.

In case the user wishes to choose a non-standardized cross-section, the ampacity $I_{max,HVAC}$ is estimated from the values given by suppliers. Finally, the number of three-core cables should be chosen.

Table 8 Ampacity of three-core cables

Cross section [mm2]	*Ampacity [A/core]*
300	530
400	590
500	655
630	715
800	775
1000	825

With those values introduced, the mean active current per cable core and the cable power rating is deduced as:

$$I_{mean,HVAC} = \frac{c_{OWF} \cdot P_{OWF}}{n_{cables,HVAC} \cdot \sqrt{3} \cdot U_{RMS}}; \qquad S_{cable,HVAC} = \sqrt{3} \cdot U_{RMS} \cdot I_{max,HVAC} \tag{8}$$

where,

$I_{m,HVAC}$: mean current in each cable core [A];

P_{OWF}: OWF rated power [W];

U_{RMS}: phase-to-phase voltage level [V];

$I_{m,HVAC}$: mean value of the active electric current taking in account the capacity factor c_{OWF}, i.e. the active current that each cable must carry in normal operation [A];

$S_{cable,HVAC}$: rated power of each cable, i.e. the maximum power the each cable can withstand in steady-state [W].

The inputs choice determines the transmission system performance, and should be chosen wisely. Note that the value of the mean active current is independent of the cable rated ampacity, as the first one is calculated with the introduced parameters, whereas the second one is given by suppliers. That could lead to unrealistic situations, where the cable rated ampacity is lower than the mean current value. The same problem will appear with LFAC and HVDC models. To prevent those situations and give indications to choose an adequate cable, a guide is available within the program that should help the user, and prevent unrealistic situations. How this guide has been made is treated in Section 3.9.

3.4.2. Base cost

The costs of transformers, switchgears, and the costs of the offshore structure are treated in this section.

3.4.2.1. Transformers

To model the transformer cost, data has been gathered from [58] and [59]. These data has been plotted to establish a relationship between costs and the rated transformer power, which is displayed in Figure 17.

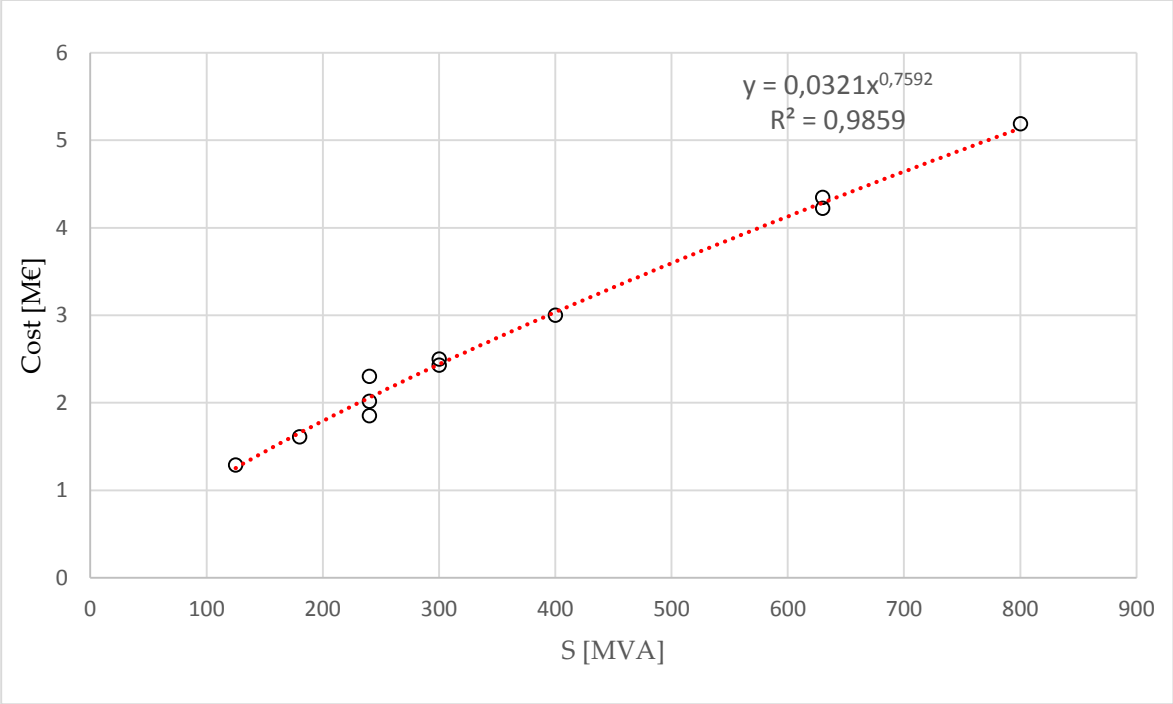

Figure 17 Transformer cost as a function of its rated power

It is observed that there is a strong correlation ($R^2 = 0.986$) between the cost and the rated power of a transformer. The fitted curve obtained from the data in Figure 17 is given by:

$$C_{TR,HVAC} = 0{,}0418 \cdot {S_{TR,HVAC}}^{0{,}7592} \quad (9)$$

where,

$C_{TR,HVAC}$: cost of a single transformer [M€];

$S_{TR,HVAC}$: rated power of the transformer [MW].

In this particular case, another equation modelling transformers costs has been found in [60], thus making it possible to contrast and verify (9). Figure 18 shows that the two curves fit well and since there is no appreciable difference, (9) can be considered validated.

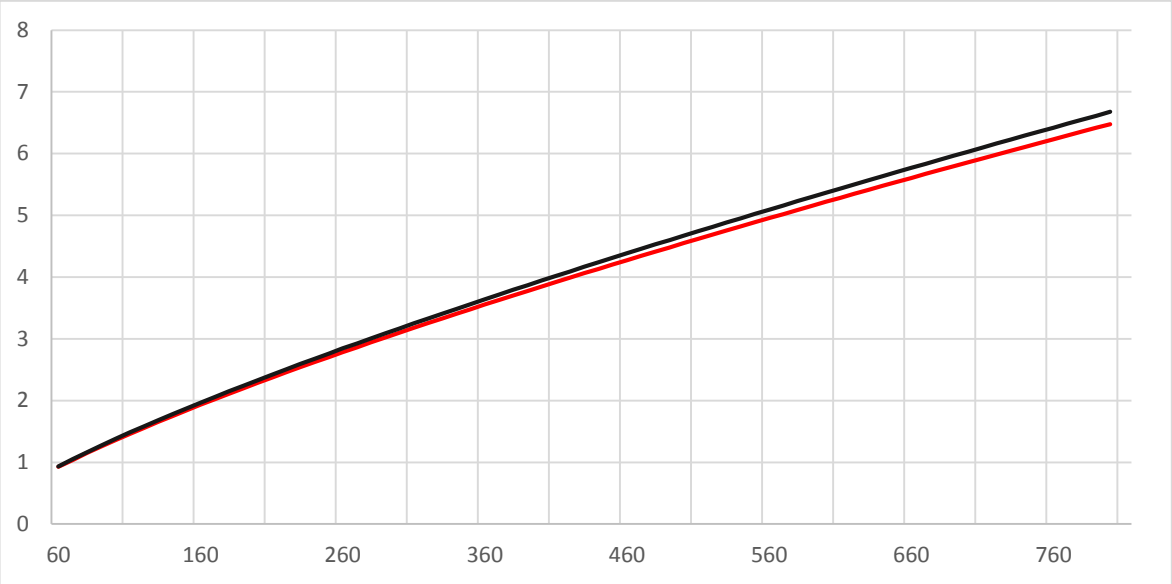

Figure 18 Transformer cost as determined by own model (red) and referred model (black)

Concerning the number of transformers employed, there will be two separate groups needed, one for each substation (cf. Section 2.1.4). Each group must be rated to the OWF full power. In [61], different transformer offshore topologies are studied, and it is concluded that the optimum topology depends on economic considerations, such as the discount rate. On the most unfavourable scenario, the optimum topology is determined as two transformers per substation, each rated at 60% of the OWF maximum power [61]. This is the configuration adopted in this work as it balances reliability and cost: in case of a transformer fault, there is still one unit with 60% capacity. Additionally, overrating transformers decreases their losses, as their load index is decreased (transformer losses are detailed in Section 3.4.4.7).

Therefore, there will be four transformers in total (two per substation), each rated at $0{,}6 \cdot P_{OWF}$. However, it has not been found information and costs for transformers larger than 800 MVA; thus it is not advisable to extend the cost analysis for OWFs bigger than 1600 MW. Therefore, to correctly model OWFs with installed capacities higher than 1600 MW, more than two transformers per substation may be necessary.

3.4.2.2. HV Switchgears

Regarding HV switchgears, interesting data is available in [58], and has been plotted in Figure 19.

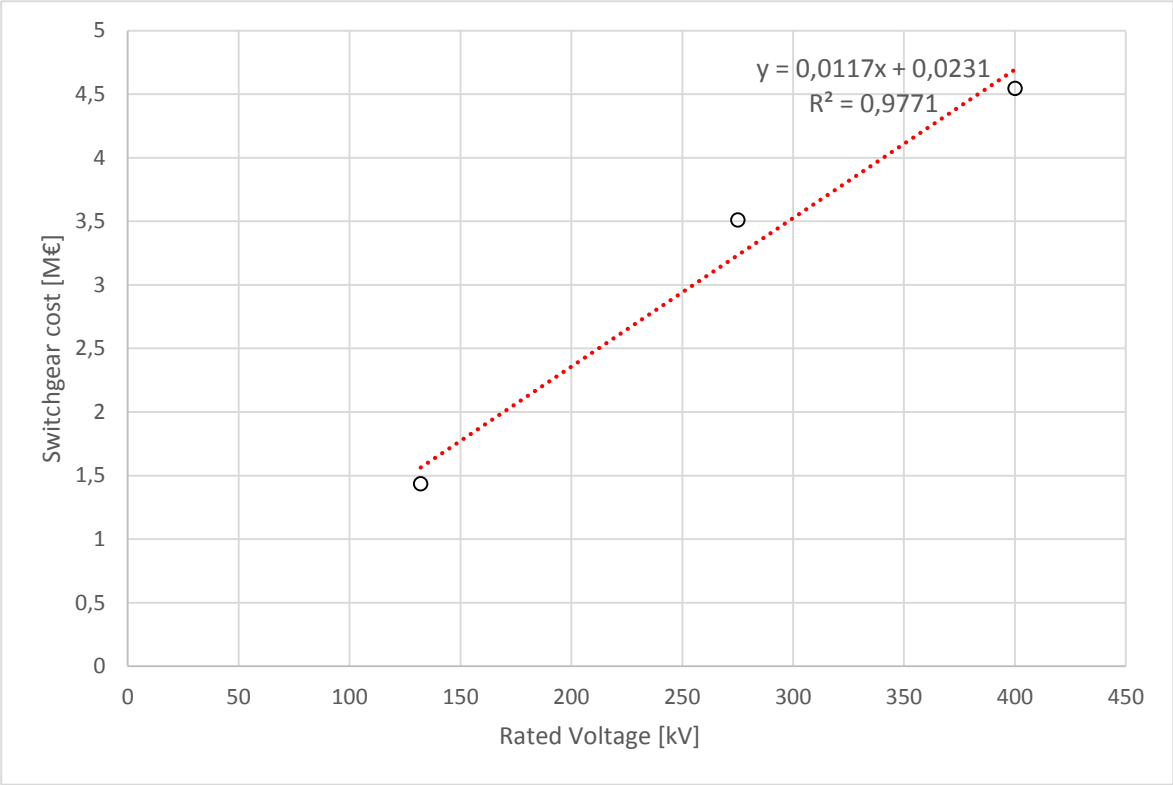

Figure 19 Cost of HV switchgear. Data source: [58]

Based on the presented data, the cost of a HV GIS can be obtained via a linear model, which yields:

$$C_{GIS} = 0{,}0117 \cdot U_{RMS} + 0{,}0231 \tag{10}$$

Contrary to most of the cost models, the GIS costs were found to be voltage-dependent and not power-dependent.

As a switchgear purpose is fundamentally protection and it is needed between critical components. As the wind farm infield collection system and the grid integration point are out of the scope of this work, the switchgear is needed at the sending and arriving point of the offshore and onshore substation. Consequently, the number of necessary HV switchgears will

be two per cable, one allocated at the offshore substation and another at the onshore substation.

3.4.2.3. Offshore substation structure

The cost of an offshore structure depends on its size. According to [60] and [62], the cost of a sophisticated offshore substation structure, i.e. with enough space for the electrical necessary equipment, living space for workers and additional services such as an heliport is modelled by the following equation:

$$C_{SS,HVAC} = 2{,}534 + 0{,}0887 \cdot P_{OWF} \quad (11)$$

where,

$C_{SS,HVAC}$: cost of the offshore substation foundation [M€];

P_{OWF}: OWF rated power [MW].

It would be interesting to relate cost of the offshore platform directly with its volume. Some volume and weight data is available in [58] for a 300-MW and a 500-MW HVAC platform. Estimating the offshore platform cost with (11), the cost per cubic meter and per ton can be calculated (see Table 9). It can be observed that as the platform cost increases, the marginal cost for its size decreases, whereas the cost per ton increases. Nevertheless, those behaviours cannot be extrapolated with only two data points.

Table 9 HVAC platform cost data

Rated Power [MW]	*Volume[m³]*	*Weight [t]*	*Cost[M€]*	*Cost [€/m³]*	*Cost [€/t]*
300	9001	2000	29,1	3238	14572
500	21600	2500	46,9	2171	18754

3.4.3. Distance dependent costs

3.4.3.1. Cable cost

Cable cost modelling was found to be very challenging, as there is few data available and the models found in literature where mostly for MV cables. The study performed in [58] reports cost of three-core HVAC cable, shown in Table 10. In [13], cost of a 250-MVA three-core cable is reported as being 0.6 M€/km, whereas [63] reports a mean cost of 0.75 M€/km for a three-

core cable.

Table 10 HVAC three-core cable cost. Data from [58]

V(kV)	*S(MVA)*	*Cost(M€/km)*
132	200	0.518 - 0.805
220	300	0.575 - 0.863
245	400	0.748 - 1.150

These data would be enough to estimate values for specific cases. However, to incorporate the cable costs to the technical-economic analysis, a modelling function should be achieved. From [62], an interesting model has been found, which is also employed in [60]. Lundberg states that the cost of three core cables can be modelled through an exponential equation with an offset constant, as in (12):

$$C_{cables,HVAC} = A + B \cdot e^{C \cdot S_{cable,HVAC} / 10^2} \quad (12)$$

where,

A, B and C: constants that depend on the voltage level;

$C_{cables,HVAC}$: cost of the HVAC three-core cables [M€/km];

$S_{cable,HVAC}$: rated power of a single cable [MVA].

The following table is reported regarding values of the constants in (12) [64][11].

Table 11 Values of constants for modelling HVAC cable costs. Data from [62]

V [kV]	*A [M€]*	*B [M€]*	*C [MVA^{-1}]*
22	0,031	0,063	6,15
33	0,044	0,064	4,10
45	0,056	0,066	3,00
66	0,074	0,068	2,05

[11] Those costs where reported in Swedish Krona, converted to euro using the 2003 exchange rate, and updated with the mean Eurozone inflation rate of 2%/year.

132	0,213	0,023	1,66
220	0,344	0,012	1,16

The approach taken to use (12) to calculate the HVAC cable costs is the following one: the three constants (A, B and C) have to be modelled for every voltage level. With this latter operation, (13), (14) and (15) were obtained[12]:

$$A_{HVAC} = 0{,}001631 \cdot U_{RMS} - 0{,}0142 \quad (13)$$

$$B_{HVAC} = 0{,}9805 \cdot (U_{RMS})^{-0{,}765} \quad (14)$$

$$C_{HVAC} = 45{,}713 \cdot (U_{RMS})^{-0{,}693} \quad (15)$$

Combining (13), (14) and (15) with (12), the cost of HVAC three-core cables can be obtained. Note that based on the data displayed in Table 11, the model cannot be deemed reliable for U_{RMS} values beyond 220 kV.

3.4.3.2. Cable laying cost

The cable laying costs data found were varied. In fact, cable laying costs depends on many factors, such as weather conditions – that can delay the laying process – and vessel availability[13].

The study done by Lancheros assumes a cost of 0,3 M€/km for each three-core cable [13], whereas Van Eeckhout considers 0,170 M€/km per three-core cable [63]. Additionally, additiofnal data is obtained from [9] and reported in Table 12.

Table 12 Data for HVAC cable laying cost. Source: [9]

Laying cost [M€/km]	*Cross-section [mm²]*	*Voltage level [kV]*
0,254	500	132
0,268	800	132

[12] With the best-fitting curves

[13] A complete review of cable installation challenges can be found in [63] , which covers vessel availability among various matters.

0,285	800	132
0,238	800	150
0,282	500	220
0,310	800	220

The costs in Table 12 are not suitable for a cost function, as they do not show a clear pattern. The reason is that there are factors which strongly affect the costs (i.e. vessel availability and weather conditions), from which no data has been found. Instead of achieving a poor model (linear multiple regression explains less than 50% of the cost variance), a more cautious assumption has been made. For this work, a constant cost of 0,273 M€/km will be assumed for each cable, which is the mean cost of the available data.

3.4.4. HVAC Losses and reactive power

To calculate the cable losses, the cable parameters (i.e. its resistance, capacitance and inductance) must be determined. Moreover, to model the losses of the cables as a function of the transmission line length, the parameters must be calculated themselves as a function of the transmission line length.

3.4.4.1. Cable Resistance

The ac cable resistance is calculated following the standards from the IEC 60287, provided in [65] and [66]. In fact, the equivalent ac resistance of a cable is the dc resistance increased by factor dependent on proximity and skin effect, as it can be seen in (16):

$$R_{ac} = R_{dc} \cdot (1 + y_s + y_p) \tag{16}$$

where,

R_{ac}: ac resistance of the conductor [Ω/km];

R_{dc}: dc resistance of the conductor [Ω/km];

y_s and y_p: unitless factors representing respectively the skin and the proximity effects.

The dc resistance of the conductors is calculated as follows:

$$R_{dc} = \frac{1{,}02 \cdot 10^9 \cdot \rho_{20}}{S} \cdot (1 + \alpha_{20} \cdot (\theta - 20)) \tag{17}$$

where,

ρ_{20}: thermal resistivity of the conductor material at 20ºC [Ω·m];

α_{20}: thermal coefficient of the conductor material at 20ºC [K^{-1}];

S: cross-sectional area of the conductor material [mm^2];

θ: conductor material operating temperature [ºC].

As the conductor material is copper (refer to Section 2.1.3 for the conductor material decision), the thermal values employed are $1{,}7241 \cdot 10^{-8}$ and $3{,}93 \cdot 10^{-3}$ for, respectively, the thermal resistivity and the thermal coefficient. Regarding the conductor temperature, it is set at 90ºC, which is the maximal operational temperature for XLPE cables [26].

The determination of the skin effect factor is made through the following equation:

$$y_s = \frac{\left(8 \cdot \pi \cdot f \cdot 10^{-7} \cdot k_s / R_{dc}\right)^2}{192 + \left(8 \cdot \pi \cdot f \cdot 10^{-7} \cdot k_s / R_{dc}\right)^2} \tag{18}$$

where f is the electric frequency [Hz].

The factor k_s is dependent on the conductor geometry, and equal to 1 when conductors are round and stranded [66], which is the case.

Additionally, the proximity effect, for three-core cables, is calculated the following (19) and (20):

$$y_p = \frac{{x_p}^4}{192 + 0{,}8 \cdot {x_p}^4} \cdot \left(\frac{d_c}{s_c}\right) \cdot \left[0{,}312 \cdot \left(\frac{d_c}{s_c}\right)^2 + \frac{1{,}18}{\frac{{x_p}^4}{192 + 0{,}8 \cdot {x_p}^4} + 0{,}27}\right] \tag{19}$$

$${x_p}^4 = \left(8 \cdot \pi \cdot f \cdot 10^{-7} \cdot k_s / R_{dc}\right)^2 \tag{20}$$

where,

d_c: conductor diameter [mm];

s_c: Spacing between conductor axes [mm];

The factor k_p is equal to 1 for round and stranded conductors *[66]*.

The conductor diameter can be calculated easily from the conductor cross section, but the spacing between conductors cannot be easily estimated[14]. As it is not desired to treat s_c as a new input, it has been necessary to estimate spacing between conductors as a function of the known variables. A relationship that explained more than 95% of the variability was achieved by linear regression, treating s_c as a function of the voltage level and the conductor diameter:

$$s_c = 20{,}491 + 0{,}15155 \cdot U_{RMS} + 0{,}78141 \cdot d_c \quad (21)$$

where U_{RMS} is the phase to phase voltage level [kV].

Combining (21) with (19) and (20), the ac resistance of the subsea cable can be calculated without the need for new inputs.

3.4.4.2. Cable inductance and cable capacitance

Determining the cable capacitance and inductance has been challenging. The formulae found in literature to calculate cable capacitance or inductance require knowing extensive geometry data from the cable, such as its sheath and insulation thickness or the laying distance between conductors. Most of these geometry data, such as laying distance between conductors, was

[14] Between the conductors inside a three-core cable the insulation is to be found, whose thickness depends on the voltage level. Consequently, the distance between conductor axes is not simply two times its radius.

found to be inaccessible or case dependent.

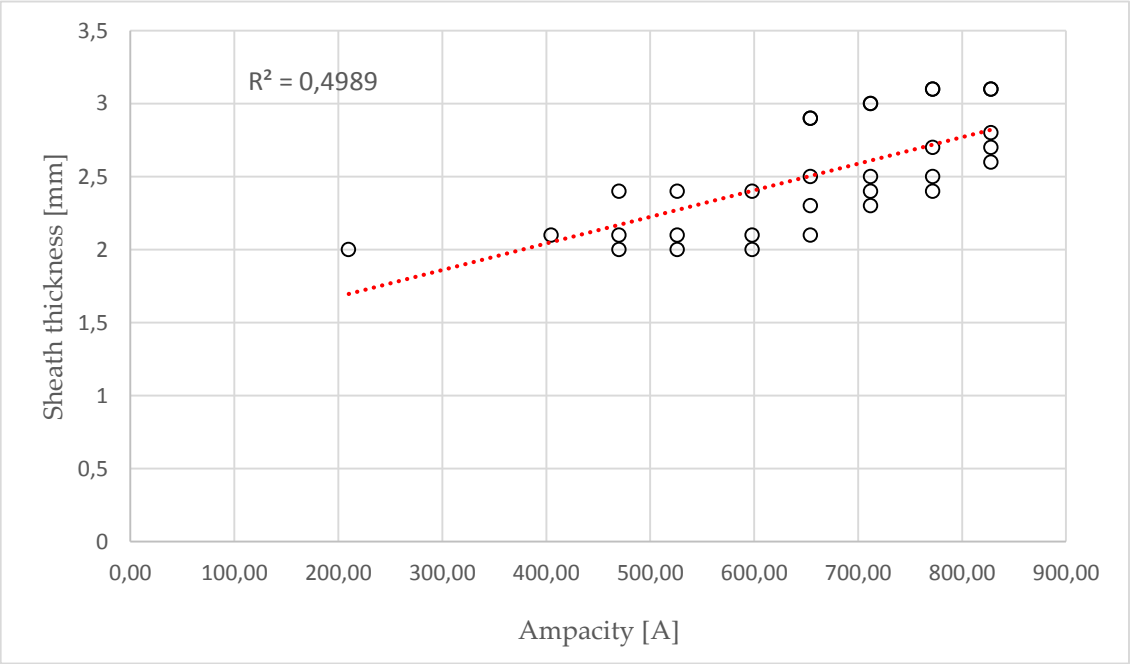

Figure 20 Sheath thickness as a function of the cable ampacity.

However, an attempt was made to model those geometry data as a function of some already considered variables, such as the cross section, voltage level and cable ampacities. Minor correlations were found, and inaccuracies were revealed when contrasting the established correlations with additional data. Figure 20 shows an example of those poor correlations, with data obtained from [67]. A modelling function that explains 49,9% of the variability has been deemed unfit for this work.

In fact, accurate determination or estimation of such geometry data would require an extensive analysis of XLPE power cables geometry, and would only be valid in case-specific analyses. Additionally, this technical-economic analysis aims to requiring a minimum number of inputs, and should be usable without the need of very specific cable geometry knowledge. Therefore, using formulae that requires extensive geometry data was not considered.

Nevertheless, capacitance and inductance of the cable must be determined somehow to calculate the reactive power. Another approach was taken, imitating procedures usually made in other fields. To reveal some correlations, data available in [67] of cable capacitance and cable inductance were sequentially plotted as a function of the entire input variables considered. Although no direct correlations were found, one interesting relationship was revealed; between cable capacitance (and cable inductance) and two of the inputs, the voltage level and

the conductor diameter (which can be deduced from the cross section).

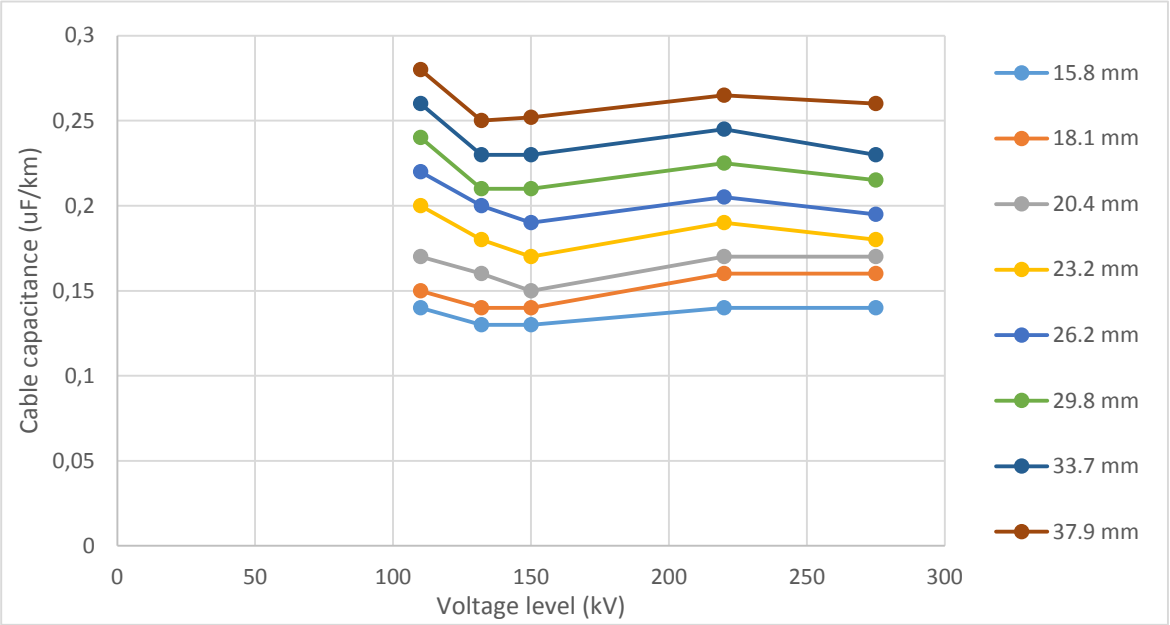

Figure 21 Cable capacitance as a function of voltage level and conductor diameter. Data from [67].

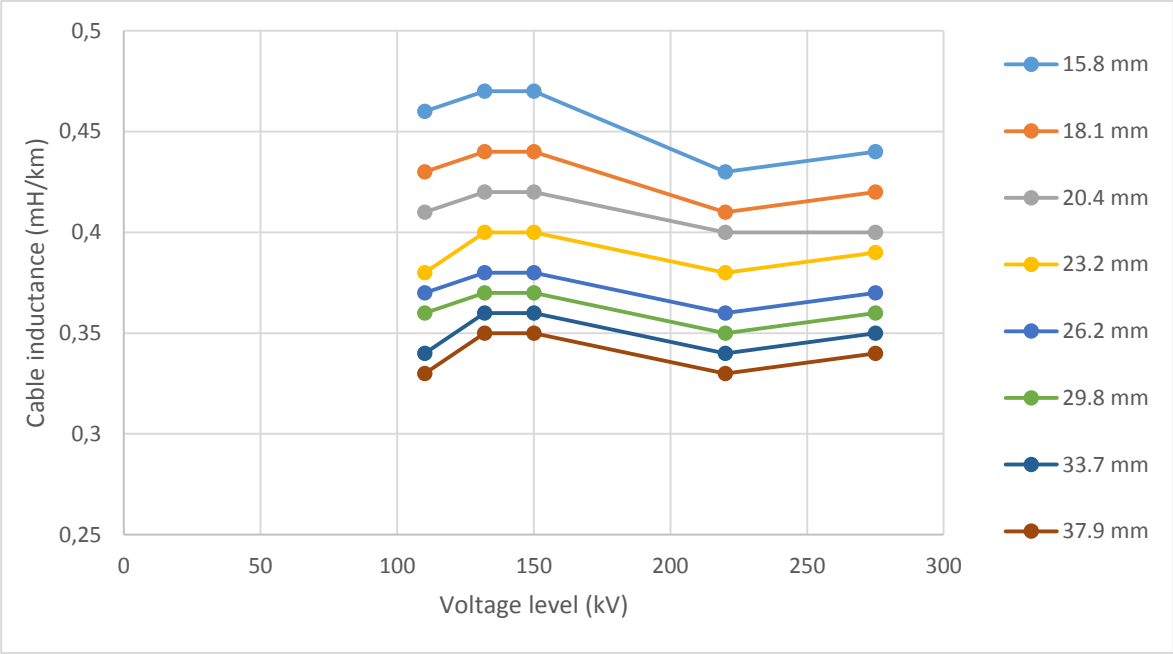

Figure 22 Cable inductance as a function of voltage level and conductor diameter. Data from [67].

Figure 21 and Figure 22 show the relationship between cable reactance, voltage level, and the conductor diameter. It can be seen that the relationship is not linear, thus it is not suitable to

model them by a linear regression, e.g. as done in (21).

Taking in account the relationship previously found, an alternative strategy was taken. Looking at Figure 22 and Figure 21, it is clear that both capacitance and inductance could be estimated by means of two-variable interpolations: interpolating from the conductor diameter and the voltage level. As double interpolation is not implemented within Excel, the function was programmed, with code found in [68] and some minimal modifications. Then finally, a method was found to correctly estimate cable capacitance and inductance, without the need for new inputs.

3.4.4.3. Dielectric loss factor

Several studies of dielectric behaviour of XLPE cables are available, albeit most of them analyse medium voltage cables [69] [70]. The main dependencies that those studies outline are an increase of the dielectric loss factor with temperature and aging, up to values of 0,0200. It is mentioned in [71] that the IEC standard is 0,004. On the other hand, suppliers claim a value of 0,0004 (10 times less than the standard), which may be achievable with their technology [26]. Anyway, a more conservative default value of 0,004 (which is modifiable), is considered for this work according to the IEC standard.

3.4.4.4. Cable reactive power

Calculation of the reactive power generated can be done once the line inductance and line capacitance has been found. As exposed in Section 2.1.2, reactive power is generated by inductive and capacitive effects, as show in (22) and (23):

$$q_c = n_{cables} \cdot 3 \cdot \left(\frac{U_{RMS}}{\sqrt{3}}\right)^2 \cdot 2\pi \cdot f \cdot C \tag{22}$$

$$q_l = n_{cables} \cdot 3 \cdot {I_m}^2 \cdot 2\pi \cdot f \cdot L \tag{23}$$

where,

q_c: capacitive power generated per kilometre of power transmission line [VAr/km];

q_l: inductive power generated per kilometre of power transmission line [VAr/km];

n_{cables}: number of cables;

U_{RMS}: phase-to-phase value of the voltage level [V];

f: electric frequency [Hz];

C: line capacitance [F/km];

L: line inductance [H/km];

I_m: mean value of the current [A].

In fact, as the inductive reactive power generated is current-dependent (i.e. load-dependent), the mean value of the current is employed for the calculation:

$$q_{tot} = q_l - q_c \tag{24}$$

Finally, the total reactive power per kilometre of line q_{tot} [VAr/km] is calculated through (24). Capacitive power generated is bigger than the inductive power, hence the compensation must be made with inductive reactive power through shunt reactors (see Section 2.1.6). As stated in Section 2.1.6 a STATCOM unit will be also considered, to meet the grid requirements.

The cost of reactors is set at 0,01 M€/MVAr, as stated by Van Eeckhout [63]. Alternatively, Lundberg considers the cost of a shunt reactor as 2/3 of that of a transformer with the same MVA rating [62] [11]. Nevertheless, this latter approach is not considered, as it implies that the distance could not be considered as a variable.

For a 100-MVAr and a 200-MVAr STATCOM, the reported costs are, respectively, in the range of 5,75 to 11,5 M€ and 11,5 to 23 M€ [58], giving an approximate cost of 0,086 M€/MVAr. As stated in Section 2.1.6, little reactive power variation is to be expected. Consequently, for this work a single STATCOM rated at 10% of the produced reactive power will be considered (this ratio is modifiable by the user). The following equation is then obtained:

$$C_{compensation} = 0{,}01 \cdot |q_{tot}| + 0{,}086 \cdot 0{,}1 \cdot |q_{tot}| \tag{25}$$

where,

q_{tot}: total reactive power generated by the cables [MVAr];

$C_{compensation}$: cost of compensating the reactive power generated [M€].

Additionally, it must be taken in account that compensation systems also present their own losses. Shunt reactors are built similarly to transformers, although they lack the secondary

windings. Their losses are reported as 0,2% of the transmitted power [72], which is consistent as they are similar to the transformer losses (see Section 3.4.4.7). Consequently, the shunt reactor losses and its cost can be calculated as in (26) and (27):

$$P_{losses,reactor} = 0{,}002 \cdot |q_{tot}| \tag{26}$$

$$C_{reactor}^{losses} = P_{losses,reactor} \cdot F_{loss} \tag{27}$$

Where,

$P_{losses,reactor}$: losses in the reactors [W/km];

$C_{reactor}^{losses}$: cost of losses in reactors [€/km];

q_{tot}: total reactive power generated by the cables [VAr] (it is here in VAr to match the units).

On the other hand, the STATCOM losses will not be accounted for, because it is not possible to known when the STATCOM will be necessary. Even if the grid coupling requirements are very strict, the STATCOM will not be operating continuously, only when there is an unpredicted imbalance in the reactive power; i.e. if there is a failure in a shunt reactor, or if the current in the transmission cables reaches its maximum value. Hence, as it is not possible to predict how long the STATCOM will be operating and at which ratings it will need to operate.

3.4.4.5. Cable active losses

Once the line parameters are calculated, the cable ohmic and dielectric losses can be deduced through (28) and (29):

$$P_{ohmic,HVAC}^{active} = n_{cables} \cdot 3 \cdot (I_{m,HVAC})^2 \cdot R_{ac} \tag{28}$$

$$P_{dielectric} = q_c \cdot \tan(\delta) \cdot \tag{29}$$

where;

$P_{ohmic,HVAC}^{active}$: losses caused lost by the active part of the current, per kilometre of line [W/km];

n_{cables}: number of cables;

I_m: mean value of the current [A];

R_{ac}: conductor resistance per km [Ω/km];

$P_{dielectric}$: power loss by dielectric effects per kilometre of line [W/km];

q_c: capacitive power per km of line [VAr/km];

tan(δ): dielectric loss factor.

And their cost is calculated with (30):

$$C_{HVAC\ cable}^{active\ losses} = \left(P_{ohmic,HVAC}^{active} + P_{dielectric}\right) \cdot F_{loss} \tag{30}$$

where $C_{HVAC\ cable}^{losses}$ is the cost of the losses in each HVAC cable [€/km].

3.4.4.6. Charging current

The cable current is split in its active and reactive component, where the reactive component corresponds to the charging current. As said in Section 2.1.2, the charging current increases along the distance due to the capacitive and inductive elements of the cable, and is calculated using (31):

$$i_c = \frac{q_{tot}}{\sqrt{3} \cdot U_{RMS} \cdot n_{cables}} \tag{31}$$

where the charging current is obtained in A/km. The cable current will therefore increase along the cables, increasing its ohmic losses. However, the compensation at both ends reduces its value, and the compensated charging current becomes half of its original value [49].

$$i_{c,compensated} = {}^{i_c}/_{2} \tag{32}$$

So for a given distance l,

$$i_{cable}(l) = I_{m,HVAC} + \frac{i_c}{2} \cdot l \tag{33}$$

The ohmic losses are calculated by (34), in W/km:

$$P_{ohmic,HVAC} = n_{cables} \cdot 3 \cdot [i_{cable}(l)]^2 \cdot R_{ac} \tag{34}$$

where R_{ac} is the ac resistance [Ω/km].

Moreover, as the active current and the reactive one are lagging 90º, the following applies

(Pythagoras theorem):

$$P_{ohmic,HVAC}(l) = n_{cables} \cdot 3 \cdot \left({I_{m,HVAC}}^2 + \frac{{i_c}^2}{4} \cdot l^2 \right) \cdot R_{ac} \quad (35)$$

Therefore, the ohmic losses can be split in its active current component, and its charging current component. The active current component is treated in section 3.4.4.5, whereas the ohmic losses caused by the charging current are calculated separately with (36):

$$P^{charging}_{ohmic,HVAC}(l) = n_{cables} \cdot 3 \cdot l^2 \cdot \frac{{i_c}^2}{4} \cdot R_{ac} \quad (36)$$

To obtain the charging ohmic losses for the total transmission length, (36) must be integrated[15]:

$$P^{charging}_{ohmic,HVAC\,\boldsymbol{total}} = \int_0^{d_{tot}} n_{cables} \cdot 3l^2 \frac{{i_c}^2}{4} R_{ac} \cdot dl = \frac{3 \cdot n_{cables} \cdot R_{ac} \cdot {i_c}^2}{12} \cdot {d_{tot}}^3 \quad (37)$$

Equation (37) indicates that the total ohmic losses due to charging current can be expressed as a coefficient multiplied by the third power of the total transmission length.

This distinction between charging and active ohmic losses is made because it is implemented in the spreadsheet tool, which needs to treat separately fixed costs, linear distance-dependent costs, and this cubic distance-dependent cost. Consequently, the cost factor derived from the charging current ohmic losses is calculated as:

$$C^{charging\ losses}_{HVAC\ cable} = n_{cables} \cdot 3 \cdot \frac{{i_c}^2}{12} \cdot R_{ac} \cdot F_{loss} \quad (38)$$

where $C^{charging\ losses}_{HVAC\ cable}$ is in fact in €/km³.

3.4.4.7. Transformer losses

Regarding the transformer losses, it was intended first to achieve the loss calculation by means of the transformer parameters. Figure 23 shows the equivalent per unit (p.u.) circuit of a

[15] Multiplying (36) by distance, in lieu of integrating it, would mean considering a constant charging current (a constant value that depends on the maximum length), which is wrong and would overestimate the value of the charging current losses.

transformer (per phase). R_c and X_m stand for the iron losses (non-load dependent) and R_{eq} and X_{eq} model the copper losses (load dependent). No direct values of the copper and iron resistances were found, but some losses indexes were available.[16]

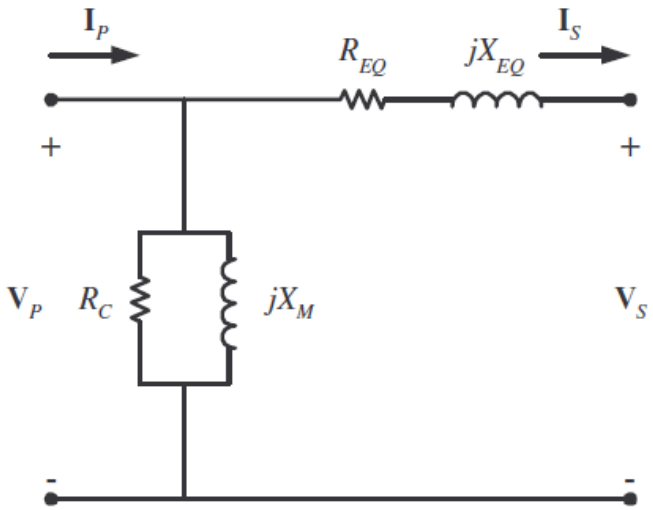

Figure 23 Transformer equivalent circuit (p.u.)

Most data available regarding large power transformer losses are global efficiencies. ABB claims efficiencies up to 99,85% for their offshore power transformers [30]. Moreover, a general equation for power transformer efficiency is provided in [29]:

$$eff_{TR} = 0{,}00082377 \cdot \ln\left(S_{TR,HVAC}\right) + 0{,}99365 \tag{39}$$

where $S_{TR,HVAC}$ is the rated power of the transformer [MVA] and eff_{TR} is the efficiency in p.u.

Additionally, data is exposed in [73], at rated power the reported non-load losses are 0,033% and the load-related losses are 0,30%, for a total of 99,67% efficiency. It is also stated in [73] that for transformers rating from 400 MVA to 1000 MVA, an efficiency of 99,6% could be assumed (0,2% of non-load losses and 0,2% load-losses at maximum load). If the values of non-load losses and load-losses are known, the losses of the transformer at any load can be calculated as:

[16] The losses indexes are in fact the values or copper and iron parameters, in p.u.

$$P_{TR,HVAC}^{losses} = NLL \cdot S_{TR,HVAC} + LL \cdot LI^2 \cdot S_{TR,HVAC} \;\; ; \;\; LI = \frac{C_{OWF} \cdot {P_{OWF}}/{\left(\frac{n_{TR}}{2}\right)}}{S_{TR,HVAC}} \qquad (40)$$

where,

NLL: non-load loss index [p.u.];

LL: load-loss index [p.u.];

LI: load index of the transformer [p.u.];

$S_{TR,HVAC}$: rated power of the transformer [MVA];

n_{TR}: number of transformers ,which equals four by default (two per substation), as stated in Section 3.4.2.1).

For this work, the non-load loss and load-loss indexes are both considered 0,002 pu. As the selected configuration has been set as twin transformers at 60% capacity (see Section 3.4.2.1), each individual transformer load will never reach its maximum value (in normal operation), thus lowering the transformer losses. Even when the OWF is at full load, the transformer load index will remain at 83,3% with the selected configuration, lowering the load-related losses in comparison with other possible configurations (e.g. twin transformers each rated at 50% of the OWF rated power, which would imply a 100% load index at the OWF maximum power).

3.4.5. MVAC costs

MVAC costs are treated as a section in HVAC costs, as excepting the cable costs the same cost functions employed in the HVAC analysis will be used. No further attention is paid on MVAC, as it is known that this technology is only suitable for OWF with low power ratings (e.g. 100 MW) and near to shore (e.g. 10 km). Consequently, MVAC is not researched in-depth.

The same cost functions will be employed as for HVAC, although the offshore substation (offshore transformers, offshore structure) is not necessary. The spreadsheet inputs are the same as for HVAC, but the voltage level is kept constant at 33 kV and the cable parameters are estimated from suppliers [28].

3.5. HVDC cost

3.5.1. Base variables

In the same way as explained in Section 3.4.1, to obtain the costs for an HVDC transmission system, the user most introduce a set of variables (see Table 13) which are the base of the cost modelling.

Table 13 HVDC main inputs

Variables	*Description*	*Units*
U_{HVDC}	Phase to phase voltage level of the transmission cables	kV
S_{HVDC}	Cable cross section	mm²
$n_{cables,HVDC}$	Number of cable pairs	-

The number of cables pairs $n_{cables,HVDC}$ is by default limited to 1 being the system bipolar (see section 2.3.4), although it can be increased. On the other hand, each cable rated ampacity $I_{rated,HVDC}$ is estimated from the values given by suppliers (see Table 14), and the mean current and the rated power of each cable pair are calculated through (41).

Table 14 Rated ampacities of HVDC cables

Cross section [mm2]	*Ampacity [A/core]*	*Cross section [mm2]*	*Ampacity [A/core]*
95	343	1200	1458
120	392	1400	1594
150	441	1600	1720
185	500	1800	1830
240	583	2000	1953
300	662	2200	2062
400	765	2400	2170
500	883	2600	2275
630	1023	2800	2373
800	1175	3000	2473
1000	1335		

$$P_{rated,cab.pair} = 2 \cdot I_{rated,HVDC} \cdot U_{HVDC} \qquad I_{m,HVDC} = \frac{c_{OWF} \cdot P_{OWF}}{2 \cdot n_{cables,HVDC} \cdot U_{HVDC}} \tag{41}$$

where,

$P_{rated,cab.pair}$: rated power of each cable pair [W];

$I_{rated,HVDC}$: rated current of each cable [A];

$I_{m,HVDC}$: mean current of each cable [A];

c_{OWF}: OWF capacity factor;

P_{OWF} : OWF rated power [MW].

3.5.2. Base cost

3.5.2.1. Transformers cost

As mentioned in Section 2.3.2, HVDC systems also need transformers to step up the voltage. The cost function shown in (9) is employed; and the same configuration with two transformers is assumed, as it constitutes the optimum relationship between reliability and cost [61].

3.5.2.2. VSC converter cost

It is known that the cost of VSC converters can be higher than 100 M€. Lancheros [13] states 120M€ for a 1000MW converter (2013), whereas Lazaridis [74] and Lundberg [62] agree on a cost of 0,11M€/MW (2005 and 2003). Schoenmakers [9] assumes a cost of 0,085 M€/MW for a ±150 kV converter and 0,093M€/MW for a ±300 kV converter (2008). The ENTSOE [58] reported costs (2011) are given in Table 3.5-3.

Table 15 VSC converter cost data [58]

Rated Power [MW]	*Cost range [M€]*	*Mean Cost [M€/MW]*
500	75 - 92	0,167
850	98 - 105	0,119
1250	121 - 150	0,108
2000	144 - 196	0,085

Being an incipient technology, VSC converters costs have decreased as the technology improved. For this reason, costs reported in recent sources are considered more reliable. Moreover, as it can be seen in Table 15, assuming a constant cost per MW would be a vague assumption, as the costs decreases with the converter rated power. Furthermore, as costs from [58] are stated to come from suppliers, they are considered particularly relevant. Therefore, those data are used to achieve a cost function, shown in Figure 24.

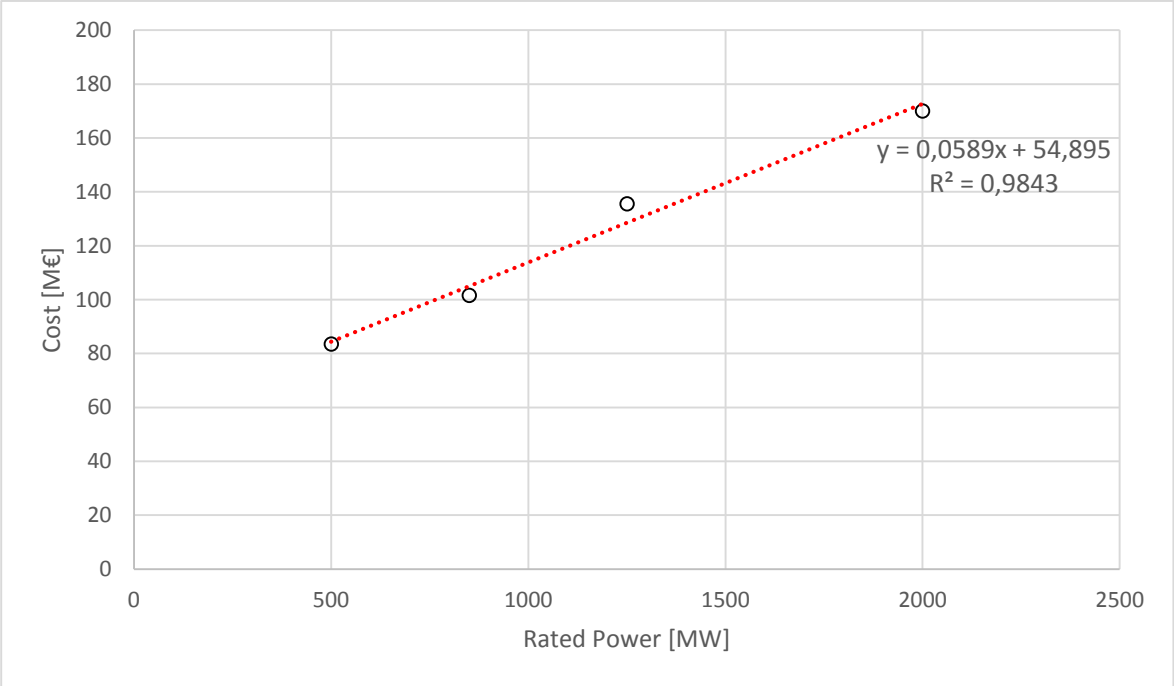

Figure 24 VSC converter cost as a function of its rated power

$$C_{VSC} = 0{,}0589 \cdot S_{VSC} + 54{,}985 \tag{42}$$

where,

C_{VSC}: cost of a single converter [M€];

S_{VSC}: converter rated power [MW].

As discussed in Sections 2.3.3.2 and 2.3.4, there will be two converters, one for each conversion operation: a rectifier at the offshore substation and an inverter at the onshore one.

3.5.2.3. HVDC Offshore substation structure

It is known that a VSC-HVDC offshore structure needs more size than its equivalent HVAC structure. Consequently, its costs will be higher. From data in [58], it can be estimated that a VSC platform costs are from 57,9% to 115,4% higher than an HVAC platform for the same rated power. Furthermore, it is stated that a VSC platform is 85% bigger than an equivalent HVAC platform [63]. As 85% falls in the middle of the cost increase range, it is a prudent value to consider. Consequently, the cost of an offshore substation structure is modelled as:

$$C_{SS,HVDC} = 1{,}85 \cdot (2{,}534 + 0{,}0887 \cdot P_{OWF}) \quad (43)$$

where,

$C_{SS,HVDC}$: cost of the offshore HVDC substation platform [M€];

P_{OWF} : OWF rated power [MW].

3.5.3. Distance dependent costs

3.5.3.1. Cable cost

To achieve a function that estimates the cost of dc cables, data has been gathered from literature. Two different approaches have been revealed: authors either assume a fixed cost [63] [13], or they consider a cost function, as achieved by Lundberg in 2003 [62] [74]. However, dc cables technology (extruded XLPE) has made significate advances since 2003 [75], thus Lundberg cost function could be outdated. Consequently, it has been intended to build a new cost function. For this purpose, data from [58] has been plotted to reveal any correlation (Figure 25).

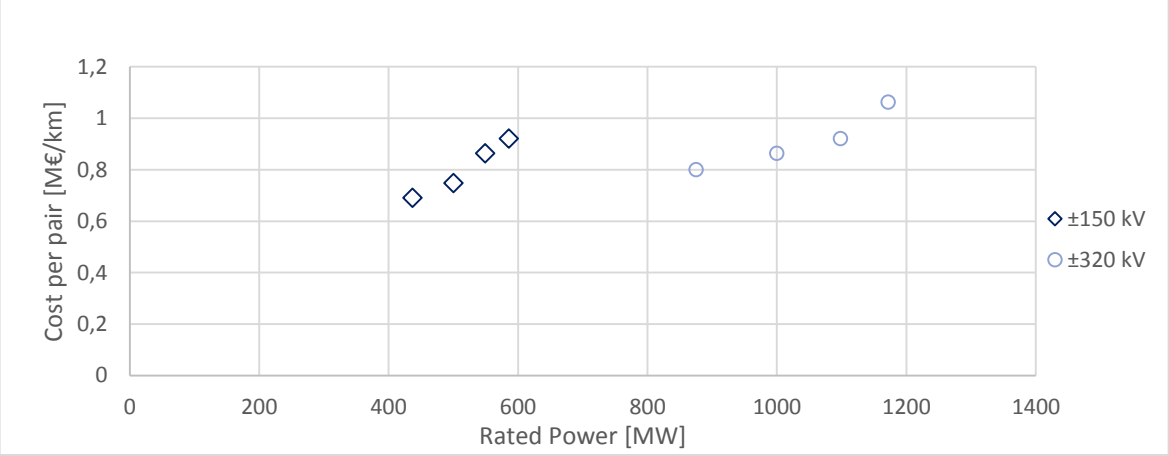

Figure 25 HVDC VSC cable cost as a function of its rated power and voltage level. Data source: [58]

It is observed that the cost of the cable is suitable for a multiple regression, with the rated power and the voltage level as variables:

$$C_{cable\ pair,HVDC} = 0{,}652 + 0{,}00098 \cdot \mathrm{P_{rated,cab.pair}} - 0{,}002363 \cdot U_{HVDC} \quad (44)$$

where;

$C_{cable\ pair,HVDC}$: cost of each cable pair [M€/km];

$P_{rated,cab.pair}$: rated power of the cable pair [MW];

U_{HVDC}: HVDC voltage level [kV].

Nevertheless, the model obtained should not be used for voltages and power rates outside the data ranges shown in Figure 25.

Note that the number of cables must be even, to match the chosen topology (symmetric monopolar). Additionally, it must be accounted that a pair of cables laid in the same trench cannot handle more than 1400MW [76]. Consequently, for OWF rated less than 1400MW a single cable pair will be enough, and their rated power will match the OWF rated power (P_{OWF}). However, for larger ratings, the number of cable pairs should be increased, and the OWF rated power should be equally distributed amongst each cable pair.

3.5.3.2. Cable laying cost

Each cable pair must be laid in the same trench to minimize the generated magnetic fields (Section 2.3.4). As for ac cable laying, there is not enough reliable data to achieve a cost function. A compromise is then made using the available information reported in Table 16.

Table 16 HVDC cable laying cost data.

Reported cost [M€/km] (per cable pair)	*Reference*
0,575 - 1,035	[58]
0,176	[62]
0,600	[13]
0,200	[74]
0,215	[63]

A compromise cost is therefore set at 0.4 M€/km for each cable pair. The cost data for this particular case is considered unreliable at some degree: as all the costs come from different sources, it is not known what is included. It could be supposed that the lower cost corresponds simply to installing the cables and digging the trenches, while maybe the higher one includes route survey among other services.

3.5.4. HVDC transmission system losses

3.5.4.1. DC cables losses

For dc cables, losses are much simpler to calculate than for HVAC cables, as there is no reactive power, and no proximity and skin effects (compare with Section 2.3.1). The dc resistance is calculated with (17) with the previously selected cross-section S_{HVDC}. The losses are calculated as:

$$P_{ohmic,HVDC} = 2 \cdot n_{cables,HVDC} \cdot {I_{m,HVDC}}^2 \cdot R_{dc} \quad (45)$$

where;

$I_{m,HVDC}$: mean current [A];

R_{dc}: cable resistance [Ω/km];

$P_{ohmic,HVDC}$: ohmic losses in the cables [W/km].

By default the number of cables $n_{cables,HVDC}$ is two.

As done for HVAC, the losses cost is calculated as the cost of the non-produced energy, taking in account the OWF lifespan:

$$C_{HVDC\ cable}^{losses} = P_{ohmic,HVDC} \cdot F_{loss} \quad (46)$$

where;

$C_{HVDC\ cable}^{losses}$: cost of the losses in the HVDC cables [€/km];

$P_{ohmic,HVDC}$: power of the losses in the HVDC cables [W/km].

3.5.4.2. Converter losses

As discussed in Section 2.3.3.2, reported VSC converter losses have gradually decreased from 3% down to 1% with newer technology generation [42]. For this work, it is assumed that the VSC losses are 1% of the converted power, obtaining the following equation:

$$P_{losses,VSC} = 0{,}01 \cdot C_{OWF} \cdot P_{OWF} \quad (47)$$

where,

$P_{losses,VSC}$: losses power of a single converter [W];

c_{OWF}: OWF capacity factor;

P_{OWF}: OWF rated power [W].

The cost of these losses is evaluated in (48). Notice that the VSC losses cost could actually be very high. As an example, for a 500 MW OWF, assuming the cost of energy (C_{energy}) at 50 €/MWh and a lifespan of 15 years, VSC losses cost amount to 26.3 M€.

$$C_{VSC}^{losses} = P_{losses,VSC} \cdot F_{loss} \tag{48}$$

where,

C_{VSC}^{losses} : Cost of the losses in both VSC converters [€]

$P_{losses,VSC}$: Losses power of both VSC converters [W].

3.6. LFAC Costs

As LFAC transmission systems are still in figuring as a theoretical proposal for OWFs, the related power transmission costs have not been extensively investigated by researchers as in comparison to HVDC or HVAC solutions. A cost comparison between VSC-HVDC and LFAC was performed in [18], whereas the cost of some components at non-standard frequencies is estimated in [55].

For this work, the same cost functions as HVAC will be considered, except for transformers and transformer losses, whose cost patterns will be established by analysing its differences with standard step-up transformers. Offshore structure costs for LFAC will also be particularly studied.

The costs of the necessary ac-ac converters (CCV and B2B-VSC) will also be analysed. For the rest of the devices, the same cost patterns as the ones established for HVAC will be utilized. Note that it is not an unreasonable approximation as, for example, it is known that standard HVAC cables can be employed for LFAC [49]. Even though the same cost functions are applied, the results will be different since, for instance, operating at a lower frequency will cause reactive power compensation to be much lower. Additionally, a lower frequency allows employing transmission cables with higher voltages than for standard HVAC without strong reductions on the power transmission capability.

3.6.1. LFAC base variables

To perform the calculations, the user must provide the following variables:

Table 17 HVAC main inputs

Variables	*Description*	*Units*
$U_{RMS,LFAC}$	Phase to phase voltage level of the transmission cables	V
S_{HVAC}	Cable cross section	mm²
f	Electric line frequency	Hz
$n_{cables,LFAC}$	Number of three-core cables	-

The electric line frequency is set by default at 16,67 Hz (50/3), but the user can choose to employ 20 Hz , which would be the standard for 60 Hz grids. As for HVAC, the voltage level should be between 110 kV and 275 kV, as the modelling equations have been made with some

limitations (estimation of cable capacitance and inductance). For the cable cross section, the user must choose from a list of standardized values, which are the same as for the HVAC subsea cables.

Once the conductor cross-section has been chosen, the three-core cable ampacity (i.e. the maximum intensity that each cable core can withstand) is deduced from values given by suppliers [28], reported in Table 18 . The same values for ampacity are employed than for HVAC. In case the user wishes to choose a non-standardized cross-section, the ampacity $I_{rated,LFAC}$ is estimated from the values given by the suppliers. Finally, the number of three-core cables should be chosen.

Table 18 Ampacity of three-core cables

Cross section [mm2]	*Ampacity [A/core]*
300	530
400	590
500	655
630	715
800	775
1000	825

With those values introduced, the mean active current per cable core and the cable power rating are deduced:

$$I_{mean,LFAC} = \frac{c_{OWF} \cdot P_{OWF}}{n_{cables,LFAC} \cdot \sqrt{3} \cdot U_{RMS,LFAC}}; \qquad S_{cable,LFAC} = \sqrt{3} \cdot U_{RMS,LFAC} \cdot I_{max,LFAC} \quad (49)$$

Where, $I_{m,LFAC}$ is calculated in Amperes per core, with P_{OWF} in Watts and U_{RMS} in Volts. $I_{m,HVLF}$ corresponds to the mean value of the active electric current taking in account the capacity factor c_{OWF}, i.e. the active current that each cable must carry in normal operation. $S_{cable,LFAC}$ corresponds to the rated power of each cable, i.e. the maximum power the each cable can withstand in steady-state.

As for HVDC and HVAC, the user is shown some parameters which should assure that a suitable transmission system is selected (see Section 3.9 for further explanations).

3.6.2. Low frequency Transformers

It is known that the cost of a low frequency transformer is higher than that for its HVAC equivalent, as weight and size are inversely proportional to the frequency (refer to Section 2.4.2). Considering that the cost of transformers at a certain frequency can be extrapolated from its cost at standard frequency yields [55][17] :

$$C_{TR,LFAC} = \frac{0{,}325 f_r + 0{,}22 f_r + 0{,}164 \sqrt[3]{f_r^{\,2}}}{0{,}35 + 0{,}22 + 0{,}164} \cdot C_{TR,HVAC} \tag{50}$$

where,

$C_{TR,HVAC}$: cost of the transformer at standard frequency [M€];

f_r : normalized frequency ($f_r = 50/f$) of the chosen electrical frequency.

The cost of the transformer at standard frequency is obtained from (9) in Section 3.4.2.1. As 16,67 Hz is chosen as the frequency for the LFAC system, substituting $f_r = 3$ in (50) gives the following cost function:

$$C_{TR,LFAC} = 2{,}69228 \cdot C_{TR,HVAC} \tag{51}$$

and combining with (9) yields:

$$C_{TR,LFAC} = 2{,}69228 \cdot 0{,}0418 \cdot {S_{TR,LFAC}}^{0{,}7592} \tag{52}$$

The latter is used in this work. As previously stated, the same considerations for HVAC apply for LFAC, and two transformers each rated at 60% of the OWF rated power are considered. Note that cost data obtained in [18] roughly indicates that the cost of the LFAC transformer is triple that of its HVAC equivalent, which is approximatively the relationship obtained in (52).

3.6.2.1. Low Frequency Transformer losses

Transformer losses are calculated as standard frequency transformer losses (see Section 3.4.4.7), but with a halved non-load loss index as stated in [18]. Although it is an approximate

[17] An accurate extrapolation is made by the authors, based on the transformer materials cost breakdown, and the effect of the frequency in each transformer part.

statement, it serves to illustrate that low-frequency transformers present lower iron losses.

3.6.3. Offshore substation structure

As done for the HVDC technology in Section 3.5.2.3, the goal is to establish a relationship between the costs of the LFAC and the HVAC offshore structure. The cost of an LFAC offshore structure, able to accommodate the offshore LFAC substation, should be lower than the HVDC offshore structure cost, as the size of the latter is known to be higher [18], but higher than the HVAC offshore structure cost, as the low frequency transformers have increased size and weight.

Combining data from [18] and [58], one can estimate that for an HVAC offshore structure, the transformers account for 10% of the total weight[18]: the weight of a 300 MW HVAC structure is reported as 2000 t, whereas the weight of two 50-Hz 180-MVA three-phase transformers is estimated from [18] at 200 metric tons. In addition, as the weight of the low frequency transformers is triple that of standard transformers (see Section 2.4.2), one can estimate that the size, and thus the cost, of a LFAC offshore structure is 20% higher than the cost of an equivalent HVAC offshore structure assuming that all the other equipment remain unchanged. The previous statement, combined with (11), results in a cost function for the cost of the LFAC offshore structure:

$$C_{SS,LFAC} = 1{,}2 \cdot (2{,}534 + 0{,}0887 \cdot P_{OWF}) \tag{53}$$

3.6.4. Power converters: CCV and B2B-VSC

The cost of a back-to-back (B2B) VSC converter can be estimated proportional to the costs of a VSC converter (section 3.5.2.2). For cycloconverters (CCVs), no cost data have been found. In fact, no information has been found for CCVs in the MW power range. Nevertheless, as CCV technology is based on thyristors, its cost could be extrapolated from the costs of line-commutated converters, which are also thyristor based and which have cost data available from [58] (see Table 19).

Indications are that three-phase/three-phase cycloconverters for LFAC should need 36

[18] Same configuration as for HVAC and HVDC : two twin Transformers per substation, each one rated at 60% of the rated power of the OWF

thyristor valves (12 valves per phase) [17], whereas LCC employs only 12 thyristor valves [77]. Assuming that most of the costs are due to the thyristor valves, it could be estimated that the power-dependent cost of a CCV corresponds to the triple of the cost of a LCC with the same rated power.

Table 19 Reported cost data of LCC [58]

Rated Power [MW]	*Cost range [M€]*	*Mean Cost*
1000	81 - 104	92,5
2000	150 - 184	167,0
3000	196 - 230	213,0

Table 19 can be used to establish a cost function for the CCVs as:

$$C_{CCV} = 3 \cdot 0{,}0603 \cdot S_{rated} + 37 \tag{54}$$

For the B2B-VSC costs, it must be accounted that two VSC are necessary. Nevertheless, as the two converters are assembled together, one may assume that the cost of the whole B2B system is not the equal the sum of the cost of two converters, but has a lower value as some components can be spared, and space can be saved by employing lower voltages and higher currents, since a transmission system between both VSCs is not needed. Consequently, the cost of a B2B-VSC is assumed as 1,5 times the cost of a single VSC converter[19]:

$$C_{BtB-VSC} = 1{,}5 \cdot (0{,}0589 \cdot S_{VSC} + 54{,}985) \tag{55}$$

However, as it is difficult to estimate the actual relationship between the costs of B2B-VSC systems and normal VSC-HVDC ones, the multiplication factor is left open for the user as an additional input that can be modified.

Regarding the converter losses, it is assumed that the B2B-VSC behaves as a VSC converter (losses equal to 1% of the transmitted power), and the reported losses of the LCC are considered for the CCV (0.7% of the transmitted power as stated in Section 2.3.3.1).

[19] As it is difficult to estimate the actual relationship between the costs of B2B-VSC systems and normal VSC-HVDC ones, the multiplication factor is left open for the user as an additional input which can be modified.

3.7. Determination of the break-even distance and area

The break-even distance corresponds to the point where the costs of a HVDC transmission system become lower than their HVAC counterpart. Even if the economic analysis is accurately done, variability is inherent to any cost function. Even though the break-even point is a useful value to determinate the optimum transmission system, accounting for the variability in cost functions translates into a more accurate estimation. If the upper and lower predictions of each model are considered, the upper and lower cost predictions can be obtained, resulting in a break-even area rather than a break-even point (see Figure 26). For every self-made cost function, its variability will be considered by calculating prediction intervals, i.e. intervals which the values are expected to lie within with a certain probability.

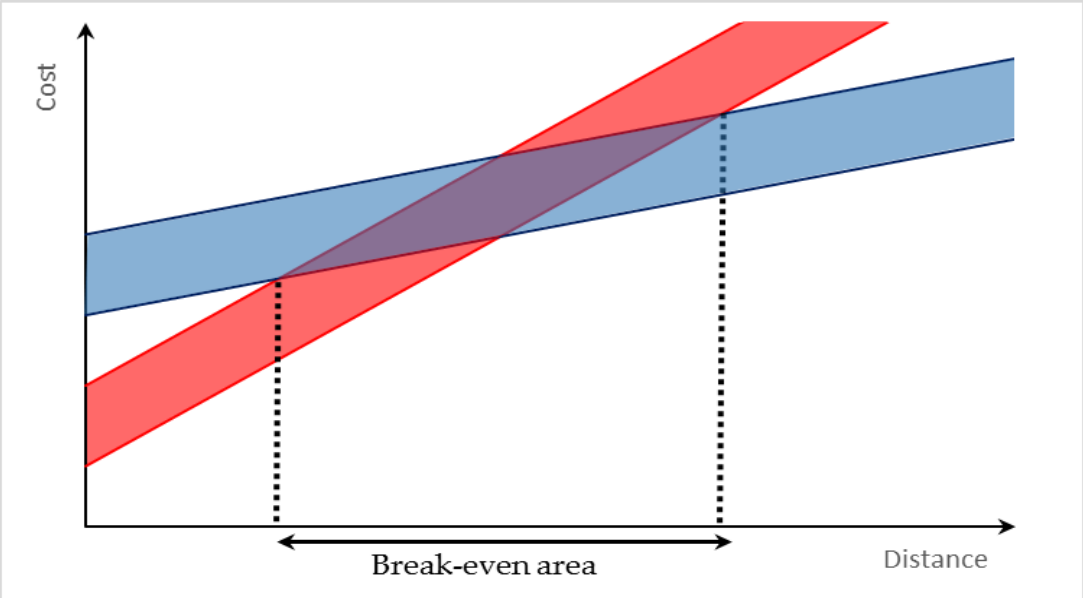

Figure 26 Break-even area when cost functions variability is considered. Distance-dependent costs variability is not considered here. Red=HVAC Blue=HVDC

Figure 26 should be similar to the obtained results. Note that as the distance-dependent costs are also subject to variability, the slope of the upper and lower limits will also be different, not only their intercept value.

As a general value, it is assumed for the statistical models that a prediction interval of 95% is accurate enough. The prediction interval for the cost functions is written as follows:

$$[\hat{y} - 1{,}96 \cdot \sigma_{est} \ ; \ \hat{y} + 1{,}96 \cdot \sigma_{est}] \quad (56)$$

where $\hat{y}$ is the value predicted by the model, and σ_{est} is the standard deviation of the model.

On the other hand, whenever a mean value has been assumed in lieu of building a cost function (e.g. cable laying costs), the following interval was considered:

$$[\overline{y} - 1{,}96 \cdot \sigma \ ; \ \overline{y} + 1{,}96 \cdot \sigma] \quad (57)$$

where $\overline{y}$ is the mean value of the considered data and σ is the standard deviation of the cost data.

Statistical results of each model can be found in the annexes. For every achieved cost function, the lower and upper 95% limits are considered, following (56) and (59). In the spreadsheet tool built, the upper and lower cost analyses are displayed to the user, along with the break-even area. For referenced cost functions, variability cannot be considered, as the original data is not known and the functions statistical parameters are not reported.

Note that the purpose of this lower and upper cost estimation is to give an idea of the break-even point variability, and not to perform an in-depth statistical study. This is why the considered prediction intervals described in (56) and (58) obviate some mathematical considerations and make some statistical assumptions, such as assuming normally distributed and uncorrelated residuals, or considering that the residual standard deviation provides a good estimate of the forecast standard deviation.

3.7.1. HVAC cost variability

For HVAC technology cost functions, the following standard deviations are obtained:

- Transformer cost function : σ_{TR} = 0,154 M€;
- GIS cost function: σ_{GIS} = 0,339 M€.

For cable laying costs, where a mean value has been assumed (see Section 3.4.3.2), the data are considered reliable enough to consider its variability (all data come from the same source), obtaining, hence, $\sigma_{cable\ laying,\ HVAC}$ = 0,025 M€/km.

3.7.2. HVDC cost variability

For the HVDC technology cost functions, the following standard deviations are obtained:

- Transformer cost function: σ_{TR} = 0,154 M€ (same as for HVAC);
- VSC cost function: σ_{VSC} = 5,86 M€;
- HVDC cable cost function: $\sigma_{cable\ pair,HVDC}$ = 0,0475 M€/km.

As said in Section 3.5.3.2, HVDC cable laying cost data are not reliable enough. Their unreliability as well as having only five data points makes any consideration of variability futile (considering the variability of this cost would translate in negative cost for the lower 95% range limit, which has no meaning).

3.8. Availability

Many factors may diminish the system availability (i.e. fraction of time in which the system is available): scheduled maintenance, repairs, and outages, among others. The unavailability translates in non-delivered energy. When choosing the most suitable transmission system, it must be accounted that a higher availability is a significant advantage. To consider that, the cost of availability is treated as a differential cost between the transmission systems.

For each transmission system j, the user introduces its availability A_j, which is given in percentage, typically of high values, e.g. 95%. Then, a comparative cost is associated to the technologies with lower availabilities, being zero for the technology with the highest availability. Considering that for 100% availability, the delivered power is equal to the generated one, the non-delivered power P_{Aj} due to lower availabilities is calculated as (59):

$$P_{Aj} = \left(MAX_k\{A_k\} - A_j\right) \cdot P_{OWF} \cdot c_{OWF} \tag{59}$$

Hence, the system with the highest availability will have an associated null power loss. The others will have a power loss that is proportional of the difference between their availability and the maximum one. Consequently, the cost of availability can be calculated with the non-delivered power as:

$$C_j = P_{Aj} \cdot F_{loss} \tag{60}$$

With this methodology, a cost is associated to an inferior availability, and included in the model. In this way, results from an availability study are incorporated to the tool, accounting for the advantages of systems with higher availabilities.

3.9. Guide for choosing adequate inputs – transmission system constraints

As previously discussed, choosing the cable cross-section, voltage level, and the number of cables must be done carefully. Due to the tool functioning, the user could theoretically introduce inputs that could make the cables exceed their ratings, making the whole economic analysis useless. Consequently, some resources are given to the user to analyse the suitability of the introduced transmission characteristics. The resources have been designed to fulfil the following criteria:

1. The transmission system (the cables) must be able to transmit full OWF rated power (i.e. the transmission systems is able to operate when the OWF produces its maximum power);
2. The transmission capability must not be reduced due to the presence of reactive power beyond the OWF rated power, within a considered distance to shore (applies to HVAC, LFAC and MVAC).

The first criterion is easy to introduce. As the user introduces the transmission parameters (voltage level, cross section, number of cables), the transmission system maximum load ratio is displayed, calculated as follows:

$$Maximum\ utilization\ ratio = \frac{P_{OWF}}{n_{cables} \cdot S_{cable}} \tag{61}$$

where S_{cable} is the rated power of each cable [MVA] , n_{cables} corresponds to the number of cables and P_{OWF} corresponds to the OWF rated power.

The maximum utilization ratio should be inferior to 100%, to transmit the maximum rated power. Along with this ratio, a large "YES" or a large "NO" is shown respectively if the utilization ratio is lower or higher than 100%.[20]

The second criterion is more challenging to implement. As mentioned in Section 2.1.2, the

[20] However, there are ongoing discussions that it would actually be more economically benefitial to implement OWFs with transmission systems rated at lower capacities than the farm itself. The reason is that since the OWFs only produce at full load hours for a small amount of time, most of the time the cable full capacity is not used.

generation of reactive power in the subsea cables gradually reduces the power transmission capability over the distance. As MVAC systems are only suitable for low distances, the reduction of transmission capability has not been considered for this technology, being the latter not noticeable for short distances (10-15 km). Thus, for HVAC and LFAC, the following approach has been taken: the transmission capability is calculated as a function of the distance, and some key values are displayed to the user.

The total reactive power generated q_{tot} has been calculated for each technology in MVAr/km. Hence, as the reactive power can be expressed as a function of the distance, the active power transmission capability is also a function of the distance:

$$S^2 = P^2 + (q_{tot} \cdot d)^2 \qquad \Longrightarrow \qquad P(d) = \sqrt{S^2 - (q_{tot} \cdot d)^2} \tag{62}$$

Where P(d) [MW] represents the transmittable power at the distance "d" [km] , and S corresponds to the maximum transmittable power of the transmission system, calculated as the power rating of each cable multiplied by the number of cables.

Nevertheless, the latter expression corresponds to uncompensated reactive power, and it has been stated that full compensation is made. For 50/50 compensation in offshore/onshore substations, the reactive power is evenly distributed at both ends of the cable; hence the charging current is reduced to the half of the charging current without compensation [9] [78]. Therefore, the transmittable power with 50/50 compensation is calculated as:

$$P(d)_{compensation} = \sqrt{S^2 - \left(\frac{q_{tot}}{2} \cdot d\right)^2} \tag{63}$$

Figure 27 shows the active power transmission capability of a 400MW OWF with a capacity factor of 0,4 ,employing two 1000 mm² three-core cables at 150 kV and 50 Hz. The horizontal lines correspond respectively to the maximum and the mean power generation of the OWF. It can be seen that approximatively beyond approximatively 70 km, this transmission system (with compensation) will not be able to transmit the OWF rated power, resulting in a loss of power whenever the OWF is at 100% capacity.

It is understood that the cables must be rated higher than the OWF to avoid any power limitation occurring throughout the transmission system. As a general value, if the distance to shore is not known, it could be established that the transmission system should be chosen to avoid any power limitation before 120 km, as OWF tend to be built at most 120 km far from

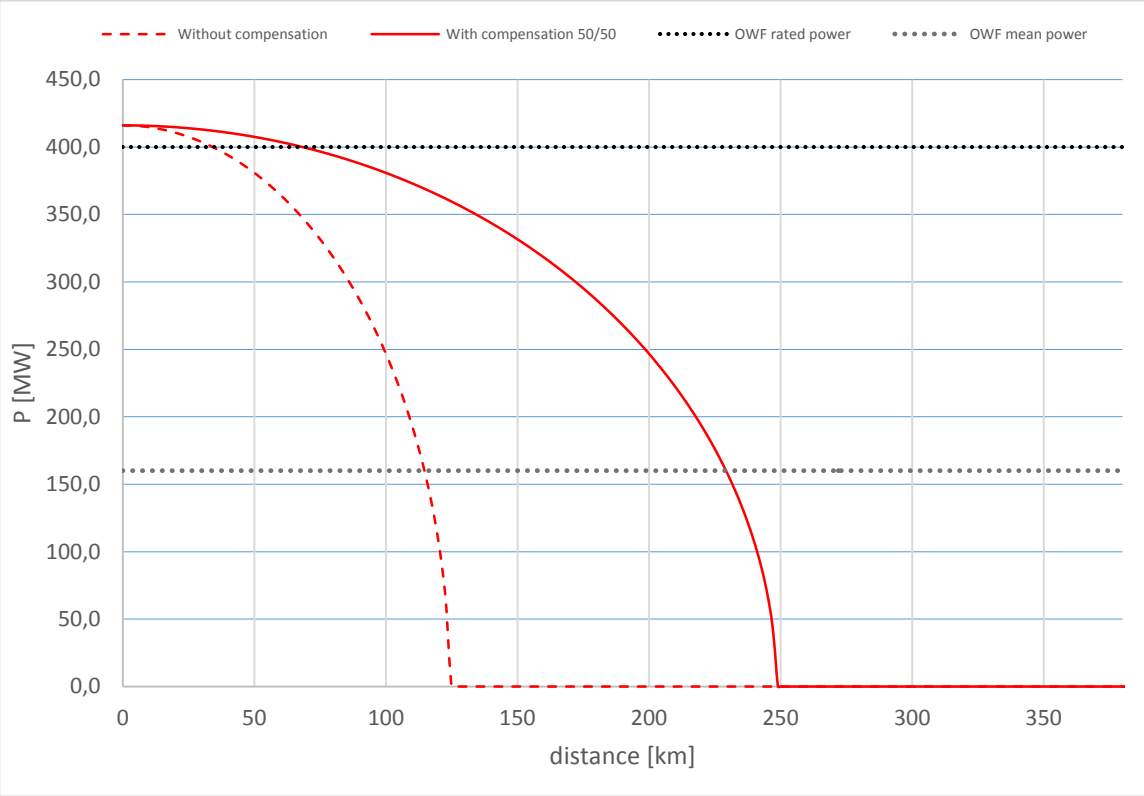

Figure 27 Power transmission capability of a 400 MW OWF employing 2·3·1000mm² HVAC cables at 150 kV (50 Hz)

shore.

To help the user, the limiting distance (the distance at which the transmission system cannot handle 100% of the OWF generated power) will be displayed for the chosen transmission characteristics. This distance can be derived from (63), and is calculated as:

$$d_{limit} = \sqrt{\left(S^2 - {P_{OWF}}^2\right) \cdot \frac{4}{{q_{tot}}^2}} \tag{64}$$

Once the user chooses the transmission system characteristics, this value is displayed along with the maximum utilization ratio. Note that if the maximum utilization ration is higher than 100%, the limit distance is 0 km, thus fulfilling the second criteria guarantees fulfilling the first one.

4. Case study

The studied case corresponds to the Bard 1 wind farm, which is the remotest offshore wind farm to date. Table 20 shows reported data over Bard1. It is situated in the North Sea (in German waters), approximatively 110 km far from shore. The power transmission is made through HVDC and this case is particularly interesting because it has suffered a series of power outages at the transmission system, translated in several months without feeding power. This leads to the following question: *Do the costs derived from the power outages compensate for using an HVDC power transmission system, instead of an HVAC one?* The following cases will be analysed:

- 1st case: a technical-economic analysis of HVAC, LFAC and HVDC power transmission systems for Bard1 will be performed, employing the designed spreadsheet tool, which incorporates the cost functions and the technical considerations presented in Chapters 2 and 3.
- 2nd case: a comparison of the actually employed HVDC power transmission system, with a chosen HVAC power transmission system and the cost of the aforementioned outages.
- 3rd case: a study of a 1000 MW OWF, taken as a general case.

Table 20 Bard 1 offshore wind farm general data [79] [80] [81]

Characteristic	*Value*	*Comments*
Rated power	400 MW	Capacity factor estimated at 0,4
Turbines	80 turbines	Each rated at 5 MW with a lifetime of 20 years
Distance to shore	112 km	Computed from the centre of the wind farm
Transmission length	194,6 km	121 km subsea and 73,6 km underground cable
Power transmission	HVDC +/-150 kV	2x1200 mm^2 Cu (Symmetric Monopolar)

The data about Bard 1 shown in Table 20 are used for the cost modelling (400MW as the OWF rated power, 20 years for the lifespan). Regarding the capacity factor and the discount rate, general values of respectively 0,4 and 6% are employed. Additionally, the energy selling price is considered 190 €/MWh, as it is stated as the Germany feed-in tariff [57]. It is also stated that the HVDC power transmission system consists in 2x1200 mm^2 copper cables (symmetric monopolar) [81]. Those data have been introduced in the model. To perform a comparison,

two alternative HVAC and one LFAC power transmission systems have been proposed. The different power transmission system data are shown in Table 20Table 21.

Table 21 Chosen power transmission system data

Characteristic	**HVDC***	**HVAC-1**	**HVAC-2**	**HVAC-3**	**LFAC****
Voltage level [kV]	±150	110	132	150	275
Electric frequency [Hz]	-	50	50	50	16,67 (50/3)
Number of cables	2 (1 pair)	3 (3-core)	3 (3-core)	3 (3-core)	2 (3-core)
Conductor cross-section [mm²]	1200	3x1000	3x630	3x500	3x300

* *Real data employed for the transmission*
** *CCV is employed for the conversion.*

The analysis considers 121 km as the transmission length, which corresponds to the subsea section of the power transmission of Bard 1. Apart from the real case employed HVDC system, four alternative transmission systems are proposed. Considering that the transmission length is 121 km , no higher HVAC voltages (e.g. 220 kV) can be considered due to the aforementioned restrictions on the power transmission capability (see Section 3.9).

Consequently, the chosen ac voltages are 110 kV and 150 kV, and the number of cables and the cross-section are selected to guarantee the power transmission capability: for lower voltage levels, a higher cross-section and number of cables is necessary. Finally, the proposed LFAC transmission system employs a cycloconverter for the frequency conversion, as it is cheaper than a B2B HVDC converter, and the goal of the analysis is to make LFAC as competitive as possible.

4.1. Results

4.1.1. First case: HVAC, HVDC, LFAC comparison

Considering a transmission distane of 121 km, the totals costs for each transmission system are presented in Table 22, whereas Figure 28 displays a general breakdown of the total costs.

Table 22 Transmission system costs at 121 km

Trans. System	**HVDC**	**HVAC-1**	**HVAC-2**	**HVAC-3**	**LFAC**
Subst. costs	238,14	56,60	58,14	59,41	158,52
Cables costs	136,41	373,48	328,87	315,74	237,93
Losses cost	138,35	157,21	161,72	171,27	129,82
Total cost [M€]	**512,90**	**587,29**	**548,73**	**546,42**	**526,27**

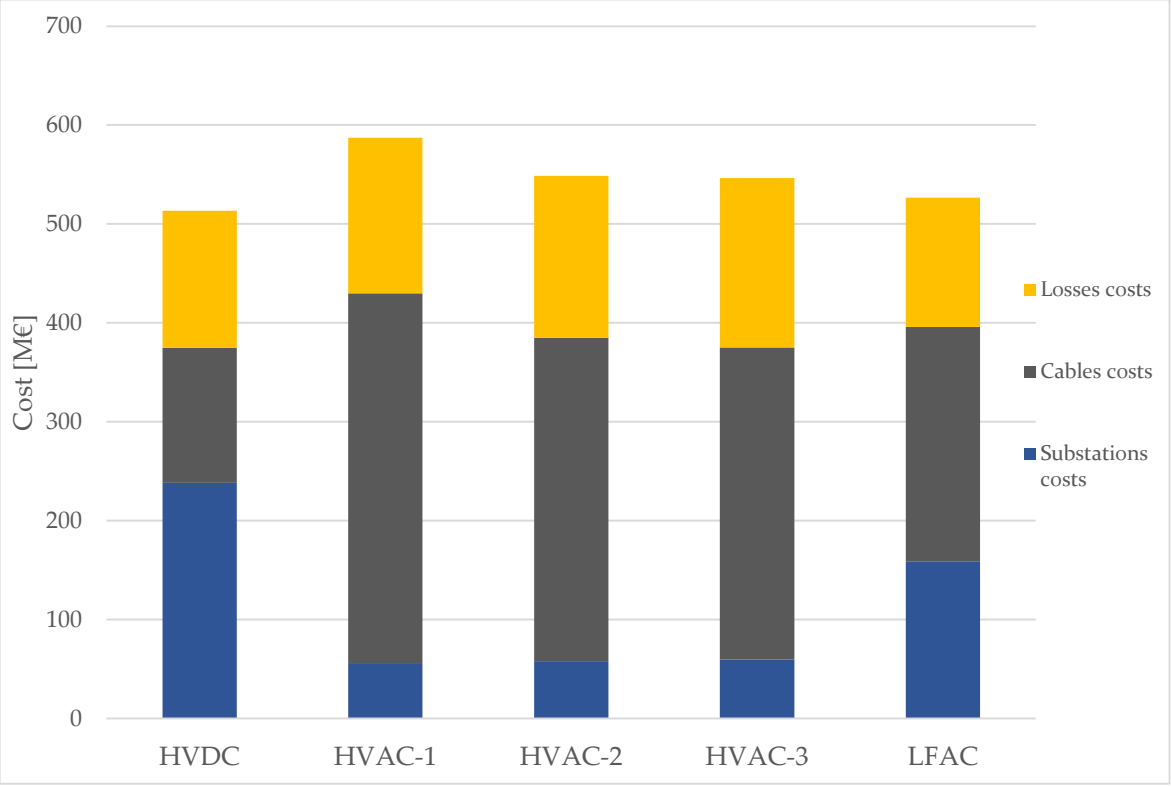

Figure 28 Costs breakdown of each transmission system. Losses cost includes all losses, cables costs include installation and supplying costs, and substation costs includes transformers, converters, switchgears and the offshore structure costs.

For the considered distance, the most economical option is the HVDC transmission system, which is indeed the actually technology chosen for the real OWF. Among the HVAC options, the transmission system at 150 kV is the most suitable. As stated in the previous sections, results confirm that substation costs are much higher in HVDC than in HVAC, whereas cables

costs remained lower. Regarding the losses, at this distance they are quite similar, due to the fact that HVDC has important losses in its converters that compensate the benefits of lower ohmic losses in the cables. On the other hand, LFAC costs are more evenly distributed between cables and substations. However, its losses remain similar to the HVAC and HVDC losses again because the converter losses compensate for lower cable losses. It should be noted that, excluding HVDC, the LFAC system was found to be cheaper than the three HVAC alternatives.

The following sections will make a more detailed analysis of the results. The first section deepens the cost breakdown, whereas the second one analyses the losses.

4.1.1.1. Costs breakdown of each proposed option

This section details the results, showing the costs of each element in the proposed transmission systems. The following tables show the costs breakdown, whereas the subsequent figures help to highlight the main cost differences between each transmission system.

Table 23 Costs breakdown of the HVDC proposed system

HVDC				
Characteristic	***Unitary cost***	***Units***	***Total***	***Comments***
Converters	78,55	2	157,09	*One per substation*
Transformers	2,68	4	10,72	*Two per substation*
Offshore structure	70,33	1	70,33	
Total substations costs			**238,14**	
Cable pair	0,73	121	88,01	*Unitary costs in M€/km*
Installation	0,40	121	48,40	
Total cables costs			**136,41**	
Cable losses	0,23	121	27,59	*In M€/km*
Transformer losses	44,31	-	44,31	*Total transformer losses*
Converter losses	66,46	-	66,46	*Total converter losses*
Total losses costs			**138,35**	
Total costs			**512,90**	

Table 24 Costs breakdown of the HVAC-1 proposed system

HVAC-1				
Concept	***Unitary cost***	***Units***	***Total***	***Comments***
Switchgears	1,31	6	7,86	*Two per cable (one in each side)*
Transformers	2,68	4	10,72	*Two per substation*
Offshore structure	38,01	1	38,01	
Total substations costs			**56,60**	
Cable pair	0,76	3x121	274,38	*Unitary costs in M€/km·cable, three cables employed*
Installation	0,27	3x121	99,10	
Total cables costs			**373,48**	
Cable losses	0,81	121	106,00	*In M€/km, includes ohmic, dielectric and compensation losses*
Transformer losses	44,31	-	44,31	*Total transformer losses*
Reactive power costs	0,06	121	6,90	*In M€/km*
Total losses costs			**157,21**	
Total costs			**587,28**	

Table 25 Costs breakdown of the HVAC-2 proposed system

HVAC-2				
Concept	***Unitary cost***	***Units***	***Total***	***Comments***
Switchgears	1,57	6	9,41	*Two per cable (one in each side)*
Transformers	2,68	4	10,72	*Two per substation*
Offshore structure	38,01	1	38,01	
Total substations costs			**58,14**	
Cable pair	0,63	3x121	229,77	*Unitary costs in M€/km·cable, three cables employed*
Installation	0,27	3x121	99,10	
Total cables costs			**328,87**	
Cable losses	0,83	121	109,91	*In M€/km, includes ohmic, dielectric and compensation losses*
Transformer losses	44,31	-	44,31	*Total transformer losses*
Reactive power costs	0,06	121	7,50	*In M€/km*
Total losses costs			**161,72**	
Total costs			**548,73**	

Table 26 Costs breakdown of the HVAC-3 proposed system

HVAC-3				
Concept	***Unitary cost***	***Units***	***Total***	***Comments***
Switchgears	1,78	6	10,67	*Two per cable (one in each side)*
Transformers	2,68	4	10,72	*Two per substation*
Offshore structure	38,01	1	38,01	
Total substations costs			**59,41**	
Cable pair	0,60	3x121	216,64	*Unitary costs in M€/km·cable, three cables employed*
Installation	0,27	3x121	99,10	
Total cables costs			**315,74**	
Cable losses	0,88	121	118,1	*In M€/km, includes ohmic, dielectric and compensation losses*
Transformer losses	44,31	-	44,31	*Total transformer losses*
Reactive power costs	0,07	121	8,86	*In M€/km*
Total losses costs			**171,27**	
Total costs			**546,41**	

Table 27 Costs breakdown of the LFAC proposed system

LFAC				
Concept	***Unitary cost***	***Units***	***Total***	***Comments***
Converter	71,37	1	71,37	*One cycloconverter at the offshore substation*
Switchgears	3,24	4	12,96	*Two per cable (one in each side)*
Transformers	7,22	4	28,87	*Two per substation*
Offshore structure	45,62	1	45,62	
Total substations costs			**158,82**	
Cable pair	0,71	2x121	171,87	*Unitary costs in M€/km·cable, two cables employed*
Installation	0,27	2x121	66,07	
Total cables costs			**237,93**	
Cable losses	0,60	121	76,33	*In M€/km, includes ohmic, dielectric*
Transformer losses	24,33	-	24,33	*Total transformer losses*

Converter losses	23,29	-	23,29	*Total converter losses*
Reactive power costs	0,05	121	5,86	*In M€/km*
Total losses costs			**129,82**	
Total costs			**526,56**	

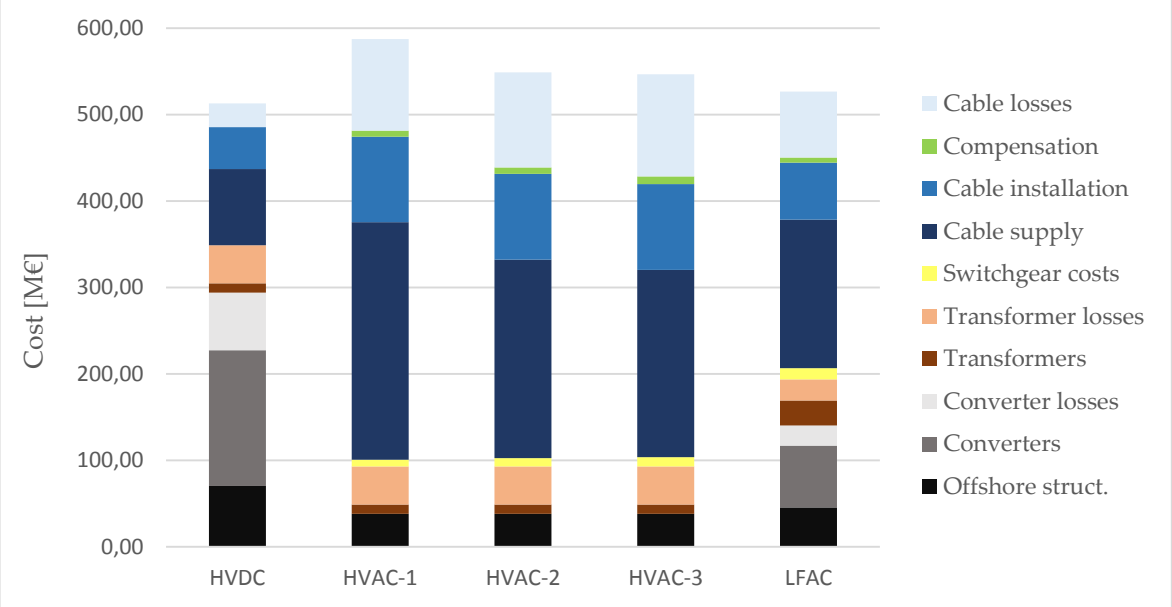

Figure 29 Costs breakdown of each proposed system

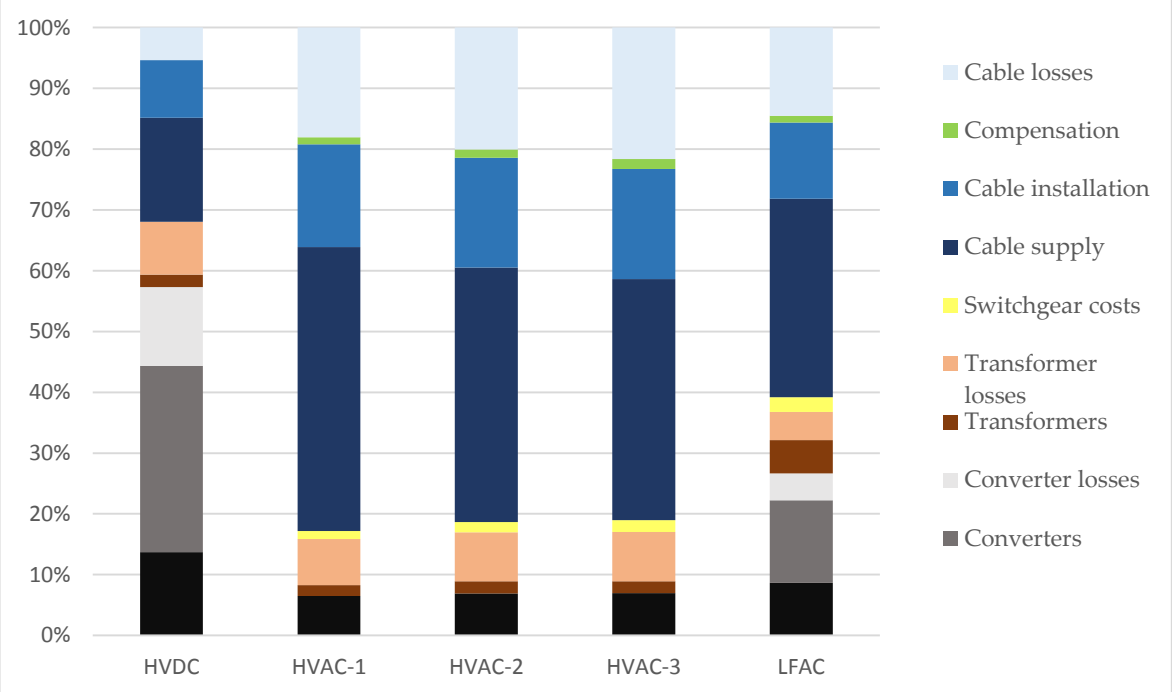

Figure 30 Costs breakdown of the HVAC-1 proposed system, in p.u.

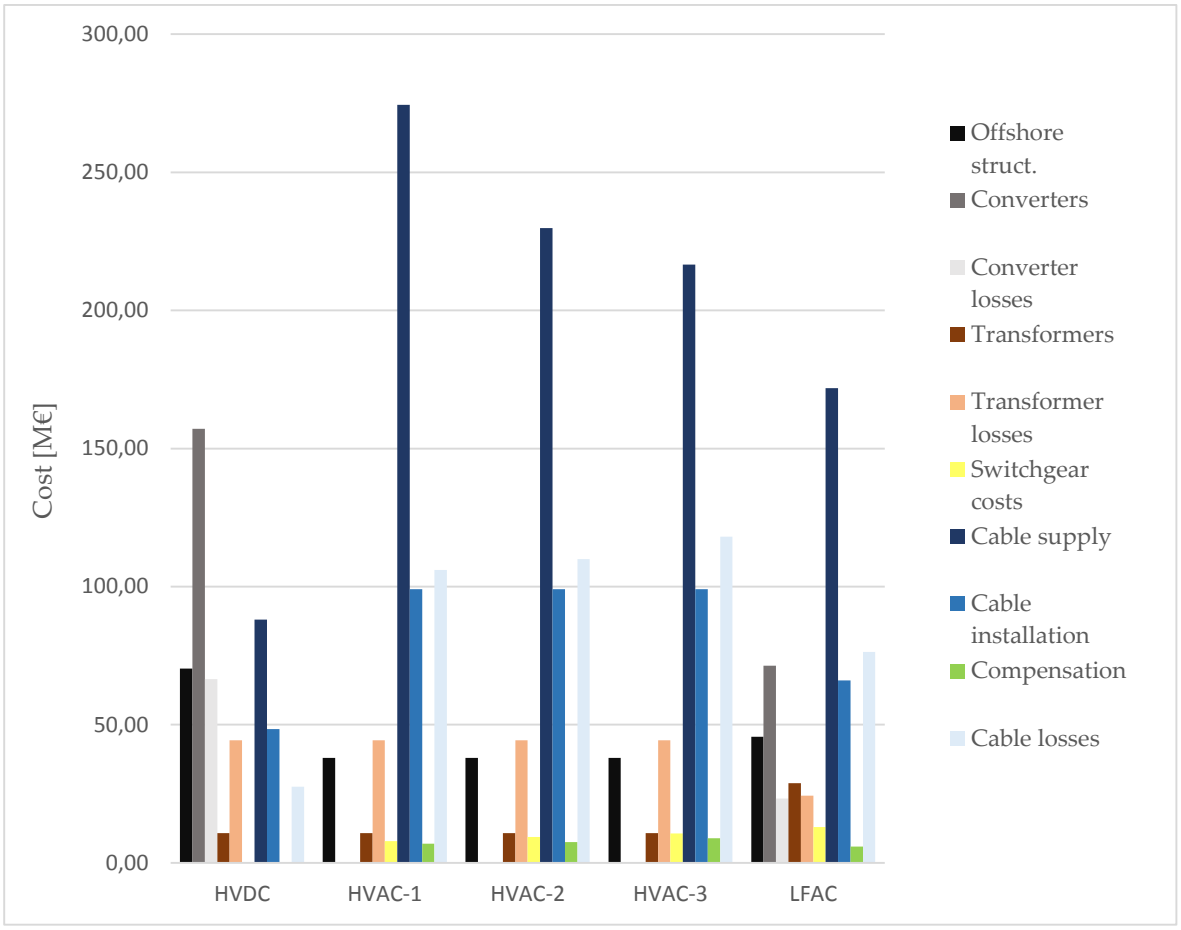

Figure 31 Costs breakdown of the HVAC-1 proposed system, comparing individuals costs

The previous figures highlight that the main costs are to be found in the cable systems (encompassing cable supply, cable installation, cable losses and reactive power compensation costs) for HVAC, which accounts for more than 80% of the total cost. The cost of the cable supply (i.e. the cost of the cables themselves) particularly stands out, representing 40-50% of the total cost. With higher voltages, a soft reduction of those costs is observed, thanks to the fact the lower cross-section can be used, which indeed translates in lower cable supply costs.

On the other hand, the converters account for more than 50% of the total cost in a HVDC transmission system. The expected cost reductions and loss reductions in the converters would definitively reduce the HVDC system costs. As the other costs are substantially lower than for HVAC, it is obvious that the further costs and losses reduction would make HVDC competitive at even shorter distances. For example, if VSC costs and VSC losses are reduced to a half, the breakeven point is to be found around 60 km, instead of around 105 km, which

is the case with the current costs.

Alternatively, the costs of LFAC are more distributed, again showing this cost behaviour in the middle between HVAC and HVDC. The cable costs also rise higher than the others do, but it could be due to the fact that no dedicated cost-function has been built for LFAC cables, employing as stated the HVAC cables cost function. It may be possible that further investigation leads to a different cost trend, more similar to those associated to HVDC.

4.1.1.2. Losses in the proposed options

Table 28 offers a detailed view of the losses in each proposed transmission system. Approximately each MW of losses equals to 20,8 M€ in costs through the OWF lifetime (considering a selling price of 190€/MWh).

Table 28 Losses breakdown for each transmission system, in MW

Losses [MW]	**HVDC**	**HVAC-1**	**HVAC-2**	**HVAC-3**	**LFAC**
Converter losses	3,20	-	-	-	1,12
Transformer losses	2,10	2,10	2,10	2,10	1,70
Ohmic losses	1,33	2,86	2,83	2,80	1,75
Dielectric losses	-	1,51	1,66	1,92	1,26
Compensation losses	-	0,74	0,81	0,96	0,63
Total losses [MW]	**6,63**	**7,21**	**7,40**	**7,78**	**6,47**

Converter losses compromise the performance of the HVDC system, accounting for almost the half of the losses. Nevertheless, with a higher cross-section and lower electric resistance, the cable ohmic losses are lower in dc. Additionally, accounting that it has no dielectric losses and no compensation is needed (thus no losses in the reactive compensation systems), HVDC presents lower losses than the HVAC systems. For higher distances, this is even more exaggerated, as ohmic losses continue to grow over the distance, whereas the converter losses remain the same.

On the other hand, the LFAC proposed system present the overall lowest losses. Although it suffers from every type of losses, each individual loss component is lower than for the other systems: higher voltage and lower frequency result in lower ohmic losses, a lower reactive power generation translates in decreased dielectric and compensation losses, and finally a lower frequency implies a reduction in the transformer losses. Additionally, it has less converter losses than a VSC-HVDC, as it employs a single converter, whose losses are

considered lower.

Regarding HVAC systems, it is noticed that the higher losses are in the 150-kV system. A higher voltage level implies higher reactive power, thus more dielectric and compensation losses. One could expect to observe a substantial decrease in the ohmic losses as the voltage level goes up, but in fact, the ohmic losses are more or less the same for each voltage level. That is because a lower cross-section is employed for higher voltages, to reduce the cable costs. The reduction on the current is compensated by the reduction on the cross-section, which increases the electric resistance.

Figure 32 and Figure 33 display interesting additional charts to enhance the comprehension of the losses patterns.

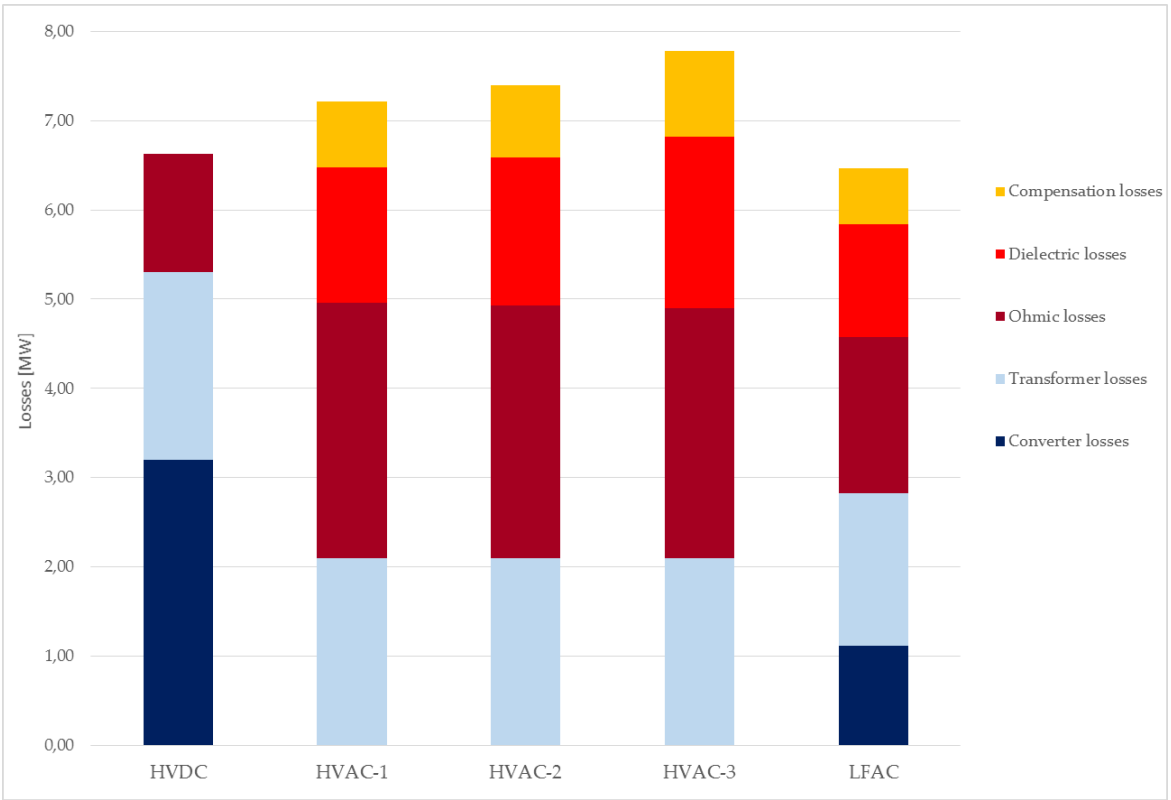

Figure 32 Losses breakdown for each transmission system, in MW

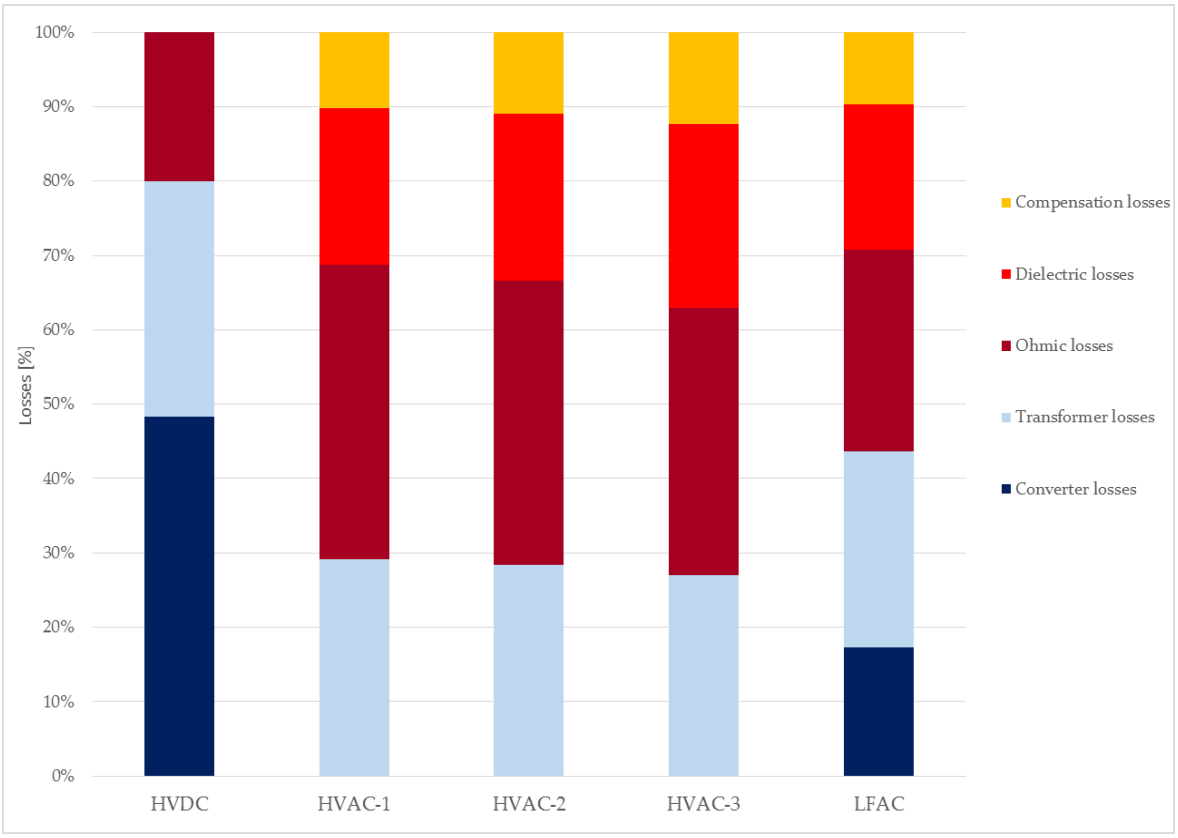

Figure 33 Losses distribution of each transmission system

Note that for HVAC systems, cable losses (ohmic and dielectric losses) make up for circa 60% of the total losses. Additionally, two interesting remarks can be made, in view of the previous figures:

- A reduction of the VSC losses would make a great impact in the losses of the HVDC-VSC system. For instance, lowering the converter losses by 50% would reduce total costs by 33 M€.
- A reduction of the transformer losses would benefit any power transmission system, as the transformer losses represent around 25% of the total losses.

This first comparison has taken a deeper look about the cost and losses of each system, highlighting the main differences between them, and comparing the obtained results. The next analysis will estimate whether HVDC is the most suitable option, considering the outages experienced at Bard 1.

4.1.2. Second case: Suitability of HVDC taking into consideration the power outages experienced in Bard 1

For this section, a comparison is drawn between the actual employed HVDC system and a proposed HVAC system. Taking into account the results obtained in Section 4.1.1, the HVAC-3 transmission system will be considered for this comparison. For the considered Bard 1 characteristics, the HVDC has a cost advantage of 33,5 M€ over HVAC-3, but the cost of the outages could surpass this cost difference.

At first, a deeper look on the experienced outages should be done. No official source from Bard 1 owner details all the power outages, although many scientific newspapers report the different and repeated transmission problems [82] [83] [84] [85] [86]. No clear information has been found about the specifics of the transmission problems, although the following facts are repeatedly reported:

- The project was three years out of schedule;
- The transmission problems are located at the offshore converter substation (named BorWin 1). A smouldering fire took place in March 2014, in the converter platform.
- The wind farm owner, instead of relying in an experienced supplier (ABB, Siemens, Alstom wind), manufactured the converter within its own company.

It seems clear that the source of problems is in the offshore substation, more precisely in the converter, which was not manufactured by any reputed supplier. Regarding the duration of outages, different power outages of variable duration are reported in the referenced sources:

- 3 months outage from October 2013 to January 2014;
- 57 days outage from 23 March 2014 to May 2014, extending to July 2014;
- Several short-duration outages. For example, 17 days of cumulated outages in January and February 2015.

The exact cumulated duration of all the power outages is not clear. However, based on the reports, it is at the very least 74 days without any power deliver, and it is probably more than 160 days.

The cost of these outages is estimated as the cost of non-delivered energy. Assuming a capacity factor of 0,4, and taking into account the German feed-in tariff of 190 €/MWh; each outage day translates into 729,6 k€ of non-delivered energy. Figure 34 shows the cost of those outages being included in the total costs of the HVDC system.

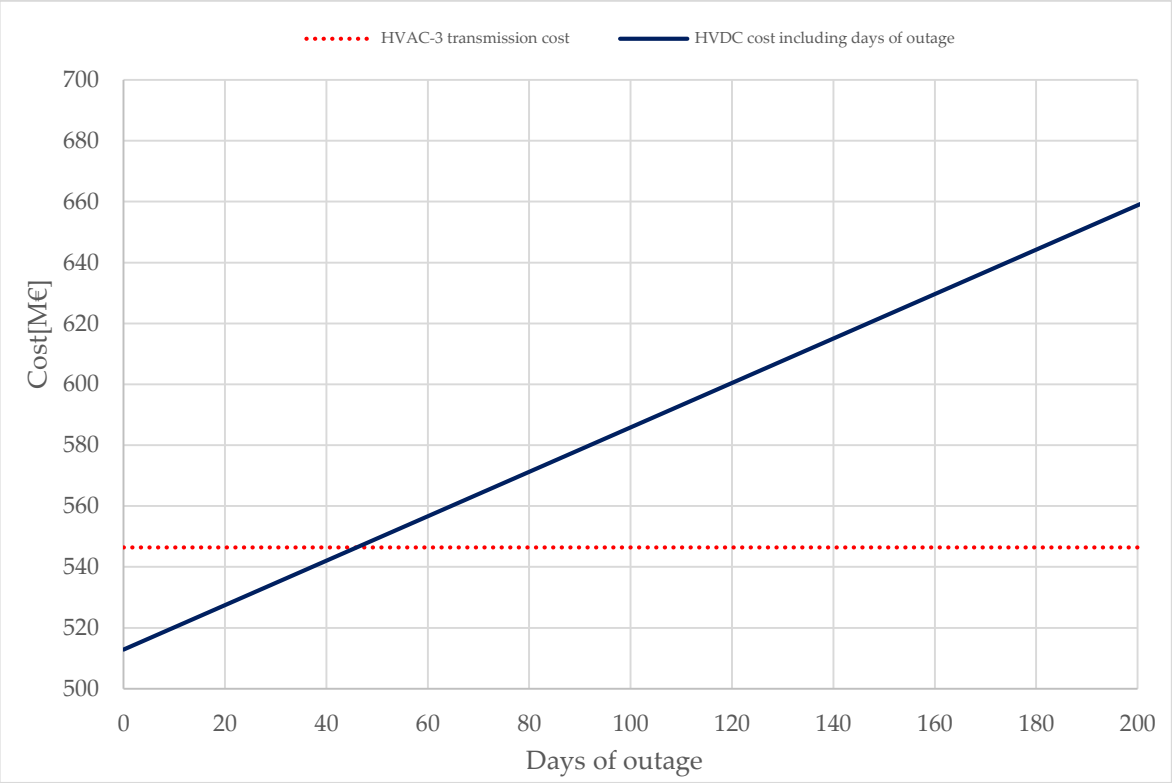

Figure 34 Costs of the HVDC transmission system for Bard 1, compared to the costs of the proposed HVAC-3 transmission system; including the cost of outages.

After 46 days of total outage, the HVDC system results more expensive than the proposed HVAC-3 transmission system. Considering that on the most optimistic point of view, there are at least 74 days without any power delivery, it is clear that an HVAC system would have been a much better option for Bard offshore 1: assuming 74 days without operation, the HVDC total costs exceeds the HVAC considered one by 21 M€. At 160 days of cumulated outage, the cost difference rises up to 83 M€.

4.1.3. Additional case study: optimal power transmission system for a 1000 MW wind farm

It has already been stated that the future of offshore wind leads to larger and more isolated wind farms [87]. For this reason, it is interesting to study the power transmission system for a

remote 1 GW offshore wind farm. Apart from a power rating of 1 GW, a capacity factor of 40%, lifespan of 20 years, discount rate of 8%, and an energy price of 100 €/MWh are considered. Table 29 shows the characteristics of proposed transmission systems for this wind farm, whereas Figure 35 shows the cost of those transmission systems.

Table 29 Proposed transmission systems for a 1000 MW wind farm

Characteristic	**HVDC**	**HVAC**	**LFAC***
Voltage level	±300 kV	132 kV	275 kV
Electric frequency	-	50 Hz	16,67 Hz (50/3)
Number of cables	2 (one pair)	6 (three-core)	3 (three-core)
Conductor cross-section	1600 mm²	3x1000 mm²	3x1000 mm²

** B2B-VSC is employed for the conversion*

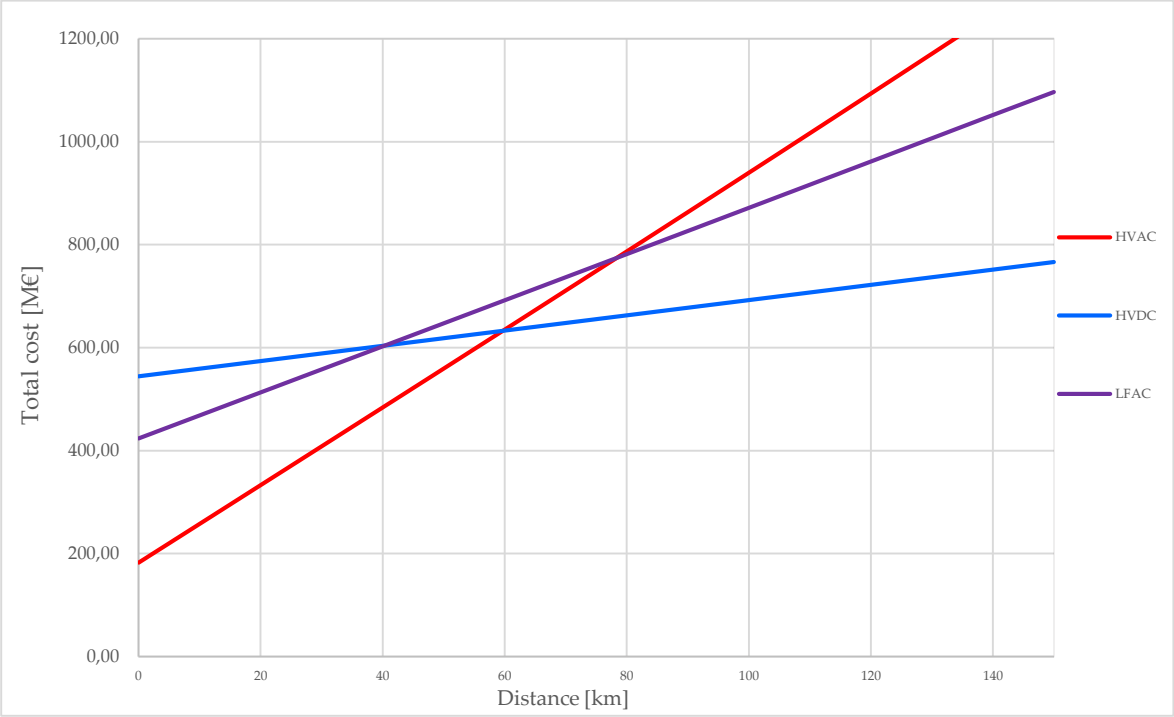

Figure 35 Costs of the proposed power transmission systems, as a function of the distance

It was expected that LFAC costs would be the lowest ones in the 50-80 km range, but LFAC is not predominant at any distance. However, the costs of the LFAC converter could have been estimated too high. In fact, if the ac-ac converter costs are halved, the LFAC transmission system becomes the optimal option in the 50-70 km range. Regarding LFAC, further

investigation is needed, particularly regarding the converter costs, but its economic feasibility is absolutely not discarded.

Excluding LFAC, the break-even point between HVAC and HVDC costs stands at 59 km. Accounting the variability, the break-even point falls in the 52-70 km range (see Figure 36).

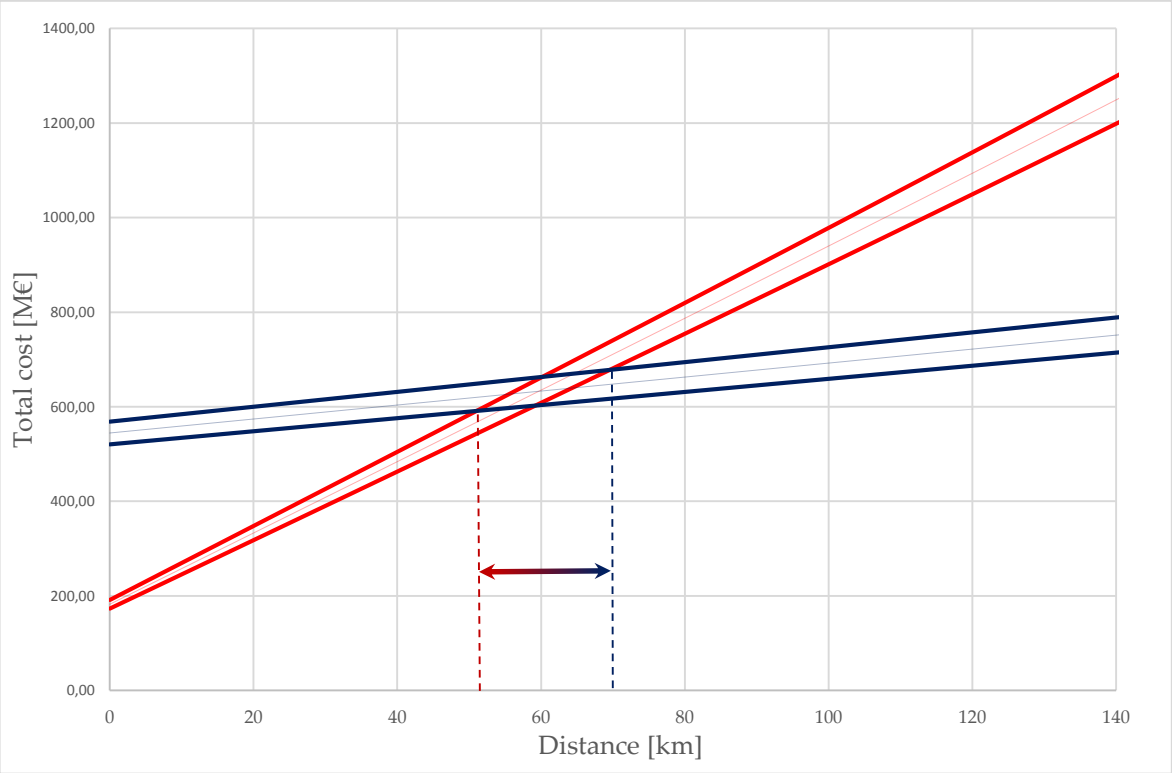

Figure 36 Break-even area for the proposed HVAC and HVDC transmission systems

Looking at the previous figure, it seems that the statement made by researchers could be confirmed for large and isolated wind farms: it is often claimed that HVDC is the most economic option for distances to shore around 50 km. This work has found that this statement remains true for large OWF, with a rated power close to 1 GW, provided that the HVDC transmission system can achieve a high availability.

Conclusions

As discussed in the introduction, the development of large and remote offshore wind farms is a reality. In the coming years, we will see offshore wind power becoming a major element of the European energy resources, thus increasing the relevance of the power transmission system. In this thesis a technical-economic analysis tool to select the power transmission systems for offshore wind farms was successfully developed.

For the technical part, the different available technologies – HVAC, HVDC, … – have been carefully examined, focusing on its main strengths and weaknesses; as well as exposing the role of the main components. The economic analysis has established cost patterns that were hitherto not available, and has combined these into a model giving the total costs of a power transmission, given an OWF design and a set of transmission parameters. The latter has been implemented in an open-access spreadsheet, that includes all the cost functions, as well as the loss calculations and availability costs. The spreadsheet includes detailed instructions for the user on how to introduce the variables, and display the necessary results, accounting the cost functions variability. Upon request, a non-protected version of the spreadsheet can be provided, in order to introduce alternative cost functions or to improve the models.

The studied cases have successfully test the economic model, providing interesting results:

- From the first case study, it can be concluded that reliability issues can completely modify the transmission costs. Because of that, reliability was included as a factor in the economic analysis and in the spreadsheet.
- The break-even point between HVAC and HVDC generally falls in the 50-100 km range. It strongly depends on the OWF characteristics and the different transmission parameters (e.g. voltage level, cable cross-section), although as a general statement it can be said it is close to 50 km for large offshore wind farms (e.g. 1000 MW) and around 100 km for lower power ratings (e.g. 400 MW).
- The feasibility of LFAC is not discarded, and is found to be very dependent on its substations costs, particularly on the cost of the low-frequency converters. Depending

on the latter, LFAC would be the most suitable technology in the medium distance range, e.g. 50-70 km.

- Although it is true that, for the studied cases, the losses in the HVDC systems are lower, the main loss-related difference between HVAC and HVDC is in the distribution of the losses. For HVAC, they are mostly situated in the cables, whereas for HVDC the biggest share of the losses is in the converters. This is particularly important because the losses in the HVDC converters are expected to further decrease (they have decreased from 3% down to 1% in the last decade), whereas not much improvement is to be expected in the HVAC cable losses (at least until superconducting cables do not appear to reduce the resistivity of copper).

Finally yet importantly, this work has provided some cost functions that were previously not found in the literature, and are encouraged to be used. The aim of this thesis is considered to be completely fulfilled, having provided a tool which determines the costs of a power transmission system for OWF, as well as having carefully studied the position of the break-even point.

On the other hand, this works leaves room for future work, which could expand the usefulness of the technical-economic analysis:

- A deeper study on the costs of ac-ac frequency converters;
- Expanding and refining the cost functions with extensive cost data provided by suppliers;
- Converting the tool into an iterative program, that accounts the power changes along the transmission (e.g., taking into account the voltage drop along the cable);
- The next step would be to achieve an optimization model, which could directly return the optimal power transmission system for a given OWF. Note that the equations provided in this work could be absolutely employed for this purpose.

References

[1] GWEC, "Global Wind Report," 2014.

[2] EWEA, "Wind Energy Scenarios for 2020," July 2014.

[3] EWEA. (2014) Annual Statistics. [Online]. http://www.ewea.org/fileadmin/files/library/publications/statistics/EWEA-Annual-Statistics-2014.pdf

[4] EY (Ernst & Young associates), "Offshore wind in Europe," March 2015.

[5] 4Coffshore. [Online]. http://www.4coffshore.com/windfarms/ravnsborg-denmark-dk06.html

[6] LORC. Middlegrunden data. [Online]. http://www.lorc.dk/offshore-wind-farms-map/middelgrunden

[7] The Crown Estate, "Offshore wind cost reduction : Pathways study," May 2012.

[8] EWEA. (March 2015) [Online]. http://www.ewea.org/press-releases/detail/2015/03/10/offshore-wind-industry-can-compete-with-gas-and-coal-within-a-decade/

[9] Dirk Schoenmakers, "Optimization of the coupled grid connection of offshore wind farms," 2008.

[10] EWEA. (2014) European Offshore Statistics. [Online]. http://www.ewea.org/fileadmin/files/library/publications/statistics/EWEA-European-Offshore-Statistics-2014.pdf

[11] N. Barberis Negra, J. Todorovic, L. Lazaridis T. Ackermann, Evaluation of Electrical

Transmission Concepts for Large Offshore Wind Farms, 2007.

[12] R. Teixeira Pinto, "MULTI-TERMINAL DC NETWORKS - System Integration, Dynamics and Control," 2014.

[13] Camilo Lancheros, "Transmission systems for offshore wind farms: a technical, environmental and economical assesment," 2013.

[14] Shanshan Wang, Guangfu Tang, and Zhiyuan He, "Comprehensive evaluation of VSC-HVDC transmission based on improved analytic hierarchy process," in *Electric Utility Deregulation and Restructuring and Power Technologies, 2008. DRPT 2008. Third International Conference on*, Nanjuing, 2008, pp. 2207-2211.

[15] Tsuyoahi Funaki and Kenji Matsuura, "Feasibility of the Low Frequency AC transmission," 2000.

[16] Xifan Wang and Xiuli Wang, "Feasibility Study of Fractional Frequency Transmission System," *IEEE transactions on power systems*, vol. 11, no. 2, pp. 962-697, May 1996.

[17] Shi You, Zhao Xu and Vladislav Akhmatov Nan Qin, "Offshore wind farm connection with low frequency AC technology".

[18] Dr. Ronan Meere and Dr. Terence O'Donnell Mr. Jonathan Ruddy, "Comparison of VSC-HVDC with Low Frequency AC for Offshore Wind Farm Design and Interconnection," in *EERA Deepwind*, 2015.

[19] K. Meah and S. Ula, "Comparative evaluation of HVDC and HVAC transmission systems," in *IEEE Power Engineering Society – General Meeting*, June 2007.

[20] J. Todorovic and T. Ackermann N. Barberis Negra, Loss Evaluation of HVAC and HVDC Transmission Solutions for Large Offshore Wind Farms, 2006.

[21] Golder Associates, "Study on the comparative merits of overhead electricity transmission lines versus underground cables," May 2008.

[22] Markel Zubiaga, "Power AC Transmission Lines, Energy Transmission and Grid

Integration of AC Offshore Wind Farms, MSc Markel Zubiaga," INTECH, 2012. [Online]. http://www.intechopen.com/books/energy-transmission-and-grid-integration-of-ac-offshore-wind-farms/power-ac-transmission-lines

[23] Vinay Mehrotra, Ajith Varghese, Hali Moleski, Richard Marek, Bill Henning, Hasse Nordman, Jim Thompson H. Jin Sim, Comparison of Standards – ANSI / IEEE and IEC , Comparison of standards.

[24] Lars Liljestrand, Flemming Krogh, Johan Karlstrand, and Jutta Hanson Stefan G. Johansson, "AC cable solutions for offshore wind energy,". [Online]. http://wind.nrel.gov/public/SeaCon/Proceedings/Copenhagen.Offshore.Wind.2005/documents/papers/Poster/S.G.Johansson_ACCablesolutionsforOffshoreWindEnergy.pdf

[25] Sthitadhee Sarkar, "Power Transmission Options for Offshore Windfarms in Scotland," Department of Mechanical and Aerospace Engineering, University of Strathclyde., 2012.

[26] Nexans. (2003) Nexans Submarine Power Cables. [Online]. http://www.nexans.com/Germany/group/doc/en/NEX_Submarine_neu.pdf

[27] Rick Schlobohm and Bill Brownell Larry Pryor. http://apps.geindustrial.com/. [Online]. http://apps.geindustrial.com/publibrary/checkout/Alum-Copper?TNR=White%20Papers%7CAlum-Copper%7Cgeneric

[28] ABB. ABB power cables. [Online]. http://www.abb.com/cawp/seitp202/9121cb7988318aecc1257b200039da24.aspx

[29] Angelo Baggini, "The updated EU energy efficiency standardisation of HV and MV transformers," in *INTERNATIONAL ENERGY EFFICIENT TRANSFORMERS WORKSHOP 2013, 42ND MEETING OF THE APEC EGEE&C*, Bangkok, November 2013.

[30] ABB. (2011) ABB power transformers. [Online]. https://library.e.abb.com/public/a2492a9e17a69c1a83257984002ada63/Global_low%20res.pdf?filename=Global_low%20res.pdf

[31] Constantinos Sourkounis and Pavlos Tourou, "Grid Code Requirements for Wind Power Integration in Europe," in *Power Options for the Eastern Mediterranean Region*, Limassol, Cyprus, 2012.

[32] Overview of line-commutated based HVDC, Document available on CIGRE website.

[33] N. Aparicio, S. Añó-Villalba, and S. Bernal-Perez R. Blasco-Gimenez, "LCC-HVDC Connection of Offshore Wind," *IEEE Transactions on industrial electronics*, vol. 60, no. 6, pp. 2372-2380, June 2013.

[34] S. Norrga, "VSC HVDC - Past , Present and Future," in *14th European Conference on Power Electronics and Applications*, Birmingham, 2011.

[35] Alstom Grid. (2011, June) alstom.com. [Online]. http://www.alstom.com/Global/CleanGrid/Resources/Documents/HVDC-VSC%20transmission%20technology%20of%20the%20future%20-%20Think%20Grid%20n%C2%B08%20.pdf

[36] J. Leon, R. Portillo, L. Franquelo, and M. Aguirre J. Napoles, "Selective harmonic mitigation technique for high-power converters," *IEEE Transactions on industrial electronics*, vol. 57, no. 7, pp. 2315-2323, July 2010.

[37] K. Friedrich, "Modern HVDC PLUS Application of VSC in Modular Multilevel Converter Topology," in *IEEE International Symposium on Industrial Electronics*, 2010.

[38] R. Belmans S. Cole, "Transmission of Bulk Power: The History and Applications of Voltage-Source Converter High-Voltage," *IEEE Ind. Electron. Magazine*, no. 6, 2009.

[39] L.A. Gregoire, J. Bélanger W. Li, "Control and Performance of a Modular Multilevel Converter System," in *Conference on Power Systems* , Halifax, September 2011.

[40] H. Duchen, M. Karlsson, L. Ronstrom and B. Abrahamsson Y. Jiang-Hafner, "HVDC with Voltage Source Converters - A powerful black start capability," in *IEEE PES Conference*, Chicago, April 2008.

[41] M. Barnes and A. Beddard, "Voltage Source Converter HVDC Links - The state of the art and issues going forward," *Energy procedia*, no. 24, pp. 108-122, January 2012.

[42] P.S. Alstom Grid, Stafford, UK Jones and C.C Davidson, "Calculation of power losses for MMC-based VSC HVDC stations," in *15th European conference on Power Electronics and Applications*, Lille, 2-6 September 2013.

[43] ABB. [Online]. http://new.abb.com/systems/hvdc/hvdc-light

[44] Kazutoshi ABE, Makoto SUIZU, Shoji MASHIO, Osamu MATSUNAGA, Shinya ASAI and Shoshi KATAKAI , J-Power Systems Corporation Yoshinao MURATA, "HVDC XLPE CABLE SYSTEMS APPLICABLE FOR HIGHER TEMPERATURE AND POLARITY REVERSAL OPERATION ," in *8th International Conference on Insulated Power Cables*, Versailles, June 2011.

[45] R. Teixeira Pinto, "Multi-Terminal DC Networks : System Integration, Dynamics and Control," TU Delft, Doctoral Thesis March 2014.

[46] A. Raza, Xu Dianguo, Su Sunwen, and Li Wiexing, "Modeling and control of multi terminal VSC HVDC transmission system for integrating large offshore wind farms," in *Multi-Topic Conference (INMIC), 2014 IEEE 17th International*, Karachi, December 2014, pp. 467-472.

[47] Silvio Rodrigues, R. Teixeira Pinto, P. Bauer, and J. Pierik, "Optimization of social welfare and transmission losses in offshore MTDC networks through multi-objective genetic algorithm," in *Power Electronics and Motion Control Conference (IPEMC), 2012 7th International* , Harbin, China, June 2012, pp. 1287-1294.

[48] S. Rodrigues, R.T. Pinto, P. Bauer, and J. Pierik, "Optimal Power Flow Control of VSC-Based Multiterminal DC Network for Offshore Wind Integration in the North Sea," *Emerging and Selected Topics in Power Electronics, IEEE* , vol. 1, pp. 260-268, September 2013.

[49] Urban Axelsson, Andre Canelhas Espen Olsen, "Low Frequency AC Transmission on large scale Offshore Wind Power Plants," in *13th wind integration workshop*, Berlin, November 2014, pp. 559-564.

[50] Y. Tang, L. Ran, T. Yang, J. Yu P. B. Wyllie, "Low Frequency AC Transmission - Elements of a Design for Wind Farm Connection," 2013.

[51] Truls Normann, Ultra-long Subsea Power Transmission Using Frequency Step-up Equipment, April 2014, Presentation from MCE deepwater development.

[52] Michael H. Johnson and Dionysios C. Aliprantis Hao Chen, "Low-Frequency AC Transmission for Offshore wind power," *IEEE transactions on power delivery*, vol. 28, no. 4, pp. 2236-2244, October 2013.

[53] K. Rudion, A. Orths, P. B. Eriksen, H. Abildgaard and Z. A. Styczynski C. Nguyen Mau, Grid Connection of Offshore Wind Farm based DFIG with Low Frequency AC Transmission System, 2010.

[54] Daniel J. Rogers, Carlos E. Ugalde-Loo, Jun Liang ,Oriol Gomis-Bellmunt José Luis Domínguez-García, "Effect of non-standard operating frequencies on the economic cost of offshore AC," *Renewable energy : an international journal*, no. 44, pp. 267-280, 2012.

[55] M. De Prada-Gil, O. Gomis-Bellmunt, A. Sumper J.L Domínguez García, "Technical and economic assessment of offshore ac hubs operating at non-standard frequencies," in *13th Wind Integration Workshop*, Berlin, November 2014, pp. 565-570.

[56] Navigant consulting, Inc. (2013, October) U.S. Office of Energy Efficiency and Renewable Energy (EERE). [Online]. http://www1.eere.energy.gov/wind/pdfs/offshore_wind_market_and_economic_analysis_10_2013.pdf

[57] offshore-windenergie.net, http://www.offshore-windenergie.net/en/politics/eeg-remuneration, Germany feed-in tariffs.

[58] ENTSOE. (2011, November) Offshore transmission technology. [Online].

https://www.entsoe.eu/fileadmin/user_upload/_library/publications/entsoe/SDC/European_offshore_grid_-_Offshore_Technology_-_FINALversion.pdf

[59] Ragnar Ulsund, "Offshore Power Transmission: Submarine high voltage transmission alternatives," June 2009.

[60] G. Forte, M. Pisani and M. Trovato M. Dicorato, "Guidelines for assessment of investment cost for offshore wind generation," *Renewable Energy*, no. 36, pp. 2043-2051, 2011.

[61] Lyndon Greedy, Fabio Spinato, Colin A Morgan Andrew R Henderson, "Optimising Redundancy of Offshore Electrical Infrastructure Assets by Assessment of Overall Economic Cost ," in *European Offshore Wind Energy Conference*, Stockholm, September 2009.

[62] Stefan Lundberg, "Performance comparison of wind park configurations," Göteborg, 2003.

[63] Bram Van Eeckhout, "The economic value of VSC HVDC compared to HVAC for offshore wind farms," 2007-2008.

[64] Eurostat, http://ec.europa.eu/eurostat/inflation-dashboard/, Eurozone statisitcal economic data.

[65] Open electrical. http://www.openelectrical.org. [Online]. http://www.openelectrical.org/wiki/index.php?title=Cable_Impedance_Calculations

[66] General Cable. http://www.generalcable.co.nz. [Online]. http://www.generalcable.co.nz/getattachment/a4c607a4-d112-40dd-9306-e1c2af3ed7d3/AC-Resistance,-Skin-Proximity-Effects.aspx

[67] ABB. (2010, April) https://library.e.abb.com. [Online]. https://library.e.abb.com/public/2fb0094306e48975c125777c00334767/XLPE%20Submari

ne%20Cable%20Systems%202GM5007%20rev%205.pdf

[68] Tushar Mehta. (2012, December) [Online]. http://www.tushar-mehta.com/excel/newsgroups/interpolation/#Two%5Fdimensional%5Finterpolation%5F

[69] Nor Akmal Mohd. Jamail, Nor Anija Jalaludi Asmarashid Ponniran, "Tan Delta and Capacitance Characteristics of Underground XLPE Cables ," in *Malaysian Technical Universities Conference on Engineering and Technology*, Kuantan, June 2009.

[70] Anuchit Aurairatch, "A PRELIMINARY STUDY OF LOSS FACTOR IN DIELECTRIC OF CABLE PRODUCED IN THAILAND," 2006.

[71] Asmarashid Ponniran and Muhammad Saufi Kamarudin, "Study on the Performance of Underground XLPE Cables in Service Based on Tan Delta and Capacitance Measurements," in *2nd IEEE International Conference on Power and Energy*, Johor Baharu, December 2008, pp. 39-43.

[72] A. Cancino and R.Malewski, "TESTING AND LOSS MEASUREMENT OF HV SHELL-TYPE SHUNT-REACTORS AT VERY LOW POWER FACTOR," 2004.

[73] Stefan Fassbinder, "EFFICIENCY AND LOSS EVALUATION OF LARGE POWER TRANSFORMERS," *ECI Publication No Cu0144*, May 2013.

[74] Lazaros P. Lazaridis, "Economic Comparison of HVAC and HVDC Solutions for Large Offshore Wind Farms under Special Consideration of Reliability," Stockholm, 2005.

[75] Masatoshi SAKAMAKI, Kazutoshi ABE, Yoshiyuki INOUE, Shoji MASHIO, Seiji KASHIYAMA, Osamu MATSUNAGA, Tsuyoshi IGI, Masaru WATANABE, Shinya ASAI and Shoshi KATAKAI Yoshinao MURATA*, "Development of High Voltage DC-XLPE Cable System," April 2013. [Online]. http://global-sei.com/technology/tr/bn76/pdf/76-09.pdf

[76] ABB, HVDC light power cables, 2006.

[77] Lie Xu, Brendan Fox Sarah Foster, "Control of an LCC HVDC System for Connecting

Large Offshore Wind Farms with Special Consideration of Grid Fault," in *Power and Energy Society General Meeting - Conversion and Delivery of Electrical Energy in the 21st Century*, Pittsburgh, July 2008, pp. 1-8.

[78] Maja Harfman T. , Song Chi, Satish K. Gunturi, Rajib Datta Joseph Song-Manguelle, "Power Transfer Capability of HVAC Cables for Subsea Transmission and Distribution Systems".

[79] http://www.4coffshore.com/windfarms/bard-offshore-1-germany-de23.html%3EBARD%20Offshore%201, Detailed data about Bard 1 offshore wind farm.

[80] http://www.lorc.dk/offshore-wind-farms-map/bard-offshore-1, Detailed data about Bard 1 offshore wind farm (2).

[81] http://www.4coffshore.com/windfarms/hvdc-converter-borwin1-converter-cid1.html, Information about the Bard1 power transmission system.

[82] Sara Knight, "Politics block German offshore wind link," *Wind Power Monthly*, May 2015.

[83] "'Dirty electricity' probe at BorWin1," *Renews*, June 2014.

[84] Sara Knight, "Bard 1 transmission problems continue," *Wind Power Offshore*, June 2014.

[85] Pierre L. Gosselin, Spiegel: Germany's Large-Scale Offshore Windpark Dream Morphs Into An Engineering And Cost Nightmare, June 2014, Science Blog.

[86] Pierre L. Gosselin, Giant 400 MW BARD I Offshore Windpark Shut-Down Extended Yet Again! Delay Is Now More Than 1 Year !, June 2014, Science Blog.

[87] C. Restrepo, E. Kontos, R. Teixeira Pinto, P. Bauer S. Rodrigues, "Trends of offshore wind projects," *Renewable and Sustainable Energy Reviews*, vol. 49, pp. 1114-1135, September 2015.

[88] Global Marine Energy, Lessons Learned: Offshore cable installation, 2010.

[89] UK government, "Contracts for Difference (CFD) Allocation Round One Outcome ," February 2015.

[90] Navigant, "Offshore Wind Market and Economic Analysis," October 2013. [Online]. http://www1.eere.energy.gov/wind/pdfs/offshore_wind_market_and_economic_analysis_10_2013.pdf

[91] IRENA, "RENEWABLE ENERGY TECHNOLOGIES - Cost analysis series : Wind Power," June 2012.

Appendix 1 : Budget

The budget of this thesis accounts for research and development of this present work, as well as involved office equipment and software.

Office equipment

A laptop is necessary in order to conduct the research and develop the cost functions, as well as to write the thesis.

Table 30 Office equipment budget

Concept	Unitary price	Units	Total
Mountain workstation	950 €	1	950 €
TOTAL			**950 €**

Development tools and software

In order to access to most of the information, purchase of various IEEE articles is required, as well as MS Excel and Minitab to develop and analyse cost patterns.

Table 31 Development tools and software budget

Concept	Unitary price	Units	Total
IEEE article subscription	27,85 € (per article)	90	2506,5 €
MS Excel	60 € (Excel Home)	1	60 €
Minitab software	30 € (six months license)	1	30 €
TOTAL			***2596,5 €***

Labour

Labour costs are divided respectively in research hours, development hours and writing hours, assuming the salary of a junior researcher at 40€/h.

Table 32 Labour budget

Concept	Unitary price	Units	Total
Research	40 €/h	200	8000 €
Development	40 €/h	150	6000 €
Writing	40 €/h	200	8000 €
TOTAL			***22000 €***

Total budget

Table 33 Total budget

Concept	Total
Office equipment	950 €
Development tools and software	2596,5 €
Labour	22000 €
TOTAL (without taxes)	***25456,5 €***
TOTAL (21% tax)	***30802,37 €***

The budget of this work is therefore set at 30802,37 €.

Appendix 2: Designed tool

The tool consists in a MS Excel spreadsheet organized in five different sheets. The first one gives the necessary instructions to correctly utilize the program, and where to find general information.

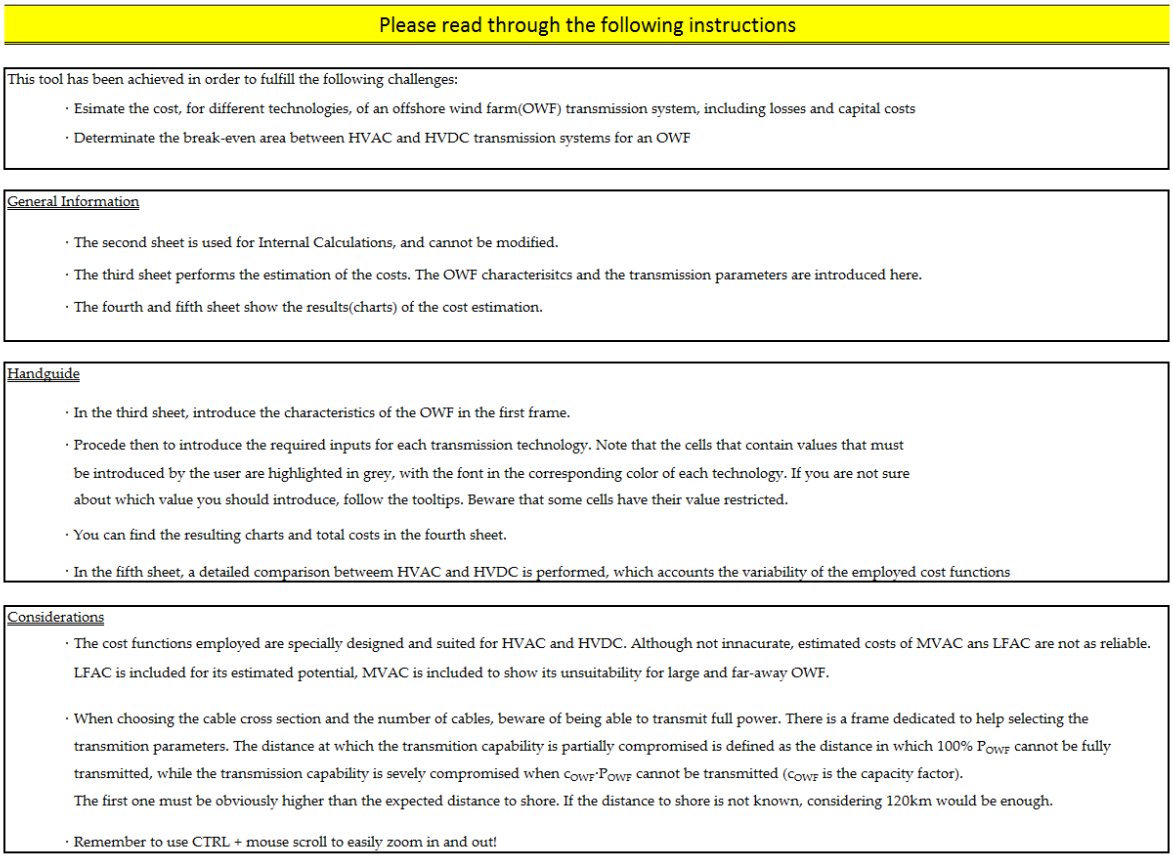

Please read through the following instructions

This tool has been achieved in order to fulfill the following challenges:

- Esimate the cost, for different technologies, of an offshore wind farm(OWF) transmission system, including losses and capital costs
- Determinate the break-even area between HVAC and HVDC transmission systems for an OWF

General Information

- The second sheet is used for Internal Calculations, and cannot be modified.
- The third sheet performs the estimation of the costs. The OWF characterisitcs and the transmission parameters are introduced here.
- The fourth and fifth sheet show the results(charts) of the cost estimation.

Handguide

- In the third sheet, introduce the characteristics of the OWF in the first frame.
- Procede then to introduce the required inputs for each transmission technology. Note that the cells that contain values that must be introduced by the user are highlighted in grey, with the font in the corresponding color of each technology. If you are not sure about which value you should introduce, follow the tooltips. Beware that some cells have their value restricted.
- You can find the resulting charts and total costs in the fourth sheet.
- In the fifth sheet, a detailed comparison betweem HVAC and HVDC is performed, which accounts the variability of the employed cost functions

Considerations

- The cost functions employed are specially designed and suited for HVAC and HVDC. Although not innacurate, estimated costs of MVAC ans LFAC are not as reliable. LFAC is included for its estimated potential, MVAC is included to show its unsuitability for large and far-away OWF.
- When choosing the cable cross section and the number of cables, beware of being able to transmit full power. There is a frame dedicated to help selecting the transmition parameters. The distance at which the transmition capability is partially compromised is defined as the distance in which 100% P_{OWF} cannot be fully transmitted, while the transmission capability is sevely compromised when $c_{OWF} \cdot P_{OWF}$ cannot be transmitted (c_{OWF} is the capacity factor).
  The first one must be obviously higher than the expected distance to shore. If the distance to shore is not known, considering 120km would be enough.
- Remember to use CTRL + mouse scroll to easily zoom in and out!

Figure 37 First sheet of the technical-economic analysis developed tool.

The second sheet is reserved for internal calculations, it is where the important parameters are calculated (e.g. cable resistance, cable reactance, elaborated cost functions, internal results of the model, etc.). Note that this sheet is not supposed to be available to the standard user, and, therefore, its design is not as important as the sheets that are available.

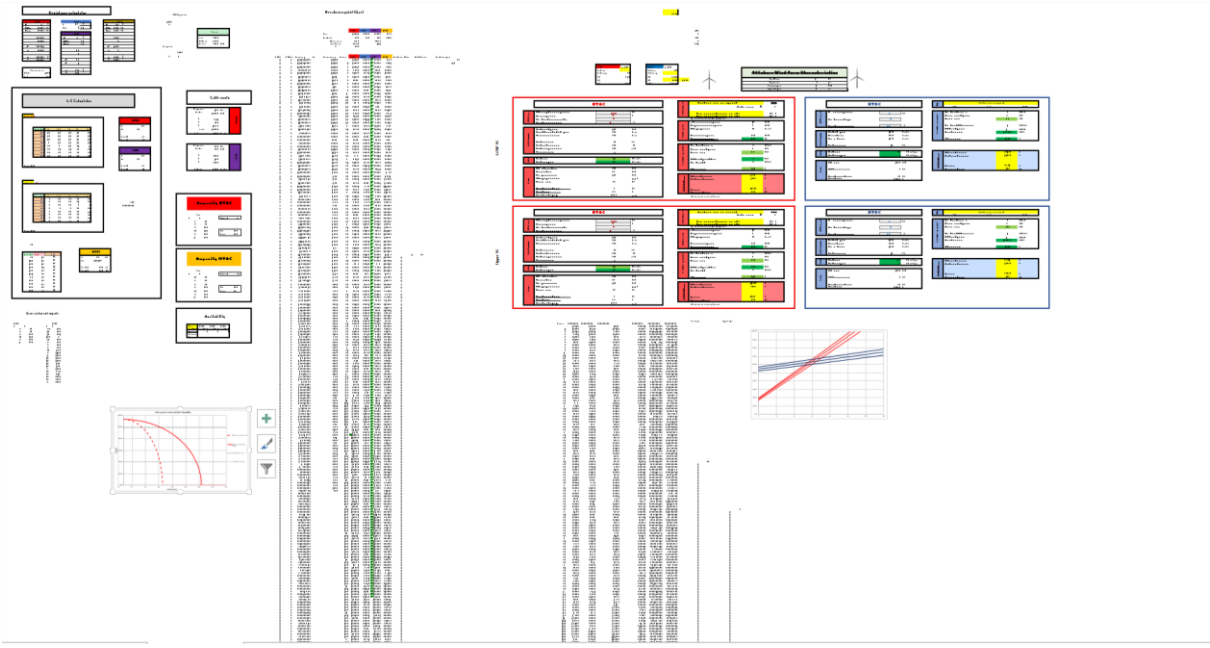

Figure 38 second sheet of the technical-economic analysis developed tool.

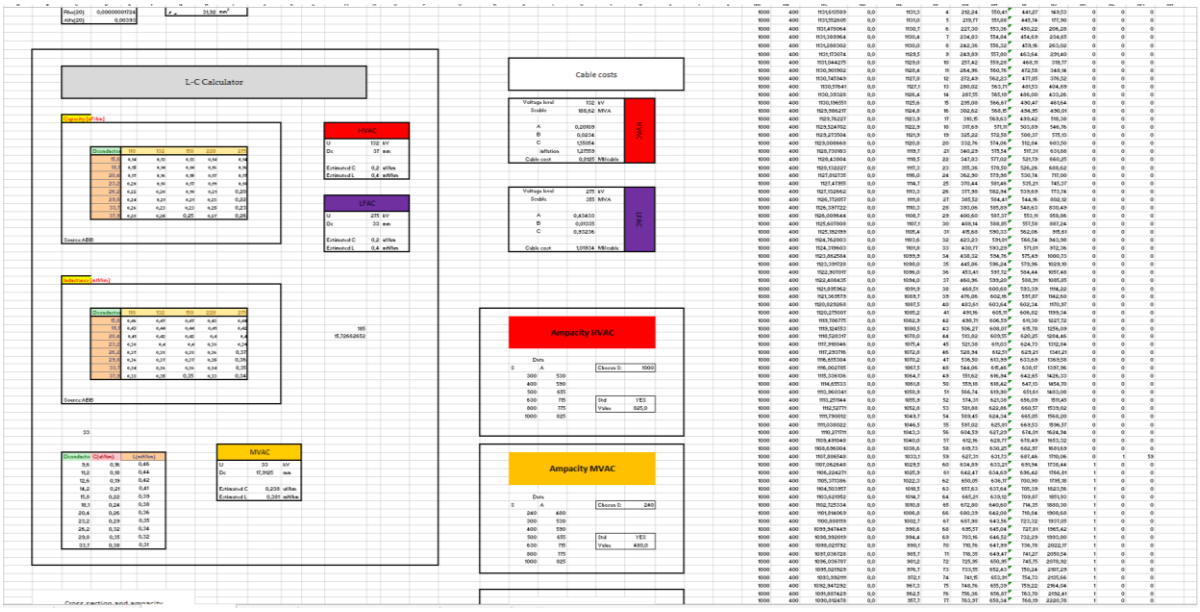

Figure 39 Closer look on the second sheet of the technical-economic analysis developed tool.

The third sheet is where the inputs are introduced by the user and it is the main page of this tool.

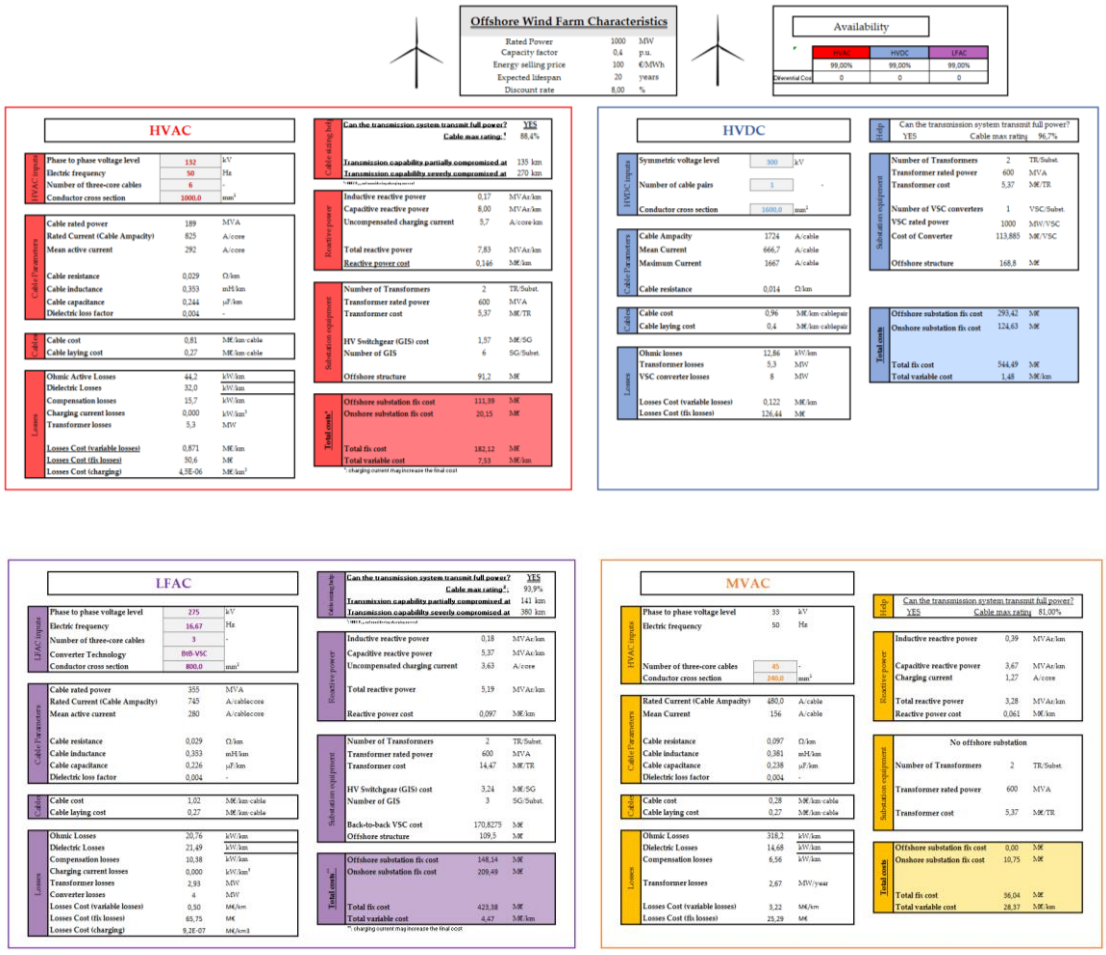

Figure 40 third sheet of the technical-economic analysis developed tool.

The fourth and fifth sheets present the results. The fourth sheets displays two charts (one including all technologies and one excluding (MVAC), along with a table that gives the costs as a function for every transmission length. The fifth sheet excludes LFAC, and is centred on the break-even point concept. It also shows the break-even range and displays a chart showing the cost variability.

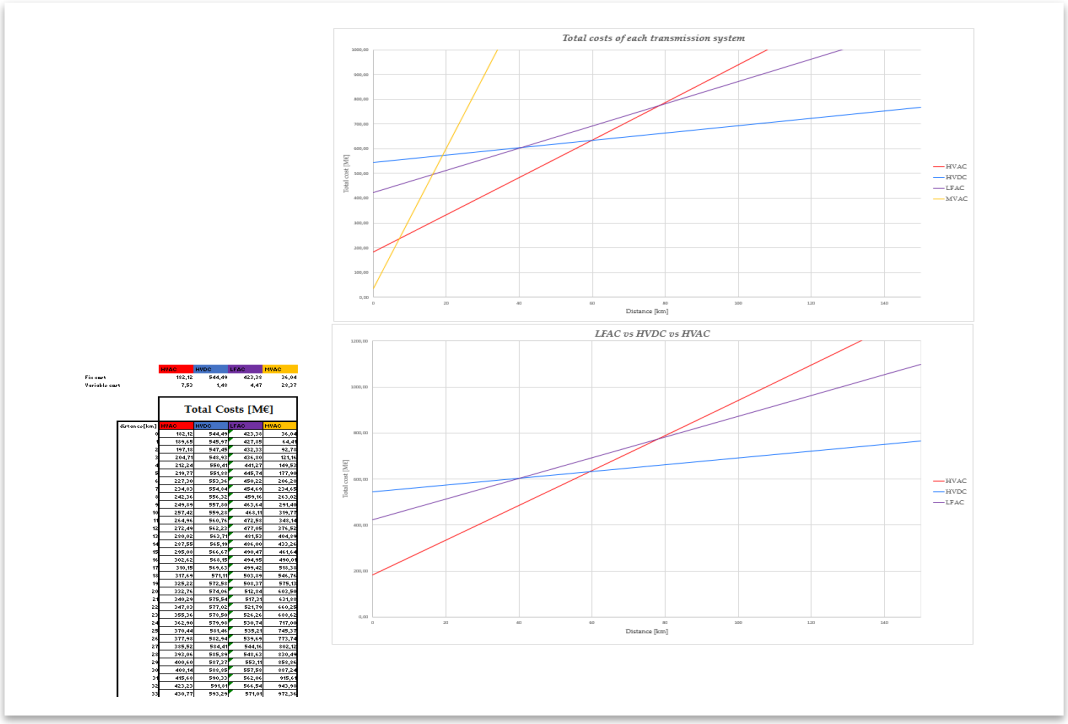

Figure 41 Fourth sheet of the technical-economic analysis developed tool.

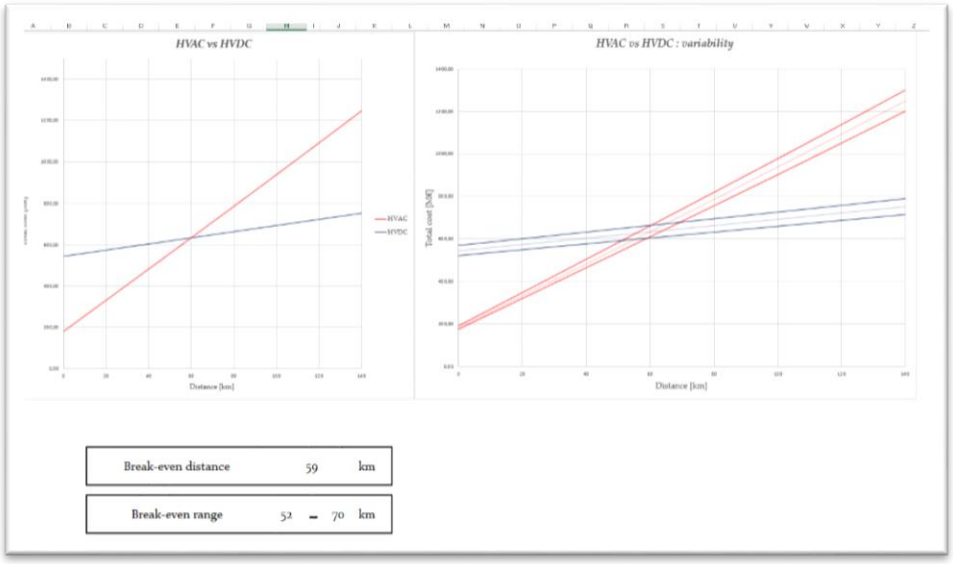

Figure 42 Fifth sheet of the technical-economic analysis developed tool.

Appendix 3: Statistical data of the self-made cost functions

This appendix contains statistical data of the self-made cost functions. Note that for the transfromers (Figure 43), the cost function is potential; hence the model is made with the natural logarithm of the variables.

Estadísticas de la regresión	
Coeficiente de correlación múltiple	0,9929336
Coeficiente de determinación R^2	0,98591713
R^2 ajustado	0,98435237
Error típico	0,05476021
Observaciones	11

ANÁLISIS DE VARIANZA

	Grados de libertna de cuadradio de los cua		*F*	*Valor crítico de F*
Regresión	1	1,88939159	1,88939159	630,0743114	1,21453E-09
Residuos	9	0,02698813	0,00299868		
Total	10	1,91637972			

	Coeficientes	*Error típico*	*Estadístico t*	*Probabilidad*	*Inferior 95%*	*Superior 95%*	*Inferior 95,0%*	*Superior 95,0%*
Intercepción	-3,17598025	0,17519898	-18,1278465	2,15646E-08	-3,572307875	-2,779652615	-3,572307875	-2,779652615
LN(STr)	0,75915713	0,03024376	25,1012811	1,21453E-09	0,690740989	0,827573267	0,690740989	0,827573267

Figure 43 Statistical data of the transformer cost function

Estadísticas de la regresión	
Coeficiente de correlación múltiple	0,98847561
Coeficiente de determinación R^2	0,97708404
R^2 ajustado	0,95416808
Error típico	0,33904826
Observaciones	3

ANÁLISIS DE VARIANZA

	Grados de libertna de cuadradio de los cua		*F*	*Valor crítico de F*
Regresión	1	4,90136294	4,90136294	42,63770478	0,096743546
Residuos	1	0,11495372	0,11495372		
Total	2	5,01631667			

	Coeficientes	*Error típico*	*Estadístico t*	*Probabilidad*	*Inferior 95%*	*Superior 95%*	*Inferior 95,0%*	*Superior 95,0%*
Intercepción	0,02308032	0,51922684	0,04445132	0,97172003	-6,574322273	6,620482906	-6,574322273	6,620482906
Voltage level [kV]	0,0116738	0,00178779	6,52975534	0,096743546	-0,011042168	0,034389774	-0,011042168	0,034389774

Figure 44 Statistical data of the GIS cost function

Estadísticas de la regresión	
Coeficiente de correlación múltiple	0,93759961
Coeficiente de determinación R^2	0,87909304
R^2 ajustado	0,83073025
Error típico	0,04753681
Observaciones	8

ANÁLISIS DE VARIANZA

	Grados de libertad	*Suma de cuadrados*	*Promedio de los cuad*	*F*	*Valor crítico de F*
Regresión	2	0,08215113	0,04107557	18,17705546	0,005083096
Residuos	5	0,01129874	0,00225975		
Total	7	0,09344988			

	Coeficientes	*Error típico*	*Estadístico t*	*Probabilidad*	*Inferior 95%*	*Superior 95%*	*Inferior 95,0%*	*Superior 95,0%*
Intercepción	0,65199257	0,05075301	12,8463816	5,08873E-05	0,521527794	0,782457338	0,521527794	0,782457338
Prated cable-pair [MW]	0,00098002	0,00019087	5,13445972	0,003662332	0,000489371	0,001470671	0,000489371	0,001470671
Voltage level [kV]	-0,00236262	0,00061455	-3,84445103	0,012068962	-0,003942383	-0,000782861	-0,003942383	-0,000782861

Figure 45 Statistical data of the dc cables cost function

Estadísticas de la regresión	
Coeficiente de correlación múltiple	0,99214306
Coeficiente de determinación R^2	0,98434785
R^2 ajustado	0,97652177
Error típico	5,85956166
Observaciones	4

ANÁLISIS DE VARIANZA

	Grados de libertad	*Suma de cuadrados*	*Promedio de los cuad*	*F*	*Valor crítico de F*
Regresión	1	4318,51857	4318,51857	125,7779565	0,007856942
Residuos	2	68,6689257	34,3344629		
Total	3	4387,1875			

	Coeficientes	*Error típico*	*Estadístico t*	*Probabilidad*	*Inferior 95%*	*Superior 95%*	*Inferior 95,0%*	*Superior 95,0%*
Intercepción	54,8950803	6,71232928	8,17824603	0,014624154	26,01425841	83,77590223	26,01425841	83,77590223
P[MW]	0,05889558	0,00525146	11,2150772	0,007856942	0,036300353	0,081490811	0,036300353	0,081490811

Figure 46 Statistical data of the VSC cost function